Utrecht University
Institute for Marine and Atmospheric research Utrecht

Carbonyl sulfide, fluxes and isotopic signatures measured in Finnish forest and wetland

Master of Science thesis

Author:
Anna de Vries 7585047

Supervisors:
Sophie Baartman MSc.
Dr. Maria Elena Popa
Dr. Kukka-Maaria Kohonen
Prof. Ivan Mammarella
Prof. Timo Vesala

2^{nd}*examinator* :
Prof. Dr. M.C. (Maarten) Krol

July 31, 2022

Utrecht University

Acknowledgement

This master thesis project would not have been possible without the help and support from my tutors, family and friends.

Especially I want to thank the following people: Firstly my supervisors who were able to create a safe and friendly learning environment where I felt comfortable to grow. Assistant Professor Dr. Maria Elena Popa, Professor Ivan Mammarella and Professor Timo Vesala; thank you for guiding me and learning me how to become an independent scientist. Thank you also for the trust you gave me and warm welcome in your research groups. Next, my daily supervisors; Doctoral student Sophie Baartman who took the job to be my main supervisor and learned me to do experimental work in the lab and Doctor Kukka-Maaria Kohonen who helped me with the data analysis as well as welcoming me at INAR. Moreover, I want to thank all the INAR staff at Helsinki University for letting me feel at home and part of their team by inviting me to their cake club, outdoor activities, numerous lunches and coffee breaks.

Thank you also to my friends Claudia, Nahid, Marta, Dilge, Angelika, Asta, Yingqi and Paulina with whom I shared unforgettable experiences. Furthermore, I want to thank the staff at the Hyytiälä field station, especially Risto Taipale and the kitchen staff.

Additionally, the following researchers were so kind to share their knowledge with me to give this project useful insights from experts: Linda Kooijman and Wu Sun for information about mosses and their research about *COS* in Hyytiälä, Mary Whelan, Camille Abadie and Marine Remaud for upscaling the *COS* wetland sink in the ORCHIDEE model, Jürgen Kesselmeier and Aino Korrensalo for sharing crucial information about mosses and providing the LAI data for Siikaneva, Anna Virkkala and Olli Peltola for the Northern Hemisphere wetland area information, Gabin Urbancic for the discussions about the boundary layer influences and Leonardo Vittori for the discussion about the chemistry behind isotopic fractionation.

Finally I am grateful for the support and love my family, including my best friend on four legs; Dazzle, gave me during this abroad experience.

Thank you all for making this adventure possible.

Abstract

Carbonyl sulfide (COS) can be used to increase our understanding of the atmospheric carbon cycle and its responses to climate change as it can serve as proxy for gross primary production (GPP) calculations. However, the utility of COS is difficult as knowledge about the global COS budget is incomplete. In this project we aim to reduce this knowledge gap.

We are the first to investigate COS fluxes measured with Eddy Covariance (EC) on a Northern latitude fen and we analyze COS fluxes at a boreal forest. Furthermore, by date, this is the first study identifying the isotopic signature of COS (^{34}S, ^{33}S and ^{13}C) at these ecosystems at various heights, light availability and seasons.

We show the fen to be a stable sink for the studied period (May-September 2019) with a median COS flux on seasonal time scale of -9.2 pmol $m^{-2}s^{-1}$ (25%-75% percentile range between -16 and -4.4 pmol $m^{-2}s^{-1}$). The diurnal cycle with magnitude around 5 pmol $m^{-2}s^{-1}$ is primarily driven by photosynthesis active radiation. Upscaling this sink for all northern latitude wetlands, results in little but significant increase of the Northern Hemisphere COS sink.

The forest is also a COS sink with a median strength of -12 pmol $m^{-2}s^{-1}$ (25%-75% range between -20 and -5.9 pmol $m^{-2}s^{-1}$) from May till October 2020. Moreover, we successfully used our results as a proxy for the GPP estimations at both sites. The mean COS isotopic signatures for the forest samples are 12.16 ± 0.96 ‰ for δ^{34}S, 1.69 ± 2.54 ‰ for δ^{33}S (calibrated against the international standard Vienna Canyon Diablo Troilite (VCDT)) and 8.89 ± 2.14 ‰ for δ^{13}C. The mean mixing ratio in the forest is 506.40 ± 15 ppt.

The fen samples have a mean of 12.77 ± 0.87 ‰ for δ^{34}S, -4.31 ± 2.53 ‰ for δ^{33}S (calibrated against the VCDT) and 13.30 ± 2.14 ‰ for δ^{13}C, with a mean mixing ratio of 531.22 ± 15 ppt. The δ^{34}S signatures fall within literature range and all signatures show little difference between the sites, seasons and among the vertical gradient suggesting non fully active ecosystems during our sampling period (February-April 2022).

Herewith, we prove the practical utility of the new pre-concentration chromatography - isotope ratio mass spectrometer developed at IMAU which gives rise to new study opportunities.

In summary, we show the importance of COS measurements on Northern latitude wetlands as we suspect them to be a stable sink and we report a new dataset of COS isotopic signatures. All this is done to improve the understanding of COS and the atmospheric carbon cycle.

Contents

1 Introduction

In this section the molecule of interest, carbonyl sulfide and its importance for climate science is introduced. Furthermore, the global budget of carbonyl sulfide, the gross primary production and the relevant theory needed for this study, are covered.

1.1 General information and motivation

Carbonyl sulfide (OCS or as here further used: COS) is the most abundant sulfur containing trace gas in the atmosphere. Recently interest in this molecule has grown as it plays an important role in understanding the atmospheric carbon cycle and its responses to climate change. Knowledge about COS can also be used to improve the simulation of the biosphere in global climate models (Fig. 1).

In the troposphere, COS is connected to the terrestrial carbon exchange. COS is directly linked to the carbon dioxide (CO_2) uptake by plants (photosynthesis) and can therefore be used to estimate the gross primary production (GPP). Quantification of the GPP is of high importance now that greenhouse gas concentrations keep increasing in the atmosphere (Masson-Delmotte et al. 2021). However, a problem scientists face, is that CO_2 is not only taken up by plants trough photosynthesis but also respired out of the plants and soil. Therefore, when estimating the GPP using CO_2, not only uptake fluxes but also the respiration fluxes, measured with the Eddy Covariance (EC) method, must be well defined. This is challenging as nighttime EC fluxes, used to estimate the respiration, can be less reliable. During calm nights when turbulence is suppressed and advection occurs, the EC system is not ideal to represent the ecosystem fluxes (Aubinet 2008). Moreover, it is uncertain if the nighttime respiration responses, are similar to daytime respiration responses (Kohonen et al. 2022, Keenan et al. 2019). This CO_2 flux partitioning problem does not occur when using COS as proxy for GPP estimations as COS is taken up irreversibly by plants meaning there is only an one-way directed flux (Kooijmans et al. 2017) (see fig. 3).

In addition, the use of COS as proxy for the GPP on global scale is, at the moment, still difficult. This because knowledge about COS is missing resulting in a non-closed global budget (Montzka et al. 2007, Whelan et al. 2018, Ma et al. 2021). Additional research is needed to increase our understanding on the interactions between COS and the climate.

Another reason to investigate COS, is that it affects the climate by influencing the radiative budget (Fig. 1 blue). In the stratosphere, COS is a source of sulphate aerosols. Stratospheric aerosols reflect incoming sunlight back to space before it can reach earth' surface causing a cooling effect on the planet.
However, COS is also a greenhouse gas warming up the planet. At the time of writing, both processes cancel each other out. However, with current changes in the climate, like changes in atmospheric circulations, COS magnitude and distribution of COS sources and sinks, this balance could be disturbed (Brühl et al. 2012, Lennartz et al. 2017).

Measurements of the isotopic composition of COS in different ecosystems, seasons and light levels can provide new insights. The isotopic composition is specific for each process, facilitating the demarcation of sources and sinks and providing information on the interaction between COS and the biosphere. This research is done to favor the adequate usage of COS for understanding the global carbon cycle and its applications in climate models.

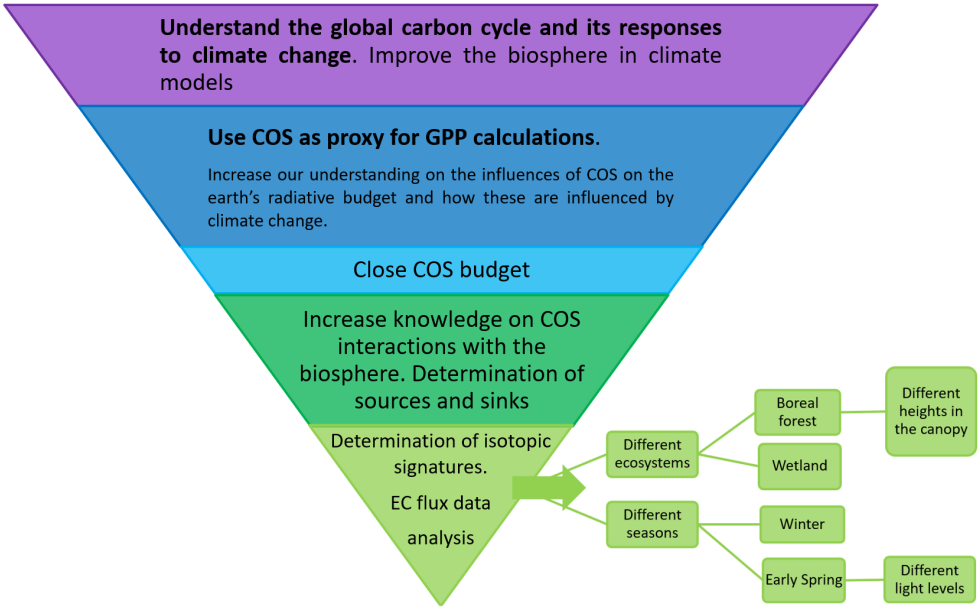

Fig. 1. Pyramid motivating our research on COS**.** With the main goal of investigating COS in purple, tools to reach this in blue, what is needed therefore in light blue and how to get there in green. In light green the focus of this project is described with a detailed ramification of the specific plan.

1.2 Theoretical framework

1.2.1 Carbonyl Sulfide

COS is a colorless gas with a sulfur-odor and toxic effects at high concentration (Biotechnology Information 2022). The linear molecule consists of a carbonyl group double bounded to sulfur (Fig 2).

Earth's COS quantities are low and non-toxic. In the troposphere the average mixing ratio of COS is 500 pmol/mol or parts per trillion (ppt) (Chin and Davis 1995) with variations between 350 ppt and 550 ppt (Kooijmans 2018).

The COS lifetime is around 2 years (Chin and Davis 1995, Baartman et al. 2021). This lifetime together with its chemical inertness (Du et al. 2017) makes it possible for COS to be transported into the stratosphere where it has a lifetime of 64 ± 21 years (Schmidt et al. 2012).

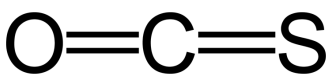

Fig. 2. Chemical structure of carbonyl sulfide (Wikimedia Commons 2007).

In the stratosphere COS is likely the main source of stratospheric aerosols. These aerosols impact the Earth's albedo causing a cooling effect and contribute to the stratospheric (ozone) chemistry. COS also contributes directly to warming due to its radiative forcing (Brühl et al. 2012, Lennartz et al. 2017).

In the troposphere the main source of COS is the ocean. Here COS is emitted directly or indirectly trough emission of the short-lived precursor gases carbon disulfide (CS_2) and dimethyl sulfide (DMS) (Kettle et al. 2002, Lennartz et al. 2017). Minor sources are anoxic soils like wetlands (Whelan et al. 2018) and volcanoes. Anthropogenic sources are oxidation of the gases emitted by rayon production, direct emission by biomass burning, coal combustion, aluminium smelting, pigment production, shipping, tire wear and several other minor sources (Stinecipher et al. 2019, Zumkehr et al. 2018, Baartman et al. 2021).

The main COS sink in the troposphere is uptake by vegetation (canopy) (Berry et al. 2013) and to a smaller extend aerobic soil uptake (Kesselmeier, Teusch, and Kuhn 1999, Baartman et al. 2021). Oxidation reactions with mainly hydroxide (OH) and to a lesser extend with the very reactive atomic oxygen ($O(^3P)$) are also a COS sink. Also the photolysis reaction is a COS sink, however, it is faster and more important in the stratosphere than in the troposphere (Schmidt et al. 2012) (Fig. 3).

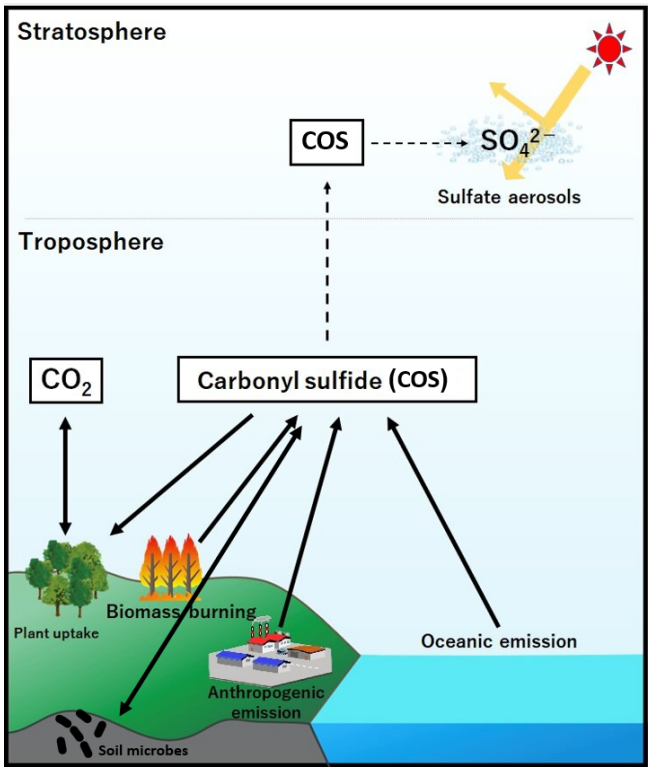

Fig. 3. Simplified overview of COS sources and sinks in the atmosphere (Modification on Shohei Hattori 2020).

1.2.2 Global Budget

To use COS to better understand the global carbon cycle and its responses to climate change, we need to close the knowledge gap in the global COS budget. Ad datum, knowledge about COS sources and sinks is missing, leading to this non-closed global budget (Ma et al. 2021). Seasonal variations (between 100 and 150 ppt in the continental sites in the Northern Hemisphere (NH) and between 40 and 70 ppt in the Southern Hemisphere (SH) and marine sites (Kooijmans et al. 2016)) together with the small atmospheric trend in COS concentrations, make the estimation of the total COS budget complicated. Especially in the NH the seasonality in COS concentrations is influenced by terrestrial vegetation (Montzka et al. 2007). When considering meteorological variables independently, temperature is the most dominant factor governing COS uptake (Vesala et al. 2022). Moreover, Sun et al. 2018 found that leaf litter can show pulses in COS uptake exceeding the plant uptake after rain fall making budget calculations more difficult. While in contrary, soil fluxes seem stable over day.

Nevertheless, an additional source of 230 - 432 Gg S/a in the SH or a larger sink in the NH is needed to match the satellite (NOAA) observations. The source probably comes from in the tropical regions. However, tropical oceans have been shown to unlikely account for the missing direct COS source (Lennartz et al. 2017). Furthermore, Ma et al. 2021, pointed out that extra COS uptake or lower emissions in the higher latitudes, could help close the budget. Finally, land surface models that are used to simulate carbon, water and energy fluxes at Earth surface / atmosphere interface as the 'Simple Biosphere Model version 4' (SiB4) and the 'Organizing Carbon and Hydrology In Dynamic Ecosystems' (ORCHIDEE), do not take into account COS sources/sinks from wetlands (Kooijmans et al. 2021).

New information about different COS isotopes together with extensive EC COS flux data analysis, can help overcome these budget uncertainties.

1.2.3 GPP

GPP is the carbon (C) uptake by vegetation during photosynthesis (Kohonen et al. 2022). Variations in the climate affect vegetation hence photosynthesis, which makes research on this topic even more important now that we experience climate change (Masson-Delmotte et al. 2021). Moreover, additional knowledge about the GPP and processes affecting it, helps to improve the biosphere in climate models leading to better climate predictions.

Flux measurements provide net ecosystem exchange (NEE) data which includes the processes of photosynthesis (GPP) and total ecosystem respiration (TER) (respiration from leaves, roots, stems and soil) (NEE=TER-GPP) (Kohonen et al. 2022). Separation between GPP and TER fluxes is needed to study the processes individually and increase our understanding of the total carbon budget on earth. COS can be a promising proxy to demarcate photosynthesis and indirectly calculate the GPP as it is an analogue of CO_2. On regional, local and leaf scale, concentrations of COS have been shown to be related to CO_2 concentrations (Asaf et al. 2013, Kooijmans et al. 2016).

Both COS and CO_2 follow the same gas transport pathway into leaves (Fig. 3). However, in contrast to CO_2, COS is irreversibly hydrolyzed by the enzyme carbonic anhydrase (CA) forming hydrogen sulfide (H_2S) and CO_2 (eq. 1) (Protoschill-Krebs and Kesselmeier 1992).

$$COS + H_2O \xrightarrow{\text{CA}} HCOOS^- + H^+ \rightarrow H_2S + CO_2 \tag{1}$$

COS is thus not respired out of the vegetation making it an useful tracer of the GPP (Asaf et al. 2013, Kooijmans et al. 2017, Whelan et al. 2018).

Besides the shared uptake pathway of COS and CO_2 and the one-way directed flux of COS, there is no interaction between COS and CO_2 (Blonquist Jr et al. 2011). A drawback of the use of COS as proxy for GPP calculation is that the hydrolyzing enzyme CA is light independent leading to COS uptake by vegetation during nighttime, when stomata do not close completely. This nighttime uptake must be taken into account when calculating the GPP using COS fluxes (Kooijmans et al. 2017).

Lastly, in the ecosystem, other than vegetation related COS fluxes (e.g. soil) need to be negligible or well quantified to be able to demarcate the COS uptake by vegetation (Kooijmans et al. 2017, Blonquist Jr et al. 2011).

To calculate the GPP with COS fluxes we use equation 2 (Sandoval-Soto et al. 2005, Campbell et al. 2008, Kooijmans et al. 2019).

$$GPP = -F_{COS}\frac{[CO_2]}{[COS]}\frac{1}{LRU} \tag{2}$$

where F_{COS} is the flux of COS at the ecosystem scale, $[CO_2]$ and $[COS]$ the mole fraction of the gases and LRU the independently determined leaf-scale relative uptake ratio.

LRU is the ratio of deposition velocity of COS over CO_2 with the deposition velocity calculated as the leaf flux scaled by the gas mole fractions (eq. 3) (Sandoval-Soto et al. 2005).

$$LRU = \frac{F_{COS}}{F_{CO_2}}\frac{[CO_2]}{[COS]} \tag{3}$$

where F_{CO_2} is the flux of CO_2 at the ecosystem scale.

The value of LRU differs among types of vegetation. Furthermore the LRU value changes during the day since light affects the fluxes of COS and CO_2 differently. Finally, during daytime and the period with most vegetational growth, vapor pressure deficit (VPD) also affects the LRU indicating a connection between stomatal conductance and humidity. Nevertheless, the value of LRU is usually larger than 1 since the deposition velocity of COS is faster than CO_2 as CA has a higher reaction rate with COS than the analogous enzyme ribulose-1,5-bisphosphate carboxylase/oxygenase (Rubisco) has with CO_2 (Kesselmeier and Merk 1993, Protoschill-Krebs,

Wilhelm, and Kesselmeier 1996, Kooijmans et al. 2019).

1.2.4 COS Isotopes

Isotopes are chemical elements with identical amount of protons but different amount of neutrons. Due to the identical atomic number, isotopes have similar chemical but different physical properties as their mass number differs. The stable isotopes investigated in this report are the Sulfur-32 (^{32}S) with a natural abundance of $94,99\%$, sulfur-34 (^{34}S) with a natural abundance of 4.25% and sulfur-33 (^{33}S) with a natural abundance of 0.75% (Meija et al. 2016). Moreover, we identify the isotopic signature of Carbon-13 with a natural abundance of 1.11%(Stute n.d.).

COS isotopologues are *COS* molecules with different sulfur, carbon or oxygen isotopes. This isotopic composition is specific for its provenance. Therefore the detection of *COS* isotopologues can be used to characterise different sources and sinks.

Because the differences among isotopic signatures are small, double relative measurements are reported. Firstly, the absolute ratio between the less abundant ($^{33,34}S$ or ^{13}C) and abundant (^{32}S or ^{12}C) isotope is calculated (eq.4 shows the example for sulfur).

$$^{33,34}R = \frac{[^{33,34}S]}{[^{32}S]} \tag{4}$$

Next, the relative deviation of the sampled isotope ratio against the standard, reference isotope ratio is calculated, resulting in the δ value (5).

$$^{33,34}\delta = \frac{^{33,34}R_{sample} - ^{33,34}R_{reference}}{^{33,34}R_{reference}} = [\frac{^{33,34}R_{sample}}{^{33,34}R_{reference}} - 1] \cdot 1000‰ \tag{5}$$

Positive δ values indicate enriched samples which contain more heavy isotopes ($^{33,34}S$) than standard, while negative δ values indicate a depleted sample containing less heavy isotopes than the standard isotopic ratio (Röckmann 2017).

Isotope fractionation occurs when isotopes are differentiated by processes that make one isotope more favored over the other. During "mass-dependent fractionation" (MDF) processes, like chemical processes, the lighter sulfur isotope is favored over the heavier due to the weaker strength of the chemical bounds between the molecules that need to be broken. Another MDF process is diffusion which is based on the differences in weight of the isotopes. *COS* uptake by plants is a mass-dependent process leading to more lighter isotopologues taken up faster by the vegetation. If the ecosystem is a sink with much vegetation, the measured air samples will be enriched in heavier isotopologues as the lighter ones are taken up irreversibly. When mass-independent processes take place, the lighter isotope is not preferred and the above mentioned effect will not be measured. However mass-independent processes rarely happen in natural processes (Röckmann 2017).

Little is known about the isotopic signatures of the sulfur atom of *COS* from different ecosystems. While, to our knowledge, no measurements on the isotopic signature of the carbon atom of *COS* have been performed. Table 1 shows an overview of the current information about *COS* isotopic signatures. Overall the δ^{34}S value from ambient air, has a range between 10‰- 14‰ in the troposphere (Baartman et al. 2021, Nagori et al. 2022, Angert et al. 2019, Hattori, Kamezaki, and Yoshida 2020, Davidson, Amrani, and Angert 2021).

COS source/sink	**δ^{34}S signature**	**Source**
Ocean source	14.7 ± 1 ‰	Davidson et al. (2021)
Ocean source	19 ‰	Hattori et al. (2020)
Antropogenic source	8.1 ± 1 ‰	Davidson et al. (2021)
Antropogenic source	4 - 5 ‰	Hattori et al. (2020)
Ambiant air Utrecht	15.7 ± 0.9 ‰	Baartman et al. (2021)
Ambiant air Israel Islands. and in the Canary	13.2 ± 0.6 ‰	Angert et al. (2019)
Biosphere different height forest	?	This study
Wetland fen	?	This study

Tab. 1. List of known isotopic signatures of sulfur-34 from *COS*

1.2.5 GC-IRMS

In this research, a continuous flow gas chromatography - isotope ratio mass spectrometry (CF GC-IRMS) method is used. With the GC-IRMS method, isotope signature of trace gases can be measured. The GC-IRMS used in this study is unique as it allows us to use smaller sample sizes (3 to 4 L).

The smaller sample sizes are possible because the systems' nonlinearity is characterized beforehand and a correction factor is applied to the measurements accounting for this. This makes sampling more convenient because without the nonlinearity correction, several hundreds of liters would be needed to overcome the non-linearity effect of rising isotope values. By the nonlinearity effect, we mean how the δ value of a certain peak in the IRMS depends on the peak area (integrated ion signal) of these isotope masses (Baartman et al. 2021).

Gas chromatography is a separation tool based on the interactions between the analyzed gas and the compounds in the column of the chromatogram. A carrier gas (mobile phase) passes the measured gas trough a stationary phase. The compounds carried by the mobile phase are attracted to the stationary phase depending on their mass. This leads to different outflow time for each component in the measured gas which is shown in the chromatogram. By selecting specifically the retention time belonging to COS, COS is separated from the other components in the gas mixture.

The IRMS contains an ion source which fragments the different compounds in the gas. The compounds pass trough a magnetic and electric field in which the ions, based on their mass to charge ratio, gain different deflection and speed. Due to the different trajectories, the ions enter the detector sorted and their relative abundance can be measured. This results in a spectrum where the relative intensity of the ion signals are plotted against the mass-to-charge ratio.

More information about the used GC-IRMS can be found in section 4.2.1 and in Baartman et al. 2021.

1.2.6 Eddy Covariance method

The Eddy covariance (EC) method is used to study interactions between the biosphere and atmosphere by measuring directly continuous ecosystem scale fluxes with high time resolution (Aubinet, Vesala, and Papale 2012, Baldocchi 2003).

The EC method measures turbulent gas exchange by measuring the amount of gases transported by turbulent eddies. Hence, the biosphere fluxes are calculated from the covariance between the turbulent vertical wind velocity and fluctuated component of the COS mixing ration (eq. 6).

$$F^{EC} = \overline{\rho_a}\overline{w'c'} \tag{6}$$

where ρ_a is the dry air molar density, w' is the turbulent fluctuating vertical wind velocity and c' is the turbulent fluctuations in gas mixing ratio ($c = \frac{\rho_c}{\rho_a}$).
To link the biosphere fluxes with the EC fluxes we need to start with the conservation of a quantity, e.g. gas molar mixing ratio in the atmosphere using the scalar conservation equation (eq. 7) (Aubinet, Vesala, and Papale 2012):

$$S_c = \frac{\partial \rho_a c}{\partial t} + \bigtriangledown \cdot (\overrightarrow{u}\rho_a c) \tag{7}$$

where S_c is the strength of the divergence of the source/sink, the first term on the right side is the rate of change of the quantity c and the second term the atmospheric transport of c with $\overrightarrow{u}$ the wind vector.

This equation can be rewritten as eq. 8 after applying Raynold's averaging rules (Appendix 8.1) and assuming $\overline{\rho_a}$ is constant based on the assumption of horizontal homogeneity.

$$\overline{S_c} = \overline{\rho_a}\frac{\overline{\partial c}}{\partial t} + \overline{\rho_a}\,\overline{\overrightarrow{u}} \bigtriangledown (\overline{c}) + \bigtriangledown(\overline{\rho_a}\,\overline{\overrightarrow{u}'c'}) \tag{8}$$

where the first term on the right hand side represents the rate of change of the dry mole fraction, second is the advection term and the last term is the divergence in eddy fluxes.

The net ecosystem exchange (NEE) can be calculated by integrating Eq. 8 from ground up to measurement height. Moreover, we assume no flux at the ground level (since we assume zero velocity at ground level) and constant flux layer which results in equation 9.

$$NEE = \frac{1}{h}\int_0^h \overline{\rho_a}\frac{\overline{\partial c}}{\partial t}dz + \frac{1}{h}\int_0^h \overline{w\rho_a}\frac{\overline{\partial c}}{\partial z}dz + \overline{\rho_a w'c'}(h) \tag{9}$$

where the first term on the right represents the storage flux (F^{STO}), the change in COS concentration between the night when turbulence is too low to be detected and early morning when turbulence is enhanced, the second term is the vertical advection flux (F^{A}) and the last term is the vertical EC flux (F^{EC}).

F^{STO} is negligible (Kohonen et al. 2022, Montagnani et al. 2018) and when assuming no net flux of dry air and steady state, also F^{A} can be neglected. So the EC flux represents the NEE of whole measured ecosystem (eq. 10).

$$NEE = F^{EC} = \overline{\rho_a w' c'}(h) \tag{10}$$

Positive sign means net COS transfer into the atmosphere (source) while negative signs indicate a COS sink (Aubinet, Vesala, and Papale 2012, Kohonen et al. 2022).

More information about EC data processing can be found in Kohonen et al. 2020.

Investigation of COS fluxes combined with isotopic composition measurements provides an unique set of information to better understand the interactions of COS with the biosphere with the purpose to use COS as a proxy for GPP calculations.

2 Project Outline

This project aims to provide additional knowledge on the global budget of COS by characterizing the isotopic signature of different sources/sinks and by the demarcation of the GPP from NEE EC flux data.

Air samples from different ecosystems (forest and wetland) in South Finland in winter and early spring season are taken and their isotopic composition is determined. Moreover, the vertical gradient in isotopic signatures in the forest is investigated and the early spring samples are taken both in high and low light circumstances. The samples are analyzed with a pre-concentrated GC-IRMS. Furthermore, EC flux measurements at the different ecosystems are analyzed to investigate the COS fluxes and their responses to environmental parameters. Lastly, we aim to find correlations between continuous NEE measurements and isotopic signatures.

2.1 Research Questions

The main research question investigated in this project is:

"Which information can be gained from measurements of the isotopic composition of COS and EC flux data of COS in different ecosystems and seasons to improve our understanding on the interaction of COS with the biosphere?"

We will investigate this question by specifically answering the following sub questions:

2.1.1 Is Hyytiälä boreal forest a COS source or sink and how does this differ among seasons?

2.1.2 What is the isotopic composition of COS at different heights in Hyytiälä boreal forest during winter/spring?

2.1.3 Is Siikaneva wetland a COS source or sink and how does this differ among seasons?

2.1.4 What is the isotopic composition of COS at different depths in Siikaneva wetland during winter/spring?

2.1.5 How do EC COS flux measurements of Hyytiälä boreal forest and Siikaneva wetland compare/differ?

2.1.6 How do isotopic signatures of COS measured at Hyytiälä boreal forest and Siikaneva wetland compare/differ?

These sub questions will guide us during the project and help us to better understand the global budget of COS and to determine the GPP by characterisation of sources/sinks trough their isotopic composition.

3 Hypotheses

Here the hypotheses on the research questions are presented based on literature study (section 1.2).

3.1 Is Hyytiälä boreal forest a COS source or sink and how does this differ among seasons?

In this report we analyze the COS EC data from Hyytiälä for a different period, April-May 2021, than Vesala et al. 2022. Besides the new analysis period, we use the data to calculate the GPP in the ecosystem, we compare the COS fluxes and GPP estimation with our wetland data and we use it to better understand our isotopic signature results. However, we base our expectations on the article of Vesala et al. 2022.

The Boreal forest is hypothesized to be a sink of COS both during day- and nighttime due to the incomplete closure of stomata and light independent enzyme, CA, hydrolyzing COS during plant uptake (Kooijmans et al. 2017). However, **we expect to see lower COS uptake during winter season** due to low enzyme activity and stomatal conductance with respect to spring when temperatures are high enough for biological activity to reconvene (Vesala et al. 2022). **When the air temperature increases over 10 $°C$ in Spring, a saturation in COS fluxes is expected** (Vesala et al. 2022).

3.2 What is the isotopic composition of COS at different heights in Hyytiälä boreal forest during winter/spring?

Taking into account the MDF principle, **we hypothesize to measure COS enriched air (higher δ^{33}S and δ^{34}S with respect to ocean and anthropogenic COS emissions (Table 1)) in the forest** as we expect this ecosystem to be a COS sink (Vesala et al. 2022, Davidson, Amrani, and Angert 2021).

Since the air in the ecosystem is affected by different sinks depending on the height in the ecosystem (e.g. mosses, leaves, needles, stems) and sources, (e.g. air from the ocean and anthropogenic sources), **different isotopic signatures are expected among the vertical gradient. Near the surface, the air is affected by the local environment (ground vegetation, soil and roots) where as above the canopy layer most of the sunlight is available for the plants. At the highest measurement point (125 m) the whole ecosystem will be represented in the air sample and enrichment in heavier isotopes can be less marked.**

Moreover, when plotting the results for δ^{34}S (on the x-axis) against δ^{33}S (on the y-axis) and making a so called 'three-isotope plot', the slope theoretically should be 0.515 (Hattori et al. 2015). This, because the ratio $\frac{^{33}S}{^{32}S}$ is of one neutron mass while $\frac{^{34}S}{^{32}S}$ differs two neutron masses. The theoretical MDF linear line connecting the two isotopes will be the ratio of $\frac{^{33}S}{^{34}S}$, and thus around 0.5.

Next, we can calculate the deviation of the sampled δ^{33}S value from the MDF line with equation 11 (Farquhar and Wing 2003, Ono et al. 2006, Hattori et al. 2015, Baartman et al. 2021).

$$\Delta^{33}S = \delta^{33}S - [(\delta^{34}S + 1)^{0.515} - 1] \tag{11}$$

where $\Delta^{33}S$ is the deviation of δ^{33}S from the MDF line.

Nevertheless, it is important to note that the slope of the MDF line is derived from lab experiments. While we are measuring isotopes from a complex ecosystem where more influences need to be considered than in a controlled lab setting. **Therefore, our 'three-isotope' plot could have a different slope and our $\Delta^{33}S$ could be far from zero.** This however, should not be directly interpreted as if no MDF took place.

In our case it is therefore more robust to plot the sulfur δ values against the mixing ratio to identify MDF. **If MDF took place, we expect a negative trend between the variables; The more COS is taken up, the higher the δ values of sulfur, and the lower the mixing ratios. For the carbon isotope the story could be different since the carbon isotope ends up in a different molecule (CO_2) than the sulfur atom (H_2S) (eq.1 and Kooijmans 2018, Ghiasi, Gholami, and Nasiri 2021, Angeli, Carta, and Supuran 2020).** H_2S afterwards has different functions in the plants while CO_2 is re-emitted into the atmosphere (Kooijmans 2018) and could therefore restore the isotopic composition of carbon (Röckmann 2017).

Moreover, COS fluxes have been shown to negatively correlate with photosynthesis active radiation (PAR) till a value of 200 $p$mol $m^{-2}s^{-1}$ (increase in PAR, decrease of F_{COS} / increase COS uptake) (Kooijmans et al. 2019). **This could lead to more COS uptake higher up in the canopy layer** where we find higher PAR levels than lower in the canopy where branches limit light penetration. However, during daytime, when VPD, which cross-correlates with PAR, increases to more than approximately 900 Pa, COS uptake decreases due to stomatal closure driven by VPD (Kooijmans et al. 2019). This could make the difference in COS uptake among the vertical gradient less pronounced. Moreover, lower in the canopy there will be more scattered light available and the leaves in the lower canopy could be more adapted to low PAR levels which could also make the difference between the COS uptake at different heights limited. Additionally, mosses, which do not have stomata and thus take up COS light independently, are present on the surface, influencing the COS uptake. Therefore, **the difference in isotopic signature caused by MDF could be low.**

Nighttime air will be enriched because of the MDF that took place in the previous hours and the low and stable boundary layer. Vegetation will thus have limited lighter isotopologues available for uptake and will take up more heavy COS isotopologues during the night. Measurements of early morning air could therefore be more enriched in heavier isotopes than COS measured later in the day when turbulence is enhanced due to sunlight heating the air. Especially near surface the influence of soil will be enhanced when turbulence is limited. However, isotopic measurements of samples taken with daylight should not be affected by this mixing in the canopy layer. Nevertheless. EC data is affected by this, therefore we take into account the storage change (eq. 9) during EC data analysis (Kooijmans et al. 2017).

Since we take our spring 'low light level' samples in the evening rather than the morning, we don't expect similar nighttime behaviour as mentioned above. Nevertheless, we do expect to see differences between the light and dark samples. Even if the stomata in the boreal forest are found to not close entirely during dark conditions (Kooijmans et al. 2016), a daily cycle in COS fluxes with more uptake during high light and PAR levels, has been identified (Vesala et al. 2022). Therefore **we hypothesize that there will be more MDF with high light levels than with low levels. This will result in more enriched isotopic signatures for the light samples with respect to the dark samples.**

On seasonal time scale, difference in isotopic signatures should be visible as we expect variations in COS uptake by vegetation. These variations are expected since temperature, one of the most important variables affecting the stomatal conductance, mesophyll diffusion and enzyme activity (Kooijmans et al. 2019), will vary among seasons. When temperatures are low, the stomatal conductance and enzyme activity are low leading to less COS uptake by the vegetation. **Winter air is expected to be less enriched in heavier isotopes with respect to the spring samples when stomatal conductance is higher and lighter isotopes are taken up faster by the vegetation leading to air more enriched in heavier isotope. Moreover, due to this temperature dependence, the difference among the isotopic signatures at different heights is expected to be little or absent during the winter period and more pronounced during spring.**

Finally, we expect the isotopic signatures for δ^{34}S to fall within, or given the argument above, to be more enriched than the known range of the ambient (background) air; 10‰ - 14‰ (Baartman et al. 2021, Nagori et al. 2022, Angert et al. 2019, Hattori, Kamezaki, and Yoshida 2020, Davidson, Amrani, and Angert 2021).

3.3 Is Siikaneva wetland a COS source or sink and how does this differ among seasons?

Wetlands can be sources/sinks depending on the oxidation state of the soil (Baartman et al. 2021, Whelan et al. 2018, Kamezaki et al. 2016, Kesselmeier, Teusch, and Kuhn 1999). **When analysing EC flux data from measurements done above the aerobic surface, we expect the fen to behave as a COS sink. While for the air samples taken deeper into the anaerobic soil, we expect to identify a COS source.**

For freshwater marshes and bogs the fluxes are lower than 10 pmol $m^{-2}s^{-1}$ (Fried, Klinger, and Erickson III 1993, DeLaune, Devai, and Lindau 2002, Whelan et al. 2018) or even negative indicating a sink (Fried, Klinger, and Erickson III 1993, De Mello and Hines 1994, Whelan et al. 2018). **Moss incubation measurements at Hyytiälä show COS fluxes between around -3 to -4 pmol $m^{-2}s^{-1}$. Since the fen is covered by mosses and other vegetation, we expect similar or higher uptake fluxes.**

However, plants in wetlands can also become a COS source instead of the expected sink due to transmission via stems of COS produced in the soil. Moreover, COS can be produced as by-product of osmotic management processes in saline environments (Whelan et al. 2018).

We exclude the photochemical production of COS from $CDOM$, sulfur radical formation and indirectly by CS_2 which can occur in water (Du et al. 2017, Whelan et al. 2018) since the water levels are expected to be too low for this.

3.4 What is the isotopic composition of COS at Siikaneva wetland during winter/spring?

COS isotopic measurements on a wetland have never been done so we cannot quantify our hypothesis based on literature. However, Kamezaki et al. 2016 was able to determine the fractionation factor of sulfur in COS caused by soil bacteria trough lab experiments.

As written above, depending on the microbes in the soil, the wetland can be a sink (aerobic soil) or source (anaerobic soil) affecting the isotopic composition of the measured COS.

Peatlands like the fen we investigate, have a surface containing oxic microbes which changes into anoxic microbes when going down into the soil (Artz 2009). Therefore, **we expect this fen to show changes in isotopic composition for the different studied depths.**

Nevertheless, since the limiting factor of the hydrolysis reaction (eq. 1) is the atmospheric concentration of COS (Protoschill-Krebs, Wilhelm, and Kesselmeier 1996), and we expect a low COS mixing ratio in the soil layer, **detection of the isotopic composition in the soil layer could be difficult.** Especially in winter when snow covers and isolates the soil layer further from atmospheric COS.

Furthermore, **we expect for the winter samples to measure background values of δ^{34}S falling within the range of the ambient (background) air; 10‰ - 14‰** (Baartman et al. 2021, Nagori et al. 2022, Angert et al. 2019, Hattori, Kamezaki, and Yoshida 2020, Davidson, Amrani, and Angert 2021) as the vegetation is covered by snow. **For the early spring samples we expect to measure enriched air in the heavier sulfur isotope based on fractionation (Section 1.2.4).**

Finally, since the fen is covered by mosses and plants which possibly have less ability to control their stomata (Zeiger, Farquhar, and Cowan 1987), **differences between COS uptake, and therefore isotopic composition, under light and dark circumstances should be low.**

3.5 How do EC COS flux measurements of Hyytiälä boreal forest and Siikaneva wetland compare/differ?

Firstly, it is good to remember that the analyzed period is different for both ecosystems. Both contain a period with the same months but the years are different. This makes comparison less direct since meteorological variables are not identical. Nonetheless, a rough comparison can be made when taking into account these meteorological differences.

The COS fen fluxes are expected to be smaller than the forest fluxes due to the different vegetation. Both ecosystems are covered by mosses and stomata containing plants. However, **the leaf area index (LAI), used to quantify the leaf material in a canopy, has a maximum of almost 7 m^2m^{-2} in the forest (Vesala et al. 2022) while for the wetland the value is expected to be lower.** Therefore, **also the diurnal cycle, governed by the opening and closing of stomata, is expected to be less pronounced at the wetland with respect to the forest.** Moreover, the fen soil usually contains more water than the forest ground. Besides, the fen surface does not have shaded areas like the forest has because of the high trees. Therefore, plants may have adapted in different ways in both ecosystems. Another adaptation that could have taken place is within the wetland plants. Due to the water and light availability these plants could have lost most of their ability to control stomata like aquatic plants (Zeiger, Farquhar, and Cowan 1987). This can also lead to a less pronounced daily cycle for the COS flux.

Also the LRU values for both ecosystems are assumed to be different due to the vegetation difference. For Hyytiälä forest we expect a LRU of 1.6 as used in literature (Kooijmans et al.

2019) **while little is known for the fen.** However, we can make an estimation using eq 3, the COS fluxes found in a bog by Fried, Klinger, and Erickson III 1993 (-8 ng S $m^2 min^-1$ which is 0,36 μmol $m^2 day^-1$ COS) and a COS mixing ratio of 500 ppt, the CO_2 fluxes of Seco et al. 2020 ($-3,1 * 10^5$ μ mol $m^2 day^-1$) and a mixing ratio of 400 ppm which leads to a LRU of 0.93 (calculated by Prof. J. kesselmeier).

3.6 How do isotopic signatures of COS measured at Hyytiälä boreal forest and Siikaneva wetland compare/differ?

Since the ecosystems are different, but both contain vegetation that can take up COS, we expect to see some similarities and some differences between the isotopic signatures measured at both sites. During winter Siikaneva is fully covered by snow and the air sample reflects only the background COS value. In Hyytiälä however, the needles of the trees are so small that snow easily falls of the needles letting them uncovered. Therefore, **we expect the forest samples to be more enriched in heavier isotopes due to the plant uptake with respect to Siikaneva. Nevertheless, the temperatures at both sides are very low so also in the forest uptake can be limited which can make the difference between the samples small.**

For the early spring samples, **we expect to see bigger differences between the light and dark samples in the forest due to the presence of plants than at the wetland which is mostly covered by mosses which can take up COS independently of light because of the lack of stomatal control.**

Lastly, since COS is transported through vegetation by diffusion, the fractionation factor can be calculated using the ratio between the diffusion coefficient of the (less) abundant isotope. The diffusion coefficient is calculated using eq. 12

$$D = (\frac{k_B T}{\mu})^{\frac{1}{2}} \tag{12}$$

where k_B is the Boltzmann constant, T is the temperature and μ is the reduced mass.
The ratio between the diffusion constants is calculated using eq. 13 (Woods-Hole-Oceanographic-Institution n.d.).

$$\frac{D_{abundant}}{D_{rare}} = \sqrt{(\frac{m_a + m_{air}}{m_a * m_{air}} * \frac{m_r * m_{air}}{m_r + m_{air}})} \tag{13}$$

where $m_a = 60.08\, g/mol$ is the molar mass of the most abundant COS isotope, $m_r = 63\, g/mol\,, 64\, g/mol$ is the molar mass of the less abundant COS isotope (^{33}S and ^{34}S) (Biotechnology Information 2022) respectively and $m_{air} = 28.92\, g/mol$ (Woods-Hole-Oceanographic-Institution n.d.).

The calculated diffusion ratio is 1.0076 and 1.010 respectively for ^{33}S and ^{34}S against ^{32}S. Davidson, Amrani, and Angert 2021 found a lower fractionation factor (-1.9 ± 0.3 ‰) for ^{34}S during plant experiments. Note however, that we are measuring in a complex ecosystem with different vegetation rather than on a specific plant in a controlled lab setting. Moreover, besides the fractionation from diffusion, further fractionation can occur during the hydrolyzing reaction with the enzyme CA, making the calculated factor possibly larger.

4 Method

In this section all the methods used to answer the research questions are described. Starting with the air sampling procedure and measurement site description. Followed by the used GC-IRMS setup and isotope data analysis and concluding with the data analysis of the EC flux data.

4.1 Sampling

For the air sampling procedure, Silico treated, pre-evacuated cannisters were used. Magnesium perchlorate ($Mg(ClO_2)_4$) dryers were made to dry out the water in the sampled air before entering the cannister. The cannisters were filled till 3 bar (2 bar over pressure) using a pump (knf, Type: PM22874-86, U: 12 V, I: 1.3 A, Pmax: 1.5bar). The 1/4" Dekabon tubes were flushed for 10 minutes before filling the cannisters (fig. 4a). Figure 4 schematically represents how the air was captured. After passing the dryer and filter, the evacuated

cannister was filled (fig. 4b). Afterwards the pump was used to overpressurize the cannister (fig. 4c). Further descriptions can be found in the manuals 8.4.1, 8.4.2 and 8.4.3.

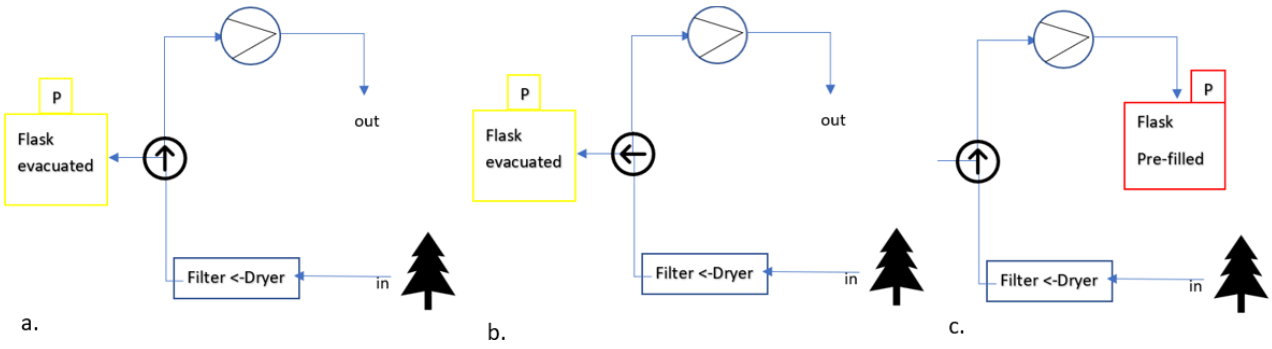

Fig. 4. Schematic representation of the used sampling setup. With a. the flushing of the line, b. the filling of the evacuated cannister and c. the over pressurizing.

Figure 5 shows how the 1 m samples were taken during spring at both locations.

Fig. 5. Photo's of sampling during spring at a. Hyytiälä and b. Siikaneva.

4.1.1 Sampling site - Hyytiälä Forestry Field station

To sample air at different heights in the forest, we sampled at the SMEAR II station in Hyytiälä, South-Finland ($61°51'N, 24°17'E, 181m$ ASL) (fig. 7). The winter samples were taken on 7 February 2022 around 2 pm and the site was covered by snow. While the early spring samples (further denoted as spring samples) were taken on 27 April 2022 around noon and in the evening with little to no snow cover.
The trees growing in a radius of at least 150 m around the measurement site are Scots pine (Pinus sylvestris L.), Norway spruce (Picea abies (L.) Karst.) and Deciduous trees (e.g., Betula sp., Populus tremula, Sorbus aucuparia) (Vesala et al. 2022). The average canopy height is 23 m.

Samples were taken at 1 m, 14 m, 23 m and 125 m height using already existing sampling lines.
The measured PAR and air temperature on the moments of sampling, are showed in figure 6.

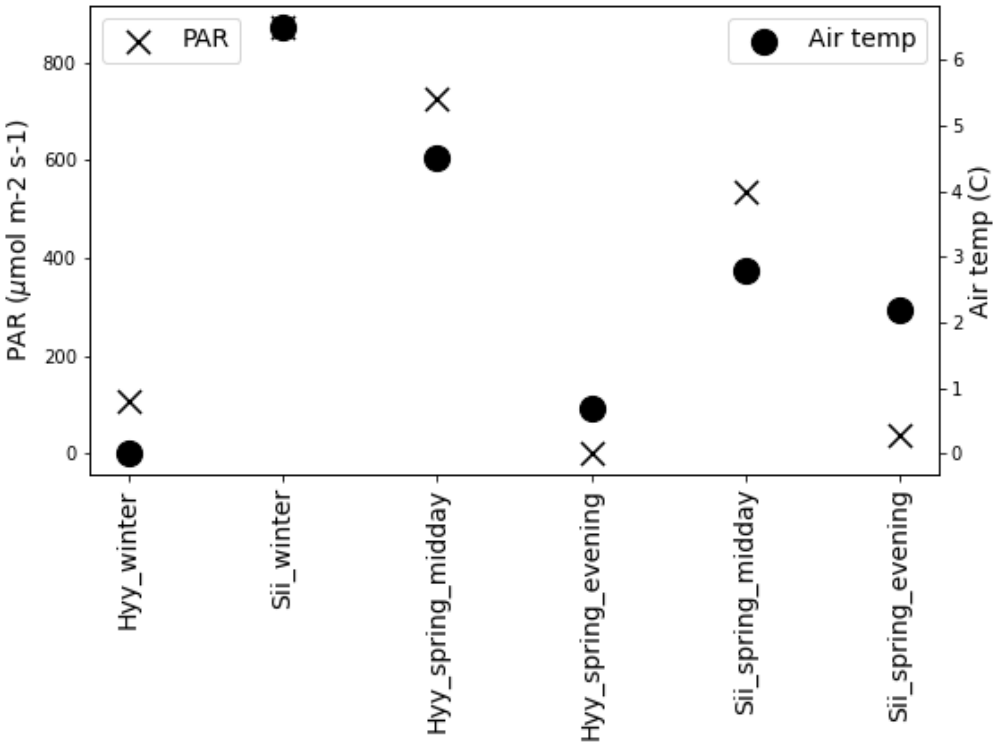

Fig. 6. PAR fluxes and air temperature measured by smartSMEAR (Aalto et al. 2019) on the moments of sampling.

The EC Flux data derives from the same site as the samples are taken.

4.1.2 Sampling site - Siikaneva wetland

The wetland samples and EC flux data have been taken on the Siikaneva fen. This is a minerotrophoc (nutrient rich) wetland located close to Hyytiälä (SMEAR II) ($61°50'N, 24°12'E, 162m$ ASL). The vegetation is dominated by peat mosses (Sphagnum spp. with S. papillosum. as main specie), Sedges and Rannochrush and the topography is flat.

This fen is homogeneous and extends around 100 m towards the east and west and 200 m to the north and south (Rinne et al. 2018). The air samples are taken approximately 1 m above the surface. We also took one winter sample below the surface, at 10 cm depth in the soil. Since the soil is expected to be anoxic at this depth and thus be a COS source, while it is oxic and a COS sink above surface, we wanted to try to identify this difference also in the isotopic signature of COS. As the sampling lines down in the soil layer contain little more than 2 L and we need double to detect isotopic signatures, one flask is filled twice with 30 hours in between to let air in the sampling line restore.

The winter samples have been taken on 16 March 2022 around 11 am with sun and snow cover and 17 March 2022 around 17:30 pm.

Since during the analysis of the EC flux data we identified a strong correlation between the COS and PAR fluxes, we decided to take the spring samples in light and dark circumstances to see if differences among the isotopic signatures also exist. These spring samples are taken on 27 April around 8 pm and 28 April around 1 pm with no snow but very wet conditions. The relevant meteorological circumstances are plotted in figure 6.

Figure 7 shows both sample sites. We like to stress the sampling sites are located nearby each other, within a distance of around 5 km.

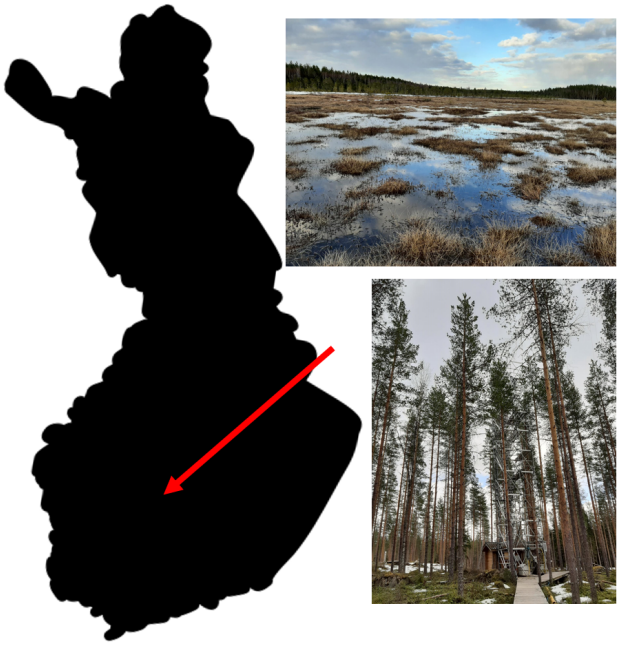

Fig. 7. Map of Finland with the red arrow indicating the sampling sites

4.2 GC-IRMS measurements and data analysis

4.2.1 GC-IRMS

To determine the isotopic composition of COS we use the CF GC-IRMS developed at the Institute for Marine and Atmospheric research Utrecht (IMAU) by Baartman et al. 2021.

The air is pre-concentrated by firstly entering a 12-port dead-end multi-position valve (Fig. 8) and then passing trough the mass flow controller (MFC). Next the air passes the magnesium perchlorate dryer, where the water is bounded to the magnesium perchlorate such that the air samples are not perturbed. Afterwards, the sample enters the two 6 port valves followed by a Tenax TA trap of $-72°C$ where the COS is trapped. Once all the gas is injected, the Tenax is heated to $130°C$ and transported by a helium carrier gas trough a 6-port valve towards the cryo-focus trap with a temperature of $-196°C$. Next, it enters the GC column to be separated from the other gases in the sampled air.

Finally the COS enters the Nafion dryer, a ConFlo interface and the IRMS where ionization and fragmentation into the sulfur ions $^{32}S^{+}$, $^{33}S^{+}$, $^{34}S^{+}$ and carbon monoxide ion CO^{+} occurs (Fig. 8) (Baartman et al. 2021). As working gas for the sulfur isotopes we inject O_2 into the IRMS as it contains all three isotope masses needed (32, 33 and 34 m/z) and is not toxic while COS is at the needed concentrations. The used working gas for the carbon isotope is CO_2. To calibrate the δ^{33}S and δ^{34}S values, both the samples as the reference measurements (calibrated against the international standard Vienna Canyon Diablo Troilite (VCDT)) are measured against the working gas. In this way we can compare our sulfur signatures with the VCDT calibration.

Note that δ^{13}C is not calibrated in this report. The calibration would however occur against the Vienna Pee Dee Belemnite (VPDB) standard rather than the VCDT. Further details about the used pre-concentrated GC-IRMS can be found in the paper of Baartman et al. 2021.

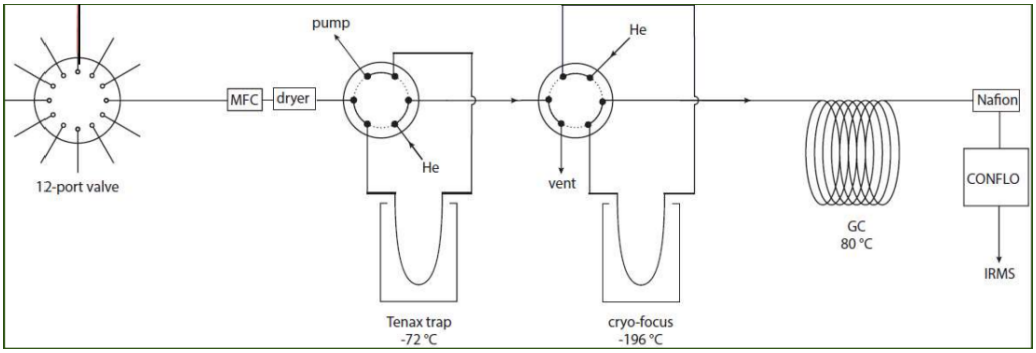

Fig. 8. Schematic overview of the used gas chromatography - isotope ratio mass spectrometer (Baartman et al. 2021)

Every measurement day started with a 3 L reference measurement and ended with a 3L reference - followed by a 3 L zero-air measurement. This to be able to make black corrections and to keep track of the possible occurring memory effect within the machine.

The Mass flow was 80 mL/min for the reference - and zero-air measurements. The samples ware measured with a flow of 50 mL/min and an injection time of 3 hours to obtain an as big as possible peak area. The Siikaneva winter sample had an injection time of 2,5 hours.

4.2.2 Isotope data analysis

For the analysis of the measured samples we used the MatLab R2020b code provided by Sophie Baartman. The injected volume in mL was calculated by multiplying the flow rate in mL/sec which is reported every 9 seconds, with 0.15.The retention time of COS was around 690 seconds.

We compared the reference and zero-air measurements with other reference and zero-air measurements and filtered out measurements that were not trustful.

For the winter samples we interpolated the samples using the reference measurements right before and after each sample. While for the early spring samples we identified a drift downwards in the results when measurements were taken one after the other. Therefore, we computed the moving mean trough the reference measurements and used these means as reference values. Nevertheless, some drift remained visible. So we marked the data points that were affected by this drift.

Moreover, we started the integration of the IRMS peak at 650 s and ended it when the slope of the peak was 17 mV/s.

Lastly, we identified outliers, datapoints that were very different than the others, and marked them in our results.

As explained in Baartman et al. 2021, the internal error on the δ values is calculated using equation 14

$$\sigma = \sqrt{\sigma_{reprod}^2 + \sigma_{nonlin}^2} \tag{14}$$

where σ_{reprod} is the reproducibility error and σ_{nonlin} is the error from the non linearity correction. This internal error represents how the measurement relates to the internal lab scale at IMAU.

Backward trajectory analysis using the NOAA HYSPLIT model (Stein et al. 2015, Rolph, Stein, and Stunder 2017) is conducted to gain information about the provenance of the ambient COS at our sampling place. The analysis went 4 days backwards with a new trajectory calculation every 4 hours, for a maximum of 6 trajectories. The trajectories for Hyytiälä are modeled 125 m above ground level (306 m ASL) while for Siikaneva 1 m above ground level (163 m ASL).

The fits on the isotope plots are done using the explicit orthogonal distance regression (ODR) method in python. This allows us to take into account the errors on the data set and make a fit without the influence of previous data points.

4.3 EC measurements and data analysis

4.3.1 EC measurements

The Hyytiälä EC flux data used in this study, was measured with an ultrasonic anemometer which measured wind components from three directions at 23 m height. COS, CO_2, water vapor (H_2O) and carbon monoxide (CO) mole fractions where measured with an Aerodyne quantum cascade laser spectrometer. Both measured with a frequency of 10 Hz and the fluxes were averaged over 30 minutes. The measurement period was from April 2020 till May 2021. More details on the equipment can be found in Vesala et al. 2022.

The Siikaneva EC flux data was also measured with an Aerodyne quantum cascade laser spectrometer between May and September 2019. The Siikaneva and Hyytiälä data were processed by Asta Laasonen (Helsinki University).

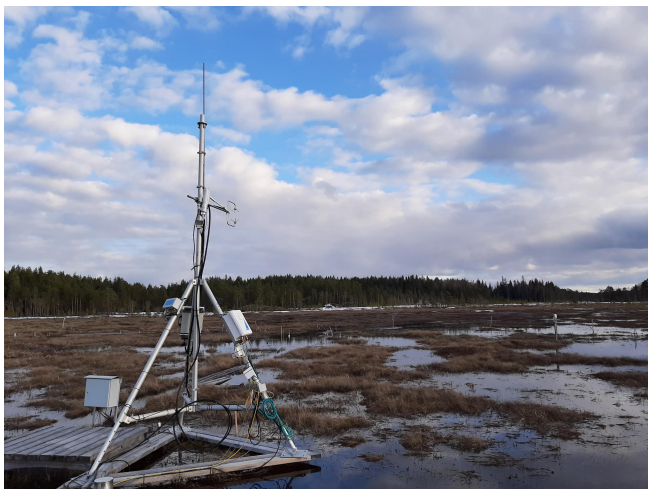

Fig. 9. Eddy Covariance measurement tower at Siikaneva

4.3.2 EC data analysis

All fluxes in the data files were filtered regarding their flag. When "flag = 2" was attributed to the data point, meaning flux stationarity (FST) larger than 1 and skewness and kurtosis criteria not met, the data point was filtered out. The skewness describes the lack of symmetry of the data set while kurtoris is a measurement for the heaviness of the tail of the data set (handbook n.d.).

Moreover, we used a 2σ threshold including only 95% of the data, assuming normal distribution. The median is chosen to be reported instead of the mean since these data sets contain many outliers and the median is more robust in this case (Leys et al. 2013). Also the 25^{th} and 75^{th} percentiles are reported.

For the Hyytiälä data file, fluxes were corrected with respect to their storage fluxes by Dr. Kukka-Maaria Kohonen.

The environmental variables taken into account for this analysis are taken from the SmartSMEAR online available database (https://smear.avaa.csc.fi, (Aalto et al. 2019).

Vapor pressure deficit (VPD) has been calculated using the air temperature and relative humidity (RH) (eq. 15).

$$VPD = e_s - e_a \tag{15}$$

where e_s is the saturation vapor pressure and e_a is the actual water vapor pressure calculated as in equation 16 and 17 (Vesala et al. 2022).

$$e_s = 0.618 \exp\left(\frac{17.27 T_a}{T_a + 237.3}\right) \tag{16}$$

$$e_a = \frac{RH e_s}{100} \tag{17}$$

5 Results

In the following section, the results from EC data analysis and isotopic signature measurements are reported following the same structure as the research questions (section 2.1).

5.1 Is Hyytiälä boreal forest a *COS* source or sink and how does this differ among seasons?

Figure 10 shows the daily median *COS* flux from April 2020 till May 2021. Hyytiälä boreal forest behaves as a *COS* sink from April till November and some days in December. In early March the *COS* fluxes fluctuate around zero while between March and April the forest seems to emits *COS* and returns into a sink from April onwards. Towards spring/summer the uptake strength increases while it decreases towards winter.

The median *COS* flux on seasonal time scale (median taken over the whole day and consequently over all the day-medians) is -8.26 pmol $m^{-2}s^{-1}$ with a 25%-75% range between -15.7 and -2.84 pmol $m^{-2}s^{-1}$.

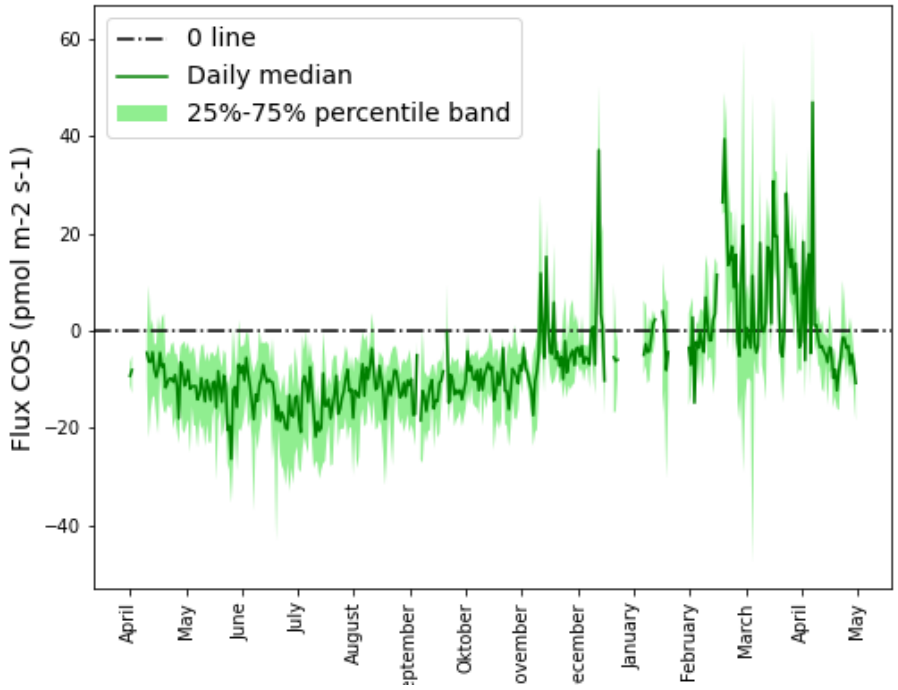

Fig. 10. Daily median *COS* fluxes from April 2020 till May 2021 with 25 and 75 percentiles. *COS* source reported as positive flux and *COS* sink reported as negative flux.

The median *COS* flux on diurnal time scale (fig. 11) is -8.23 pmol $m^{-2}s^{-1}$ with a 25%-75% range between -16.1 and 0.72 pmol $m^{-2}s^{-1}$. Due to change in averaging, these values differ from the previous ones but both indicate that Hyytiälä boreal forest is a *COS* sink in the studied period. When taking into account only the growing season, defined from May till October 2020, the sink strength is larger with a median of -12.4 pmol $m^{-2}s^{-1}$ and a 25%-75% range between -19.9 and -5.91 pmol $m^{-2}s^{-1}$.

Figure 11 shows that nighttime *COS* fluxes are nonzero.

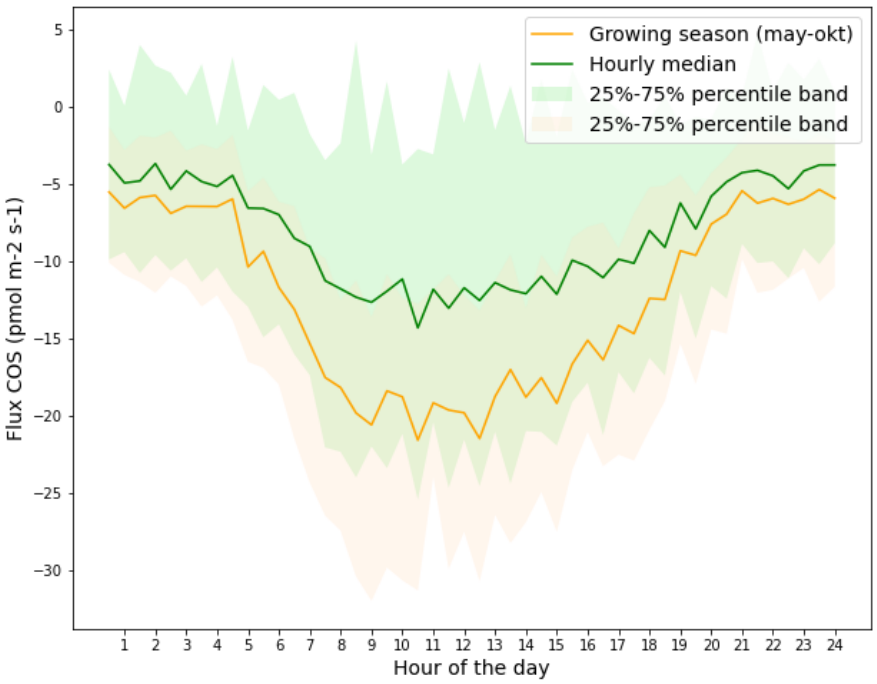

Fig. 11. Diurnal cycle COS flux with 25 and 75 percentiles. Median over whole data set in green and hourly median of growing season (May-Oct) in orange.

The daily COS fluxes, correlate well with PAR fluxes as found by Vesala et al. 2022 due to the stomatal aperture/closure driven by PAR (Kooijmans et al. 2017) (tbl. 2). However, since the hydrolisation of COS is light independent, in contrast to photosynthesis, the correlation between CO_2 fluxes and PAR is higher. Other relevant parameters, next to the COS (FCOS) and CO_2 fluxes (FCO2) are RH, precipitation (prec) and air temperature (Tair). However, these meteorological components have little correlation with FCOS.

	FCOS	FCO2
FCOS	1.00	0.87
FCO2	0.87	1.00
PAR	-0.85	-0.99
RH	0.44	0.69
prec	-0.10	-0.19
Tair	-0.42	-0.67

Tab. 2. Correlation of diurnal cycle of COS flux, CO_2 flux, PAR, RH, precipitation ($prec$) and air-temperature ($Tair$). Source reported as positive and sink reported as negative.

5.2 What is the isotopic composition of COS at different heights in Hyytiälä boreal forest during winter/spring?

Figure 12 shows an example of the chromatograph resulting for the Hyytiälä winter 23 m air sample measurements and is a good representation of all chromatographs we produced. The first three blocks (fig. 12 a.) result from the working gas, O_2. This is likely followed by a O_2^+ signal from CO_2 that remained after the trapping phase in the Tenax. The next peak with a retention time around 695 s is the COS peak. In fig. 12 b. it is visible that the 33 m/z and 34 m/z signals have larger amplitude than the 32 m/z due to their higher resistors. The final peaks in fig. 12a. are probably due to organic compounds (Baartman et al. 2021).

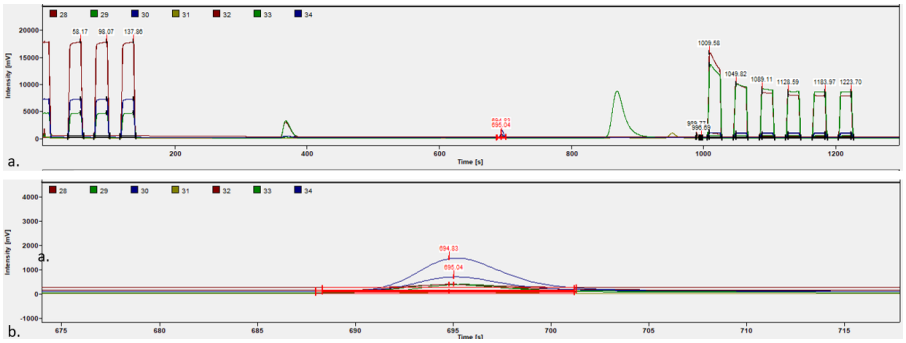

Fig. 12. Full chromatogram of the Hyytiälä 23 m winter sample in a. and a closer look to the *COS* peak in b.

From this and similar chromatographs we derived the isotopic signatures plotted in figure 13. The δ values reported, are calculated with equations 4, 5 and 14. A table with all results can be found in the appendix 3.

In winter the mean *COS* isotopic composition is for δ^{34}S 13.79 $\pm$ 1.05 ‰ , for δ^{33}S 3.79 $\pm$ 2.61 ‰ and for δ^{13}C 3.78 $\pm$ 2.14 ‰. The mean mixing ratio in winter is 474.51 $\pm$ 15 ppt.

In spring the mean *COS* isotopic composition is for δ^{34}S 10.91 $\pm$ 0.90 ‰ , for δ^{33}S 0.11 $\pm$ 2.49 ‰ and for δ^{13}C 14.00 $\pm$ 2.14 ‰. The mean mixing ratio in spring is 530 $\pm$ 15 ppt.

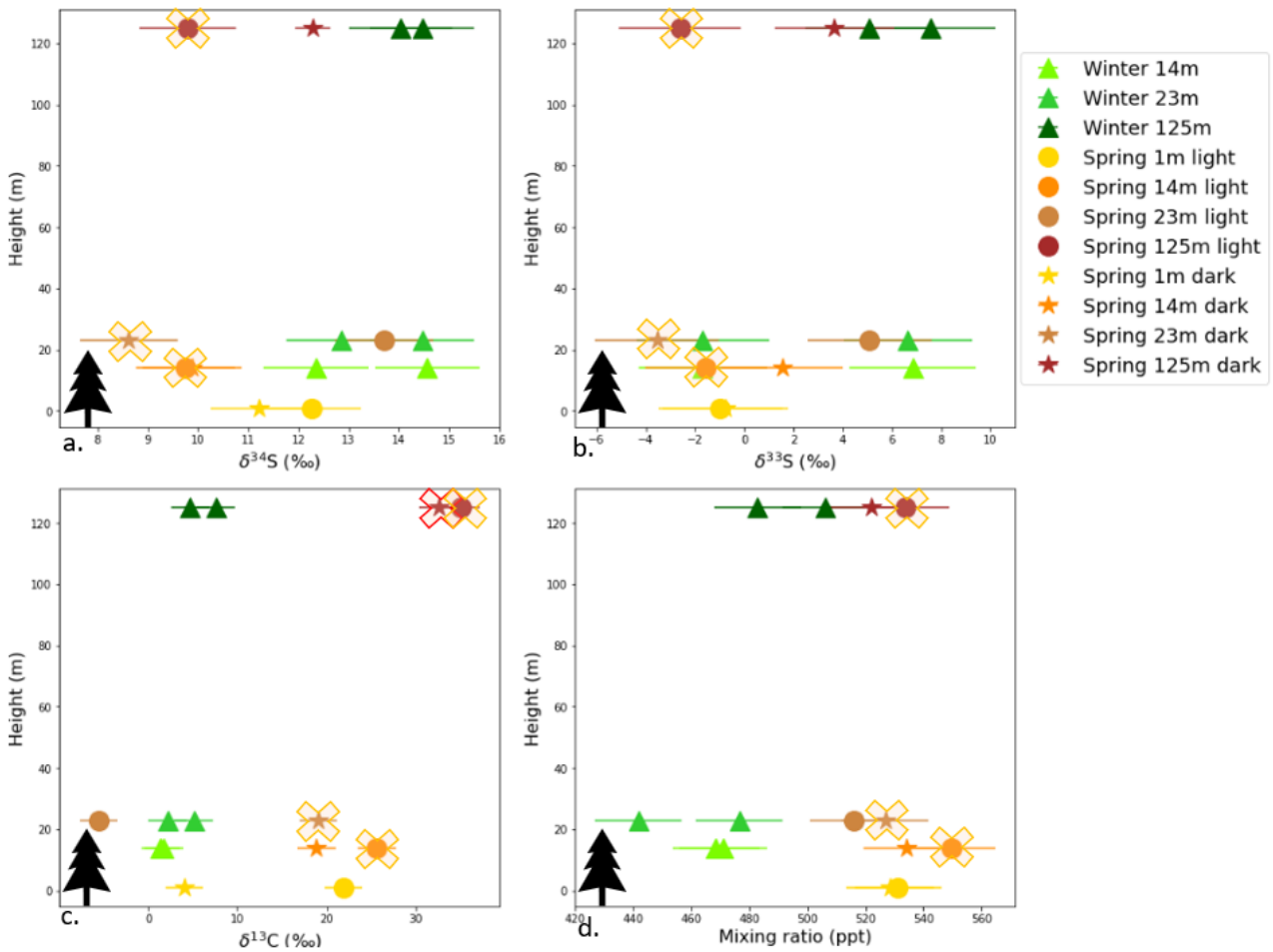

Fig. 13. GC-IRMS results of air samples with a. δ^{34}S, b.δ^{33}S, c. δ^{13}C and d. mixing ratio against the sampled height. Tree pictogram indicating the height of the trees in the forest. Green indicates the winter forest samples and orange the spring forest samples. Orange crosses on the drifted values and red cross on the outlier.

No significant difference is seen among the heights in the canopy layer for the winter samples. The spring samples, however, do show different behaviours. From fig. 13 a. we see that within the canopy (1 m, 14 m, 23 m) the samples become more enriched in δ^{34}S when going down towards the ground, with the exception of the 23 m light sample which is more enriched in δ^{34}S. For δ^{33}S we see similar but statistically less significant result. Even less or not significant is the similar result for δ^{13}C which however, has the 23 m light sample which is, in contrast to the above mentioned isotopic signatures, less enriched. No significant difference in height is visible for the mixing ratio (fig 13 d).

Besides the differences found among the vertical between winter and spring samples, the spring samples show lower δ^{34}S and δ^{33}S at 125 m with respect to the winter samples (fig. 13 a, b). The opposite occurs for the δ^{13}C and the mixing ratio (fig. 13 c, d). The samples within the canopy are less enriched than the winter samples for δ^{34}S with the exception of the 23 m light sample. This difference is less pronounced for δ^{33}S and opposite for δ^{13}C and the mixing ratio. Also, when looking at the mean for all the winter samples and spring samples at the forest (Appendix table 3), we see that the δ^{34}S and δ^{33}S are higher in winter than in spring and the opposite occurs for the δ^{13}C and mixing ratio values.

The spring samples are taken with high and low PAR fluxes, denoted in figure 13 with light and dark respectively. At 23 m we see both for δ^{34}S and δ^{33}S that the light sample is enriched in the heavier isotope with respect to the dark sample (13 a,b). For δ^{13}C the opposite occurs, higher isotopic values result from the dark sample rather than the light sample (13 c). Also the mixing ratio shows slightly higher values under dark

than light circumstances. At 125 m height, the dark samples seem more enriched in δ^{34}S and δ^{33}S.

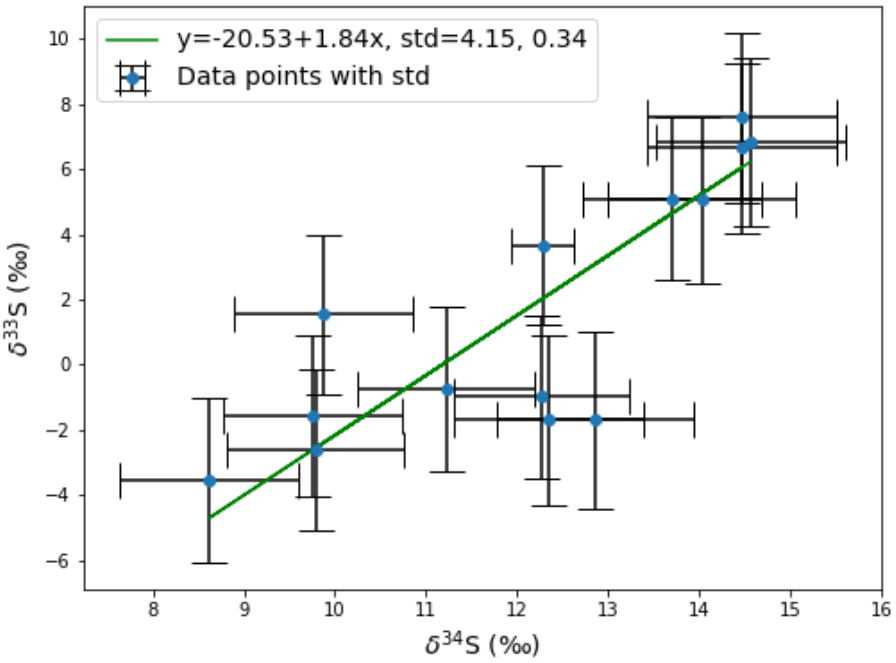

Fig. 14. δ^{34}S plotted against δ^{33}S for all samples without outliers results and explicit orthogonal distance regression fit.

When filtering out all outliers (indicated with an red cross in fig 13 and in orange in the Appendix 3) we are able to compute a 'three-isotope plot' (fig. 14) to visualize if mass dependent fractionation (MDF) took place. The slope of the plot is not around a half as we would expect from MDF but is 1.84 ± 0.34. The Δ^{33}S value (the deviation of the sampled δ^{33}S from the MDF line) has a mean of -1.08 ± 3.6.

We cannot identify a trend when plotting δ^{34}S against δ^{13}C (Appendix fig. 36).

Fig. 15 shows a negative trend between the measured mixing ratio and δ^{34}S values from both the forest (green, orange) and wetland (blue, purple) site. The more *COS* is taken up, the lower the mixing ratio and the more δ^{34}S is enriched in heavier isotope.

This dependence is not clearly visible when plotting the δ^{13}C against the mixing ratio (Appendix fig. 38).

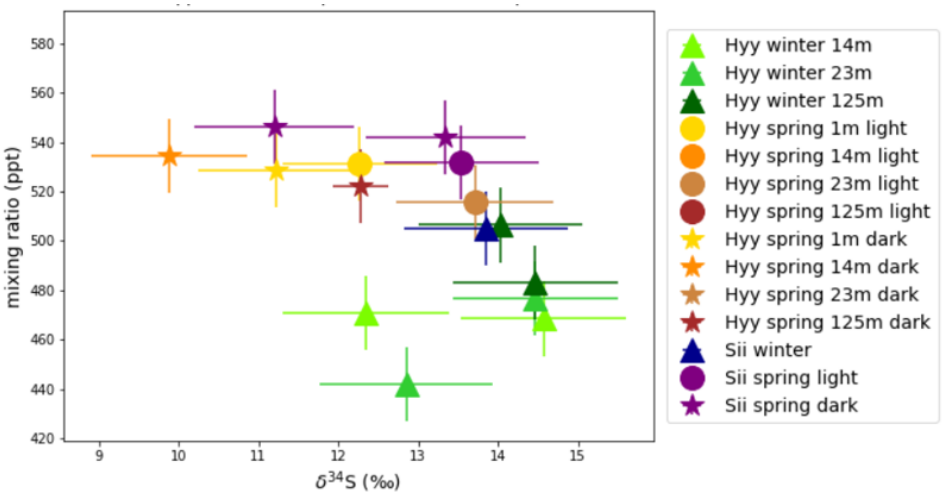

Fig. 15. δ^{34}S plotted against the mixing ratio for all COS samples. Green triangles indicates the winter forest samples, orange dots/stars the spring forest samples taken by high/low PAR values, blue triangles the wetland winter sample and purple dots/stars the spring wetland samples taken by high/low PAR values. Drifted samples and outliers are excluded.

5.3 Is Siikaneva wetland a COS source or sink and how does this differ among seasons?

Figure 16 shows that Siikaneva wetland is a COS sink for the analyzed period (May-September 2019). The median COS flux on seasonal time scale is -9.15 pmol $m^{-2}s^{-1}$, with a 25%-75% percentile range between -16.2 and -4.42 pmol $m^{-2}s^{-1}$.

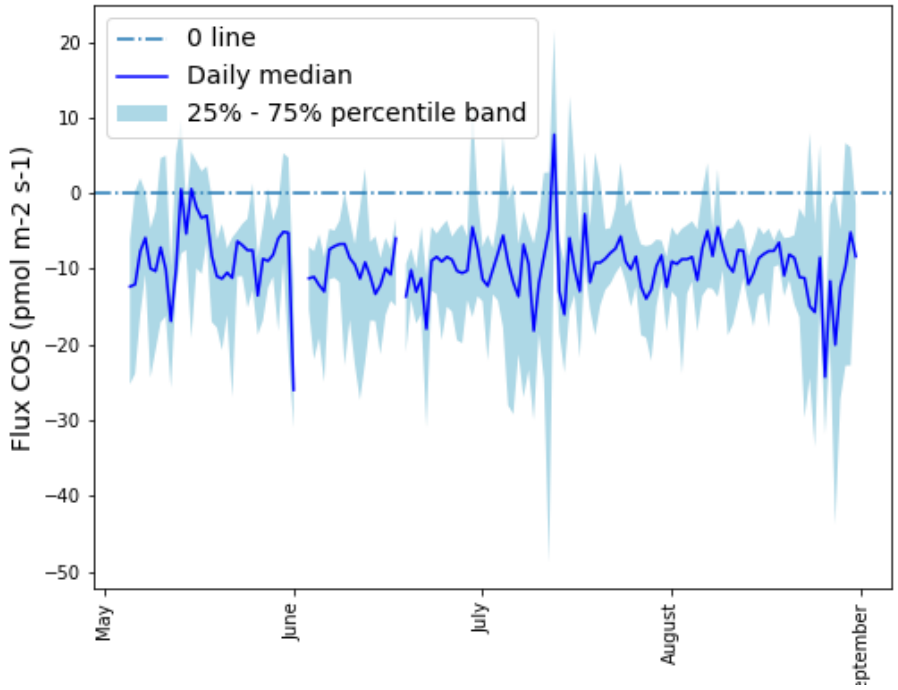

Fig. 16. Daily median *COS* fluxes from May till September 2019 with 25 and 75 percentiles. The median is computed for each day and plotted against the analyzed days. *COS* source reported as positive flux and *COS* sink reported as negative flux.

Despite the stability of the sink, we identified a diurnal cycle showing net *COS* uptake (fig. 17). The median *COS* flux on diurnal time scale is -10.0 pmol $m^{-2}s^{-1}$, with a 25%-75% percentile range between -16.5 and -4.16 pmol $m^{-2}s^{-1}$.

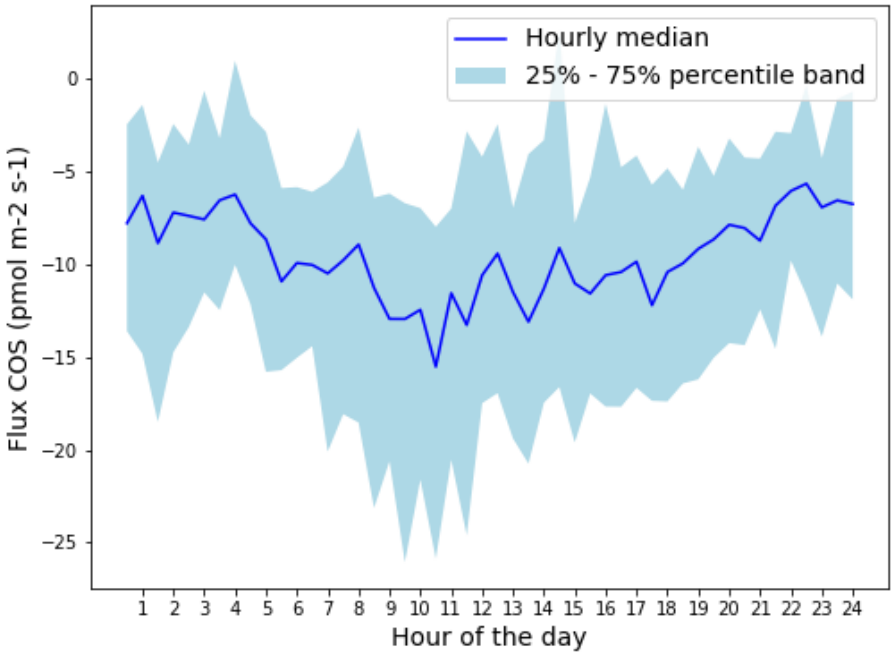

Fig. 17. Diurnal cycle *COS* flux with 25 and 75 percentiles. The median is computed over all the same hours in the analyzed days.

The median *COS* flux over the daily cycle is for May, June, July, August and September respectively; -8.16 pmol $m^{-2}s^{-1}$, -11.32 pmol $m^{-2}s^{-1}$, -9.18 pmol $m^{-2}s^{-1}$, -8.73 pmol m-2 s-1, -10.3 pmol $m^{-2}s^{-1}$. These values suggest a strengthening of the *COS* uptake which is disturbed in July, August.

Secondly, we analyzed the magnitude of the daily cycle found in the flux data. Nighttime/daytime fluxes were calculated using a threshold for *PAR* fluxes lower than 10% /higher than 60% of maximum *PAR* flux respectively. Next, the mean of both nighttime and daytime fluxes is calculated to derive the difference; the magnitude of the daily cycle. This amplitude is 4.4 ± 2.0 pmol $m^{-2}s^{-1}$.

The magnitude is bigger (5.15 ± 11.8 pmol $m^{-2}s^{-1}$) when calculated on the whole data set instead of the daily cycle. The maximum PAR level is computed for each day and the 10% (night) and 60% (day) thresholds are calculated for each day. Next, the night- and day *COS* fluxes are selected for each day and the magnitude is calculated.

Lastly, we binned the whole data set against the environmental parameters PAR, VPD, air temperature (air temp) and water table depth (WTD) to identify meteorological drivers (fig. 18). The choice of these specific parameters was done after computing a correlation matrix with many variables to select promising parameters that did not cross correlate (Appendix fig. 32). Also no correlation was found between the leaf area index and *COS* fluxes (Appendix fig. 33).

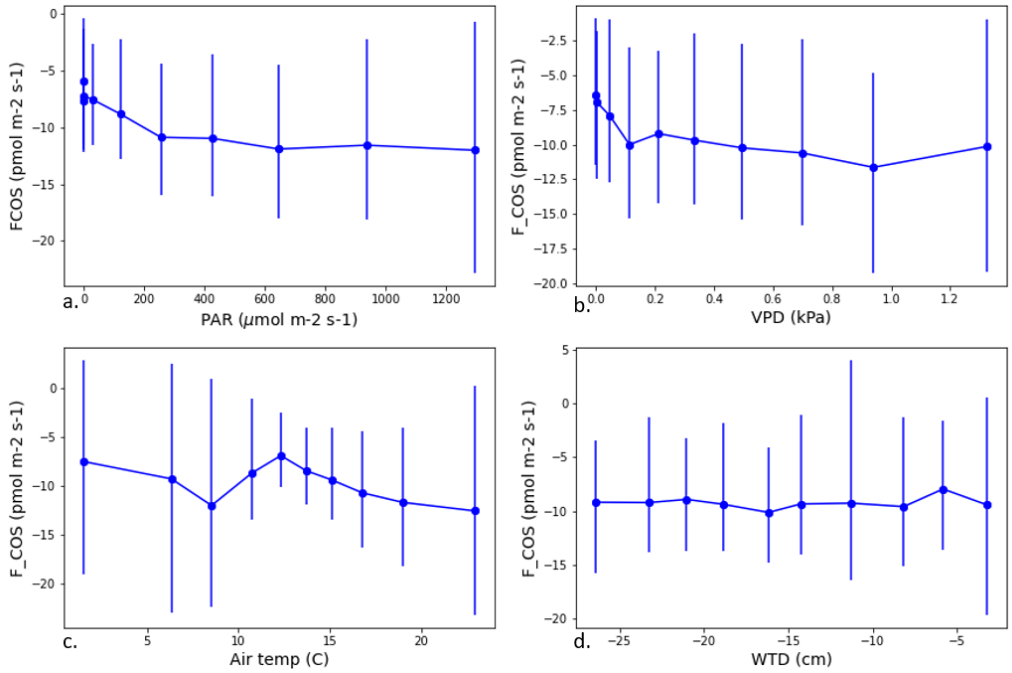

Fig. 18. *COS* **flux relationship with meteorological variables.** Data is collected in 10 equally sized binns. Errorbars represent 25 and 75 percentiles.

From fig. 18a. we see negative correlation (R=-0.89) between PAR levels from 10 to 600 μmol $m^{-2}s^{-1}$ and *COS* fluxes. This is verified in figure 41 in the Appendix. For increasing PAR values, an equilibrium is found around a *COS* flux of -11.7 pmol $m^{-2}s^{-1}$ with a 25%-75% percentile range between -20.9 and -3.19 pmol $m^{-2}s^{-1}$.

Negative correlation (R = -0.61) is also found between *COS* fluxes and low VPD levels (fig. 18b.). However, when VPD reaches levels of 0.2 kPa, the *COS* flux tend to saturate (Appendix fig. 42). At VPD levels higher than 1 kPa the *COS* sink strength decreases again. The correlation between PAR and VPD is 0.668, suggesting cross-correlation.

Figure 18c. shows a strengthening of the *COS* sink with increasing temperatures. However, a weakening of *COS* uptake is seen between air temperatures of 9 and 13 C° (R=0.83) (Appendix fig. 43).

Lastly, the *COS* flux seems stable under changing WTD conditions (fig. 18d.).

Figure 19 show a parametrization of the *COS* fluxes using PAR fluxes as stated in the hyperbola equation (eq. 18) (Vesala et al. 2022). To fit the parameters, the python non-linear least squares function '*scipy.optimize.curve_fit*' has been used. The fitted values with their standard deviations are; a = -5.97 ± 0.718, b = 183 ± 84.6, c = -6.89 ± 0.326.

$$FPAR = (\frac{a * PAR}{PAR + b}) + c \tag{18}$$

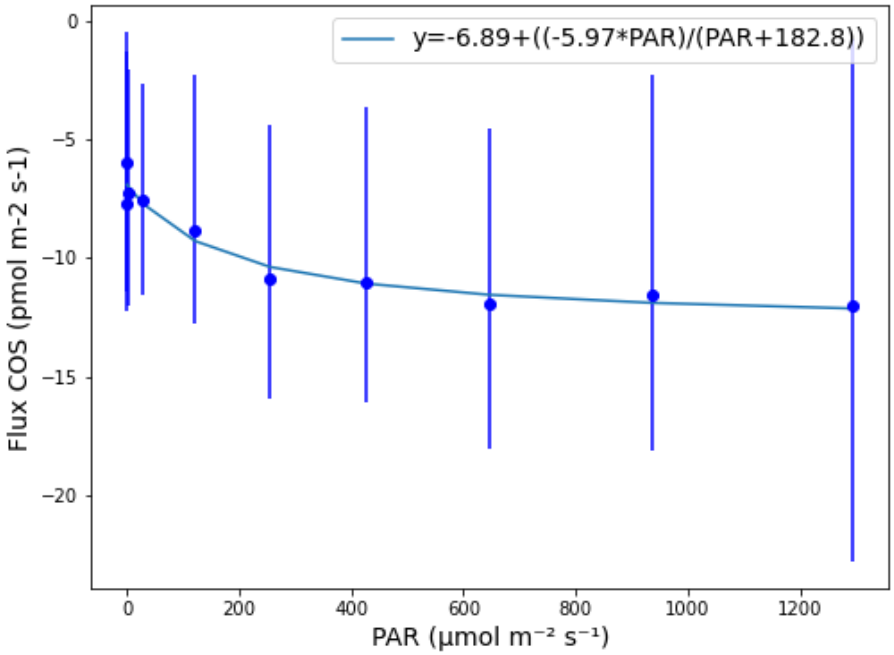

Fig. 19. *COS* **flux and fit using equation 18 against PAR values.** Data is collected in 10 equally sized binns. Errorbars represent 25 and 75 percentiles.

The parameterization suggests that when *PAR* fluxes go towards infinity, the *COS* fluxes tend saturate towards a + c = -12.86 ± 0.789 $m^{-2}s^{-1}$. This parametrization is able to reproduce the daily cycle of observed *COS* fluxes with a correlation of 0.857 (fig. 20). The fit on seasonal time scale is shown in figure 21.

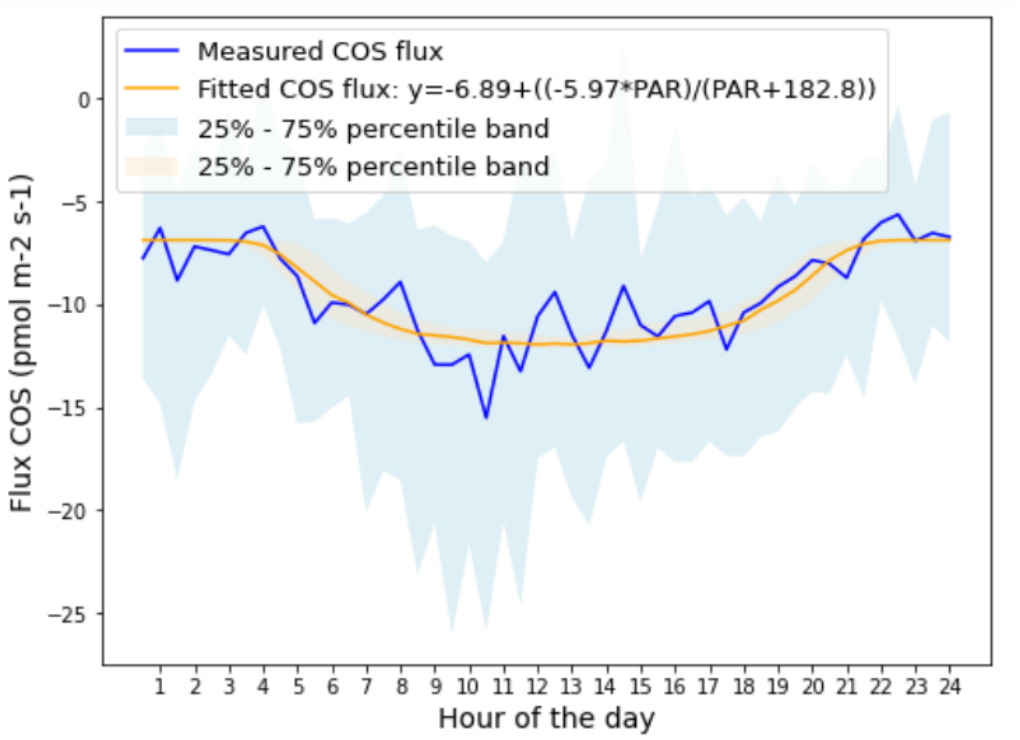

Fig. 20. Diurnal cycle COS flux and fit using equation 18 with 25 and 75 percentiles.

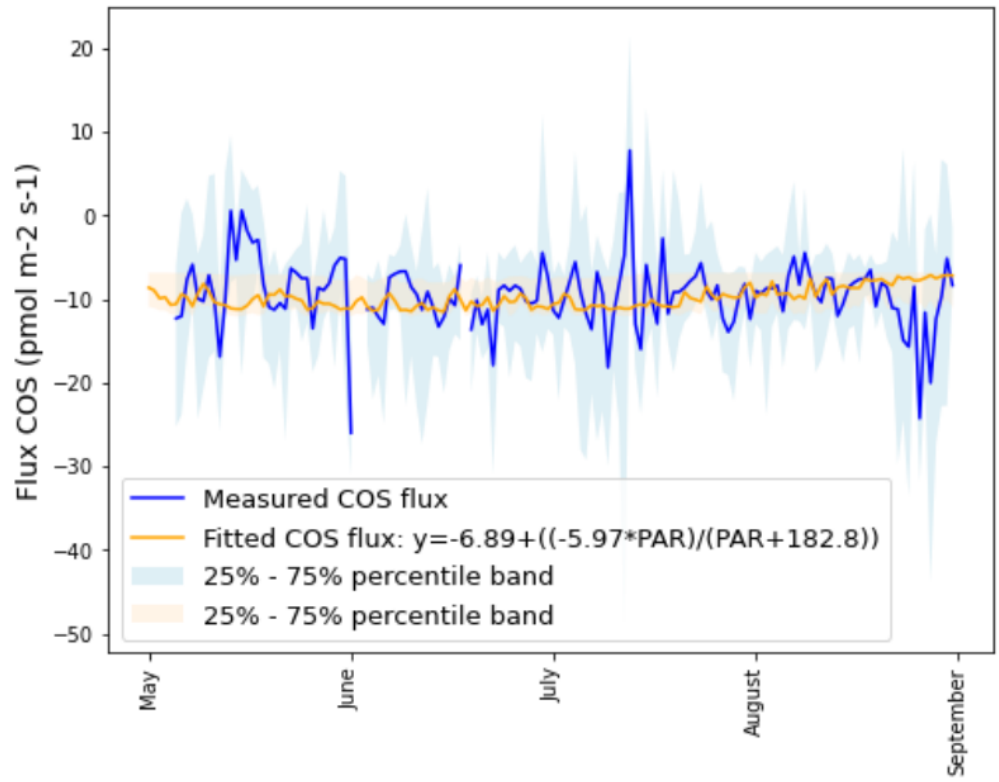

Fig. 21. Daily median COS fluxes and fit using equation 18 with 25 and 75 percentiles.

5.4 What is the isotopic composition of *COS* at Siikaneva wetland during winter/spring?

All results can be found in table 3 in the Appendix.

The winter sample below ground, at 10 cm depth, contained too little *COS* to measure the isotopic signature. The winter sample above ground has a δ^{34}S value of 13.85 ± 1.03 ‰, a δ^{33}S value of 12.58 ± 2.56 ‰ and a δ^{13}C value of 3.32 ± 2.14 ‰. The measured mixing ratio is 504.83 ± 15 ppt.

The mean of the spring samples is 12.50 ± 0.83 ‰ for δ^{34}S, -7.60 ± 2.52 ‰ for δ^{33}S and 23.27 ± 2.14 ‰ for δ^{13}C. The mean mixing ratio in spring is 540.02 ± 15 ppt.

When analysing the spring samples we see that two samples are significantly less enriched in δ^{34}S and all are less enriched in δ^{33}S than the winter sample. Also, when comparing the winter sample with the mean of the spring samples, the values of δ^{34}S (12.50 ± 0.83 ‰) and δ^{33}S (-7.60 ± 2.52 ‰) are less enriched in spring than in winter (δ^{34}S: 13.85 ± 1.03 ‰ and δ^{33}S: 5.58 ± 2.56 ‰).

Unfortunately, most of the δ^{13}C results are identified as outliers. And no uniform difference is seen between high and low *PAR* levels. Nonetheless, the wetland values fit well together with the forest values when plotting δ^{34}S against the mixing ratio (fig. 15).

Lastly, the mixing ratios found in early spring with a mean of 540 ± 15 ppt are higher than the mixing ratio found in winter (504.83 ± 15 ppt).

5.5 How do EC *COS* flux measurements of Hyytiälä boreal forest and Siikaneva wetland compare/differ?

Figure 22 shows the seasonality for the median *COS* fluxes measured between May and September as these months overlap in both data files. For Hyytiälä the data is from 2020 while for Siikaneva the data is from 2019.

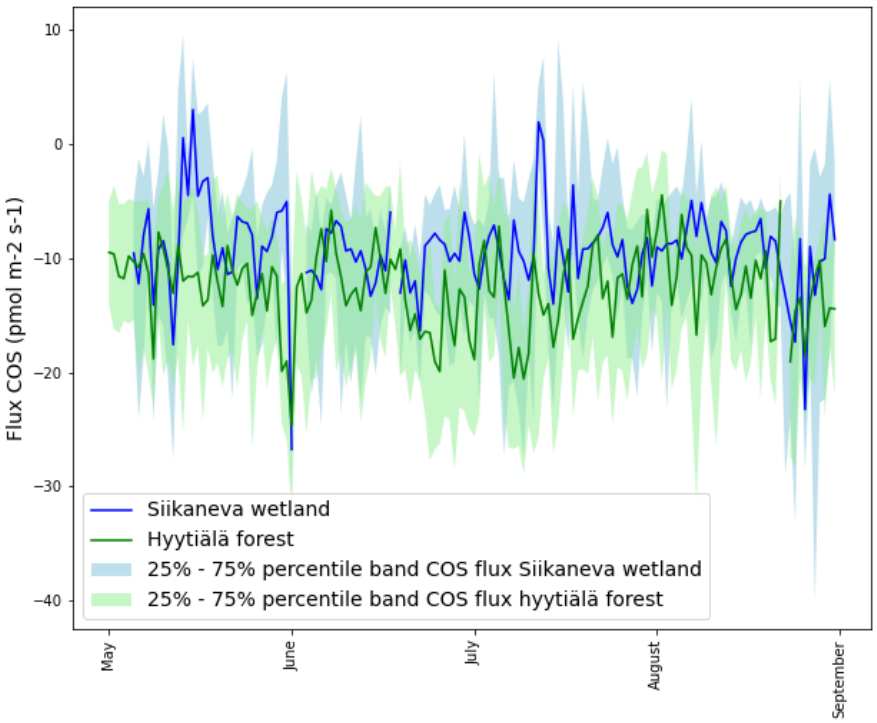

Fig. 22. Daily median *COS* fluxes for Siikaneva wetland and Hyytiälä forest with 25 and 75 percentiles.

When comparing these two data sets the difference in median COS flux is 3.23 $\pm$ 5.13 pmol $m^{-2}s^{-1}$. While the difference in daily cycle fluxes is more pronounced as shown in figure 23.

Between 21h and 5h (nighttime) the magnitude of the fluxes is similar. Where as during day, the difference between COS uptake in both ecosystems becomes visible. The forest is a larger COS sink than the wetland with a difference in maxima (taken as average between 8h and 16h) of 7.74 $\pm$ 2.08 pmol $m^{-2}s^{-1}$ or a factor Sii:Hyy of 1.68 $\pm$ 0.0860. (error calculation example in Appendix section 8.2).

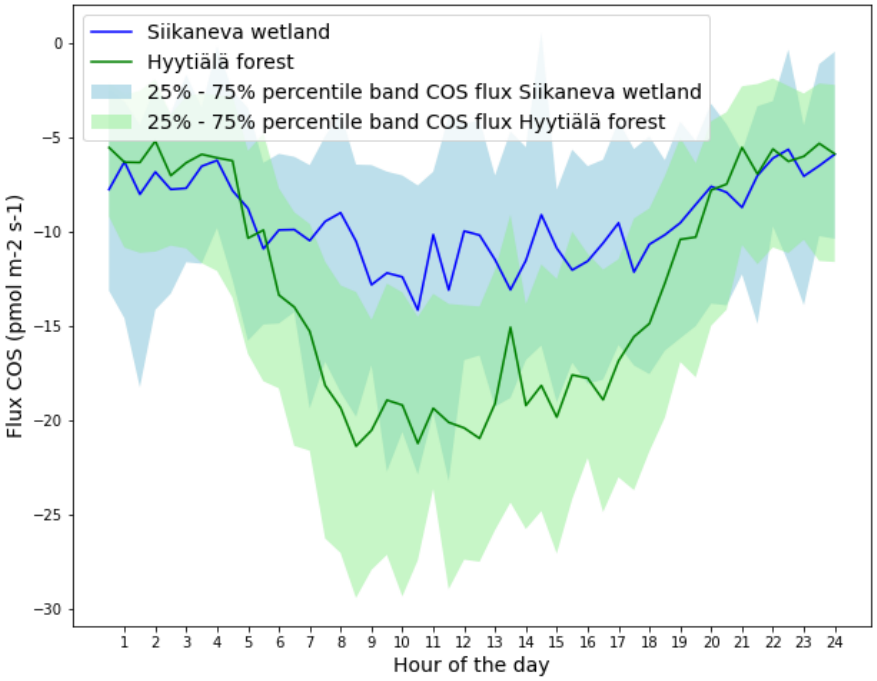

Fig. 23. Daily cycle COS flux for Siikaneva wetland (blue) and Hyytiälä forest (green) with 25 and 75 percentiles.

Furthermore we compared the GPP data of both ecosystems with the computed GPP using equation 2 (fig. 24). We used a leaf-scale relative uptake ratio (LRU) value for Hyytiälä of 1.6 as this is most frequently found in literature (Whelan and Rhew 2016, Kooijmans et al. 2019). For Siikaneva we fitted the LRU minimizing the root mean square error using Python 3.8 which resulted in a LRU value of 0.966. The offset needed to match the GPP calculated with COS fluxes with the GPP data derived from the CO_2 flux (smartSMEAR Aalto et al. 2019), was fitted afterwards for both ecosystems with a non-linear least squares algorithm.

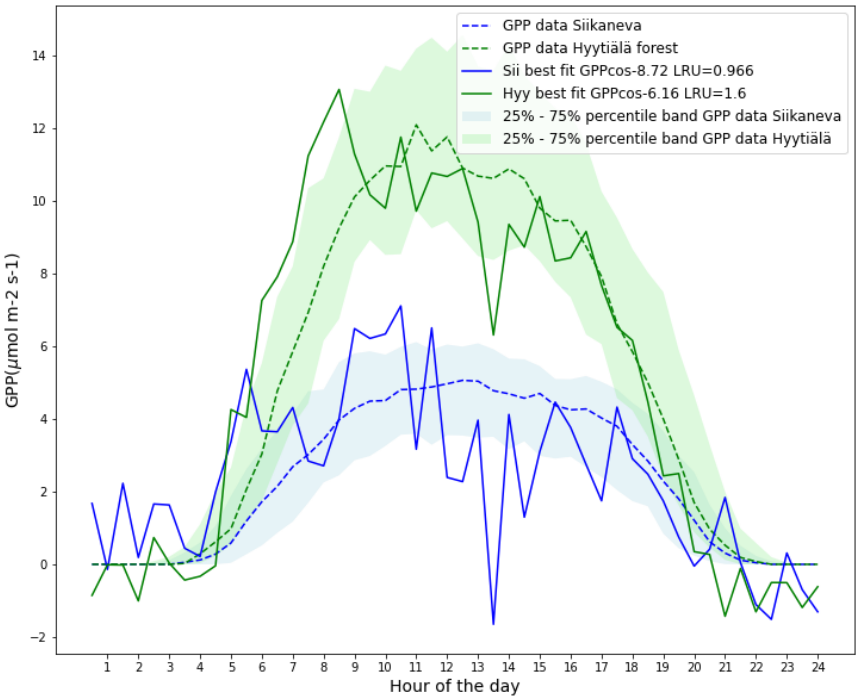

Fig. 24. Daily cycle GPP. Siikaneva GPP in blue, Hyytiälä GPP in green. Fitted GPP using COS fluxes represented with straight lines. GPP data with dotted lines with 25 and 75 percentiles.

5.6 How do isotopic signatures of COS measured at Hyytiälä boreal forest and Siikaneva wetland compare/differ?

For the winter samples we see that the air measured at 125 m in the forest is similar to the sample taken at the wetland (around 14 ‰for δ^{34}S, 6 ‰for δ^{33}S and 5 ‰for δ^{13}C) with exception of the mixing ratio which is higher at the wetland, although considering the uncertainties, statistically not significant (504.83 ± 15 ppt at the wetland against 474.51 ± 15 ppt in the forest).

The mixing ratio at the wetland (540.02 ± 15 ppt) is also slightly, but not significantly higher than the forest mixing ratio in spring (530.32 ± 15 ppt).

Lastly, when excluding outliers and drifted measurements, the spring samples have similar δ^{34}S values (also shown in fig. 15), lower δ^{33}S and similar δ^{13}C values on the wetland than in the forest.

6 Discussion

This section discusses the results following the order of the research questions (section 2.1).

6.1 Is Hyytiälä boreal forest a COS source or a sink and how does this differ among seasons?

As a general note on EC data; underestimation of the fluxes can occur at night (with low wind velocity) and during sunrise (Baldocchi 2003). Moreover, the EC method works the best over a flat terrain (Baldocchi 2003). This could affect the quality of the data in Hyytiälä where the terrain contains hills.

Nevertheless the fluxes we found, agree with the previous measured COS fluxes at Hyytiälä by Vesala et al. 2022.

The absence in the data from December till February (fig. 10) is caused by the wintertime interruption of the measurement installation. Moreover, in the following months, March-April 2021, temperatures were very low (Appendix fig. 34) and the measurement setup experienced wintertime challenges that are common after breaks in measurements. Therefore, this data could be unreliable. To understand when the COS flux data starts to be reliable, we checked that the measured fluxes were detected above the detection limit (provided by Asta Laasonen trough personal communication) and we compared the CO_2 flux data from this measurement setup with the SMEAR II station CO_2 flux measurements at 27 m height. From April onwards both CO_2 fluxes agree, meaning we can neglect data from January till March 2021.

The seasonal behaviour can be explained with seasonal air temperature and PAR fluxes (Appendix fig. 35 and fig. 34 respectively). As found by Vesala et al. 2022 and hypothesized, there is a negative correlation between PAR levels and COS fluxes (Appendix 8.3 fig. 35); when PAR levels are low (dark, winter periods), stomata tend to close leading to less COS uptake by the plants. When air temperature is low, enzyme activity is low which also leads to low COS uptake. Moreover, microbes are in dormancy at these low temperatures. Lastly, the site is covered by snow during the winter period which partly isolates the soil and mosses from interacting with COS. This however, has minor effects since gases can still diffuse trough the snow layer.
On daily time scale this negative correlation between PAR and COS fluxes is even more pronounced (R$\approx$ -0.86, fig. 2).

Nighttime fluxes are non zero as expected. COS uptake is light independent and the vegetation consists of mosses, which do not have stomata and thus can take up COS contentiously and other plants and stems which do not close stomata entirely during nighttime. So the light independent COS hydrolyzing enzyme combined with the vegetation, makes the nighttime COS uptake possible (Kooijmans et al. 2017).

6.2 What is the isotopic composition of COS at different heights in Hyytiälä boreal forest during winter/spring?

Firstly, we noticed similarity among the winter samples, suggesting no influences caused by the flasks, other sampling material or measurement settings.

The mean of the δ^{34}S values (12.16 $\pm$ 0.96 ‰) is withing the expected range of 10-14 ‰(Angert et al. 2019 Hattori, Kamezaki, and Yoshida 2020 Davidson, Amrani, and Angert 2021). The air measured in winter at 125 m representing the background, has similar values δ^{34}S value with respect to the background value found by Angert et al. 2019 (13.2 $\pm$ 0.6‰). The spring background samples have a lower mean (10.94 $\pm$ 0.9 ‰). Also the mean of all the samples has a lower δ^{34}S value (12.16 $\pm$ 0.96 ‰) than reported by Baartman et al. 2021 and Angert et al. 2019. Only based on mass dependent fractionation (MDF) we would expect to have higher isotopic values since our ecosystem should be a strong sink of COS as we have seen in the EC data analysis and is reported by Vesala et al. 2022. Nevertheless, our samples are taken in winter and early spring at low temperatures thus the uptake by vegetation is expected to be low as enzyme activity is low.

From backward trajectory we see that the air came from the south/west when we took the winter samples (fig. 25 green). This is a region in Finland and Sweden with big cities. The sampled air could have lower δ^{34}S values as it is affected by the anthropogenic emission of COS from these regions (Davidson, Amrani, and Angert 2021, Hattori, Kamezaki, and Yoshida 2020). Especially the air sampled at 125 m is most affected by this, as seen above, since this height is less influenced by other sources/sinks (e.g. vegetation).
The spring samples were taken when air came from north/west direction, passing forests and the Gulf of Bothnia. Air from the ocean could be enriched in heavier δ^{34}S isotopes (Davidson, Amrani, and Angert 2021, Hattori, Kamezaki, and Yoshida 2020) which is not what we see from our measurements. Therefore we think that the effect of the provenance of the air is little with respect to the effect of the local ecosystem.

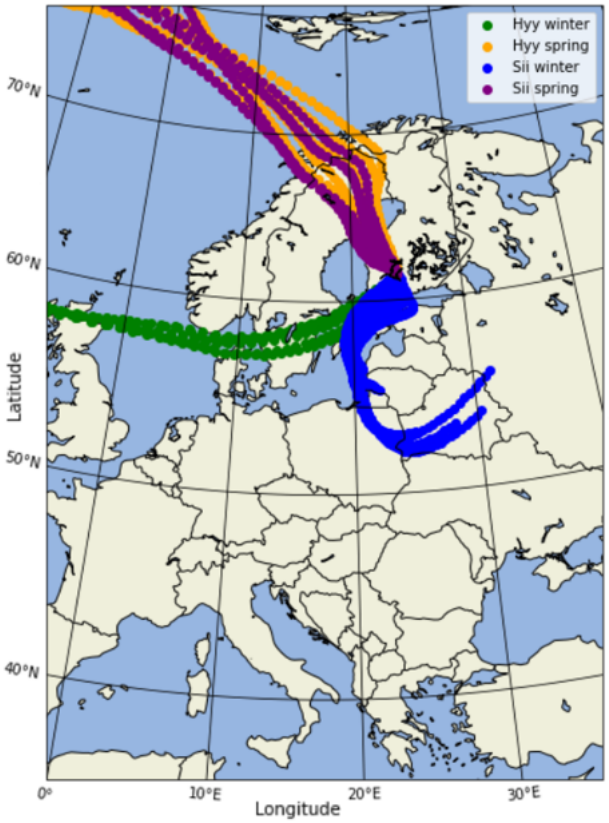

Fig. 25. Backward air parcels trajectory modeling results using HYSPLIT (Stein et al. 2015, Rolph, Stein, and Stunder 2017). Trajectories go 4 days backwards. Sampling day for Hyytiälä winter in green, Hyytiälä spring in orange, Siikaneva winter in blue and Siikaneva spring in purple.

As expected, considering the cold circumstances, the winter samples do not differ significantly among the vertical. The behaviour of the spring samples is, however, less comprehensive. The hypothesis that higher in the canopy layer the air would be more enriched due to more COS uptake and mass dependent fractionation cannot be confirmed, nor can we confirm that the difference is small/absent due to the scattered light available in the lower levels of the canopy, possible plant adaptation to lower PAR fluxes and mosses presence. The isotopic signatures give contradictory results and the data amount is too little. For example, the δ^{34}S and δ^{33}S value at 23 m light, are more enriched than the ones at 1 m, which would be expected, but in contrary, the carbon isotope is less enriched. This difference in behaviour between the sulfur and carbon isotopes can be caused by different end product of the atoms in the hydrolysis reaction (eq. 1) as hypothesized. And mostly, these results are based on only one data point per circumstance since we did not have more canisters available. More data would help clarify our results.

We also investigated the difference between isotopic signatures measured with high and low PAR fluxes. As expected, little difference is seen at 1 m, with exception of the carbon isotope. The ground vegetation consists of plants and mosses with the latter having no stomata and being able to take up COS light independently. At 23 m we see for both sulfur isotopes that during day, fractionation took place as expected as the samples are more enriched in heavier isotopes. We cannot confirm this when looking at the mixing ratio since the samples are statistically not significantly different and some are drifted.

The contradiction between the behaviours of the sulfur and carbon isotopes continues when looking at the seasonal variations. Also the hypothesis that the samples would be more enriched in spring cannot be confirmed nor rejected based on our measurements. The samples are measured in different periods because of the limited amount of canisters available to be shipped to Finland. This could have impacted the results since the GC-IRMS had some troubles right before the spring measurement sequence. These problems were not fully resolved since we identified a downward drift in the results when measuring samples right after each other. We tried

to compensate this drift using the best possible IRMS-peak integration method (section 4.2.2) but a small downward drift remained.

Moreover, the boundary layer (BL) height, deduced from diurnal cycles of air temperature and the Monin-Obukhov length, was lower and the BL was more stratified in winter than in spring (Appendix fig 39). Therefore less mixing could occur in winter, like we hypothesized for nighttime air, while in spring fresh COS could enter the measurement height. This can also help explain the lower mixing ratio found in winter with respect to spring. The trees are evergreen and, similarly to COS nighttime uptake (Kooijmans et al. 2017), winter uptake could have taken place. Some COS in the BL could thus have been taken up while no new COS was able to enter the layer due to the heavy stratification. The air that we measure in this layer can thus have lower mixing ratio than when measured in spring when new COS is allowed to enter trough mixing in the measurement layer.

When comparing the mixing ratios of the early spring samples with the mean mixing ratio derived from EC flux measurements in the same month (April) of 2020 and 2021, we see that our results are higher. The COS mixing ratio in April 2020 was 341 ppt, and in 2021 407 ppt. This difference is probably caused by the difference in measurement setup. The GC-IRMS tends to result in around 100 ppt higher mixing ratios than the EC method and the absolute accuracy of the EC method can also be low and should be interpret with caution. Unfortunately no trusted EC flux data exists for the period in which the winter samples were taken so no comparison between seasons can be made.

Another explanation of the not well distinguished results is that the forest might not behave as a net COS sink yet. When plotting the COS fluxes derived from EC method for the years 2020 and 2021 (Appendix fig. 40) we see that the forest is a sink in 2020 but with noise and a source in 2021. Also in the years 2013-2017 April shows a small or no diurnal cycle (Vesala et al. 2022). This would let us wonder if the forest was behaving as a net sink with diurnal cycle during the timing of our spring samples or not. If the forest would be both taking up and emitting COS without a distinct diurnal cycle, this explains our isotopic signature results that do not agree among each other.

Also the three-isotope plot does not show the slope we expected based on MDF literature (Hattori et al. 2015). Indeed, the $\Delta^{33}S$ value is slightly negative and most importantly has a large standard deviation suggesting high deviations in the $\delta^{33}S$ value from the MDF based expectations. This enforces our suspects about the reliability of our $\delta^{33}S$ results. Moreover, these results suggest that one cannot deduce MDF by making a three-isotope plot for samples that reflect a complex ecosystem as we hypothesized.
Besides, the plots of the sulfur isotopes against the carbon isotope (fig. 36 and Appendix 37) contain new information which we, at our stage of knowledge and taking into account our doubts about the $\delta^{33}S$ results, find hard to interpret. More measurements could help frame our results.

Lastly, to our knowledge, no information is available on the carbon isotope of COS which makes it even more difficult to interpret the results. Difference in behaviour between the carbon isotope and sulfur isotopes could be caused, as written above and in the hypothesis, by the different end product of the atoms during the hydrolysis reaction. Since these are the first results of $\delta^{13}C$ for COS, they provide a starting point for further research where hopefully, based on more evidence, the behaviour of this carbon isotope can be understood properly.

6.3 Is Siikaneva wetland a COS source or a sink and how does this differ among seasons?

First we need to be aware that the data availability is scarce. We only have data from May till September 2019 which also contains some missing data points. The amount of data points with more than 75% data available in one day is very limited, however, the data quantity is larger for days with more than 50% data availability. In figure 26 this is shown together with the weekly medians for weeks with more than 50% data available.

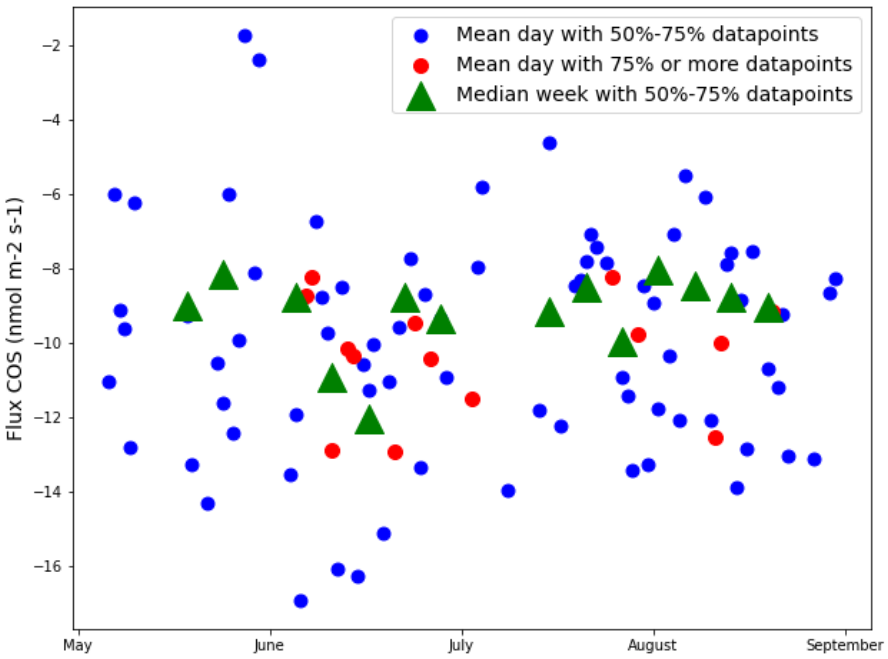

Fig. 26. *COS* **flux data averaged over the day.** More than 75% data availability in the specific day in red, more than 50% in blue and weekly medians with more than 50% data for the specific week in green.

Nevertheless, till date of writing, this is the first and only *COS* EC flux data measured over a Northern latitude fen, which makes the data, even if scarce, interesting to study.

The most important finding is that the data shows Siikaneva fen to behave as a stable *COS* sink between May-September 2019 with a median similar to what is reported by Whelan and Rhew 2016 for grassland wetland (sink between -10 and -20 pmol $m^{-2}s^{-1}$).

Even with variations in meteorological circumstances as heat (fig. 27) and drought (fig. 28), the sink strength remains remarkably stable. Also the correlation analysis with many meteorological variables showed the fen to be a very stable sink for *COS* without being influenced by other parameters (Appendix fig. 31). This stability can be explained when looking at the vegetation covering the fen. Approximately 90% of the area is covered by mosses which do not have stomata (Zeiger, Farquhar, and Cowan 1987) and therefore can take up *COS* independently of PAR and/or VPD. Moreover, since water is usually abundantly available in the fen, the plants with stomata most probably have lost their ability to control stomatal closure. Therefore, also the plants can take up *COS* continuously.

When looking more into the details of the data set shown in fig. 16, we see a source spike in July. However, this day also shows a big spread in data and finds itself in between two days of *COS* uptake. This suggests the spike to be caused by the high random variations with respect to the low *COS* fluxes. Since this is a solitary spike, we do believe it is irrelevant for this study. Nevertheless, the month July experienced very warm and dry conditions (fig. 27 and fig. 28). There is even a specific spike in temperature overlapping the spike in *COS* flux in July which could suggest that the weather conditions this day led to abnormal high microbial activity producing *COS*. Future studies covering longer time periods are needed to identify the importance and reason of this and maybe other *COS* source spikes.

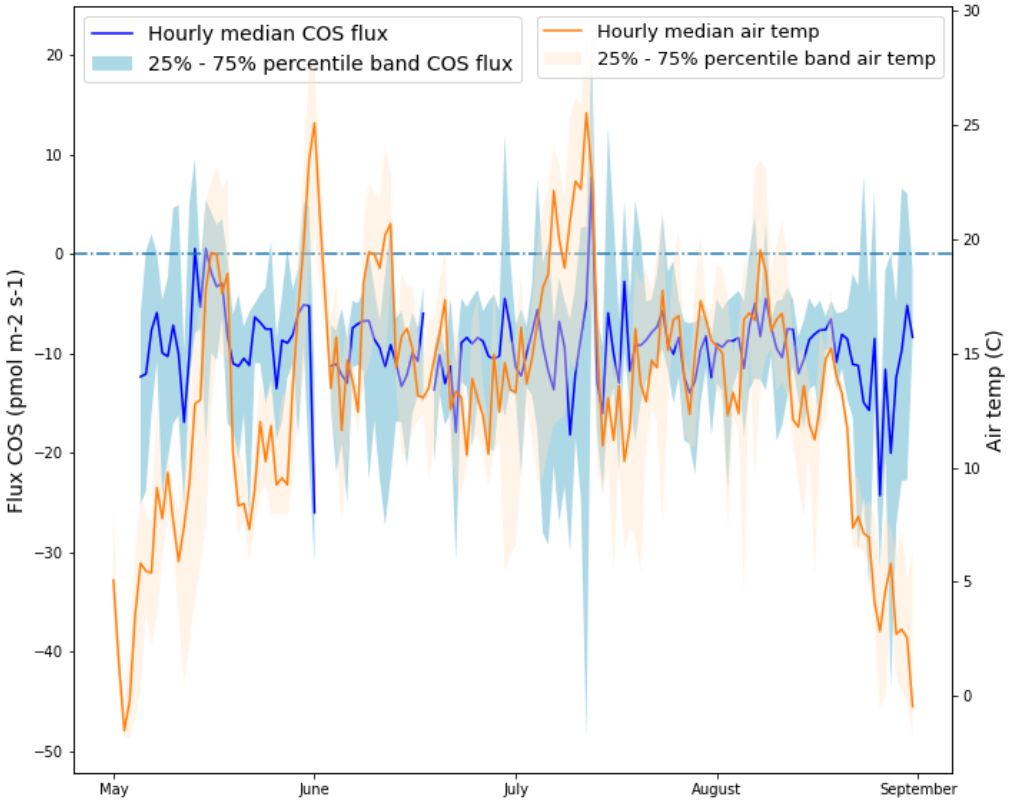

Fig. 27. Seasonal cycle COS flux and air temperature with 25 and 75 percentiles.

Also when looking at the COS sink found for each month, we see some differences. The sink strength tends to increase from May (COS flux of -8.16 pmol $m^{-2}s^{-1}$) towards September (COS flux of -10.3 pmol $m^{-2}s^{-1}$) but shows less uptake during July and August (see results 5.3). These were indeed the months with high air temperatures and low water table depth (WTD) levels (fig. 28).

Fig. 28. Seasonal cycle COS flux and water table depth with 25 and 75 percentiles. COS source reported as positive flux and COS sink reported as negative flux.

When WTD is low, the soil is very dry and little nutrients can be transported to the soil by water. Since there is low water availability, plants close their stomata to prevent to dry out which can explain the spike in emissions. Mosses however can continue take up COS and wetland plants too as they tend to (partly) lose their ability to control stomata closure. Additionally, the roots of the plants still have access to water, even in dryer periods. The vegetation in the fen thus seems to be resilient against this dry and warm event and can continue behaving as a stable COS sink.

Moreover, the EC method works with steady environmental conditions (Baldocchi 2003). This could affect the quality of the data in this period with extreme events.

The data shows, even when the daily median is computed, noise (fig 16). The EC method comes with random error, however, the amount of randomness decreases a lot when taking daily medians. For Siikaneva the fluctuations remain with little noise even after averaging. This could be because of the relative small COS fluxes (in comparison with Hyytiälä for example). More data availability could help clarify the small fluctuations found.

The small daily cycle with magnitude of around 5 pmol $m^{-2}s^{-1}$ can be explained with the found correlation on diurnal time scale between COS fluxes and low PAR values. Figures 18 and 41 show an intensification of COS strength of around the same magnitude as found for the daily cycle.

The strongest increase of COS uptake seems to appear for PAR levels till 200 mol $m^{-2}s^{-1}$ (fig. 19) as found with chamber measurements in Hyytiälä (Kooijmans et al. 2019). But in contrast to that study, we detected that the increase in COS uptake continues till PAR levels of around 600 μmol $m^{-2}s^{-1}$. The COS sink strength increase in relation with PAR can be explained by the correlation between PAR and stomatal conductance (Kooijmans et al. 2019, Vesala et al. 2022). The difference can be caused by the difference in vegetation (different mosses and wetland adapted plants who (partly) lost their stomatal control) and measurement method. Higher PAR fluxes do not influence the COS uptake as all stomata are opened.

VPD can have similar effects on the COS uptake (Linda Kooijmans personal communication). Indeed we could parameterize the COS fluxes using the VPD with equation 18 (Vesala et al. 2022) and fitted parameters:

d = 8.57 ± 1.21 and e = -15.2 ± 0.866.

$$FVPD = (\frac{d}{1+\sqrt{VPD}}) + e \tag{19}$$

This fit (Appendix fig. 44) however, is a result of the cross-correlation between PAR and VPD with value of 0.669. To disentangle the contribution of PAR, the driver of opening the stomata in the morning and VPD the driver of closing them in the afternoon, we parameterize using VPD (eq. 19) only for PAR levels higher than 600 μmol $m^{-2}s^{-1}$. The resulting parametrization shows that the COS flux is not driven by VPD (Appendix fig. 45). Thus the daily cycle is primary driven by PAR. The plants with stomatal control open their stomata when PAR increases and close them when PAR decreases resulting in a diurnal cycle for COS uptake.

Lastly, we can use the found stable COS sink in Siikaneva to represent the behaviour of northern latitude wetlands with respect to COS. Here we add a 'back of the envelope' calculation to upscale the found sink:

We assume a COS flux of -10 pmol $m^{-2}s^{-1}$ which is multiplied with 10^{-12} to mol m-2/s-1. The molecular weight of sulfur is 32,065 g/mol (Biotechnology Information 2022) and we assume a year of 31556926 seconds. Finally, we divide the result of eq. 20 by 2 since we assume COS uptake only in growing season (which we assume to be half of a year).

$$GgS/y = [F_{COS}] * [A] * sec * m_S * 10^{-9} \tag{20}$$

With F_{COS} the mean COS flux in mol $m^{-2}s^{-1}$, A the area covered by fens in the NH in m^2, sec the amount of seconds in a year and the final factor to covert the result to Giga unit.

When assuming a peatland area above 45 °N of $2.8 * 10^6 km^2$ (provided by Dr. O. Peltola based on Xu et al. 2018) this results in a COS sink of -14.3 Gg S /y.

When assuming the area of Boreal arctic fen regions to be $0.91 * 10^6 km^2$ (Olefeldt et al. 2021) the result is a sink of -4.64 Gg S/y. Whereas when assuming the area of all arctic boreal wetlands to be $3.18 * 10^6 m^2$ (Olefeldt et al. 2021) the result is -16.2 Gg S/y.

We compared these 'back of the envelope' calculations with upscalings done by Camille Abadie and Marine Remaud the ORCHIDEE land surface model (Krinner et al. 2005). The estimated wetland area is provided by the map of Tootchi, Jost, and Ducharne 2019 taking only Northern latitudes between 50° N and 70°N and a period from April till September. When upscaling the median COS flux of -10 pmol $m^{-2}s^{-1}$, so without assuming environmental relations with the COS flux, the modeled result is -15 Gg S/y.

When using the found relationship with PAR (eq. 18) and assuming for the same area and period, a mean PAR level of 465 W/m2, the COS flux becomes -11.1 pmol $m^{-2}s^{-1}$ and the total sink -20 GgS/y.

For this upscaling estimation we assume wetlands in the northern latitudes to behave similarly. We also assume the fen to be only a COS sink during half of the year based on the different mixing ratio found with the isotopic measurements in winter and the seen snow cover in winter which leads us to suspect no COS uptake during winter. With these assumptions the found wetland global yearly sink by the ORCHIDEE land surface model, is not enough to close the total global budget gap (which needs 230 - 432 Gg S/a to be closed (Ma et al. 2021) but it is an additional sink in the NH which would have remained unknown without this study.

6.4 What is the isotopic composition of COS at Siikaneva wetland during winter/spring?

The too low COS concentrations for measuring the isotopic composition, found in the soil sample taken at 10 cm depth, can be explained by the weather circumstances in the winter period. The soil temperature was around 1 °C and the water table depth 0 cm which makes soil circumstances not impossible for COS uptake by CA (Kesselmeier, Teusch, and Kuhn 1999). However, the soil was covered by approximately 1 m snow and ice which partly isolated the soil from the ambient COS mixing ratio. Little COS was available to be taken up by the microbes in the vegetation. Note that in the wetland more water is available than in the forest which leads to not only snow cover in winter, as seen in the forest, but also ice cover. The ice cover makes the diffusion of

gases from the air towards the ground vegetation more difficult and should therefore be taken into account in the discussion of these wetland results.

Theoretically, COS can be produced by microbes in the deeper soil layers and taken up in the upper soil layer we sampled. However, the microbes were in dormancy due to the low temperatures and even if some COS was produced, the COS found in our air sample was too low for isotopic detection. We did measure presence of methane (CH_4), Oxygen (O_2) and CO_2 suggesting microbial activity. Moreover, higher than normal concentrations of CH_4 are released after snow/ice melt, strengthening the hypothesis that the ice layer isolated the soil from ambient COS.

Nevertheless, since these meteorological conditions are typical for NH wetlands during winter, similar findings can be expected every winter in NH wetlands.

Both the mixing ratios measured in winter (504.83 $\pm$ 15 ppt) and spring (540.02 $\pm$ 15 mean ppt) are higher than the mean mixing ratio measured with the EC tower in May-Sept 2019 (around 350 ppt). The COS mixing ratio is known to vary among seasons between roughly 500 ppt and 350 ppt (Montzka et al. 2007) which is not far from our findings, taking into account that the GC-IRMS tends to reveal at least 100 ppt higher results than EC method. The found higher mixing ratio in spring than in winter can be, similarly to the situation in Hyytiälä, a result of the low BL in winter with respect to spring. The winter background sample has a $\delta^{34}S$ value of 13.85 $\pm$ 1.03 ‰ which is similar to the background value found by Angert et al. 2019.

Backward wind direction analysis shows that the winter samples (25 blue) contained air coming from the South of Finland and East Europe. Here some major cities are located that could have affected the sampled air since lower isotopic signatures are found in urban areas (Davidson, Amrani, and Angert 2021) with respect to forest or seas. The spring samples are taken when air came from the north/west direction passing forests (both in Finland as in Sweden and Norway) and the Gulf of Bothnia (25 green). This could result in higher δ^{34}S values (Davidson, Amrani, and Angert 2021, Hattori, Kamezaki, and Yoshida 2020) than when air passes anthropogenic sources. However, like seen for the forest samples, we do not have measured this behaviour in our samples which suggests that the samples were not affected by the air provenance.

The lower mean mixing ratio found in spring is rather a result of the wetland behaving as a COS source. Snow had just melted away, the water levels were very high and the plants were senescent which suggests that the wetland plants behaved as a source of COS. Stems of wetland plants can conduct the COS produced in the soil towards the atmosphere (Whelan et al. 2018) which after snow melt can be higher than the COS uptake we identified during summer with our EC flux data analysis.

Difference is found between the spring duplicates (light and dark). The first measured sample resulted in higher values than the second measured. This is most probably caused by the GC-IRMS which we identified to have a drift downwards when measuring samples one after the other. As mentioned we tried to compensate this in our analysis but we did not succeed entirely.

6.5 How do EC COS flux measurements of Hyytiälä boreal forest and Siikaneva wetland compare/differ?

One on one comparison cannot be made as the data sets are from different years, however, a general comparison is possible since we believe the mean weather conditions remain roughly identical.

As hypothesized, figures 22, 23 show larger COS uptake by the forest with respect to the wetland due to the different vegetation and LAI (Appendix fig. 33). The maximum LAI found in Siikaneva was around $0.6 m^2 m^{-2}$ while the maximum in Hyytiälä is around $7 m^2 m^{-2}$ (Vesala et al. 2022).

We see from fig. 22 that Hyytiälä is a less stable COS sink with respect to Siikaneva. This also can be explained by the differences in vegetation. The forest in Hyytiälä contains more plants with stomatal control which leads to more pronounced reactions to PAR -, VPD and air temperature as investigated by Vesala et al. 2022 and in the correlation analysis (Appendix fig. 46 for Hyytiälä and fig. 31 for Siikaneva).

The diurnal cycle is more pronounced at Hyytiälä than at Siikaneva which is expected when taking into account the different vegetation. Also the correlation analysis shows a larger correlation between COS fluxes

and for example PAR at Hyytiälä (Appendix fig. 47) than at Siikaneva (Appendix fig. 32).

When looking at fig. 23, it is notable that during nighttime (between 21h and 5h) the fluxes have similar magnitude. This can be caused by COS uptake by mosses which are present in both ecosystems and incomplete nighttime stomatal closure which is occurs in Siikaneva as most wetland plants tend to lose their stomatal control and in Hyytiälä as the roots and stems also take up COS.

Figure 24 shows the necessity of different LRU values for both ecosystems. A higher LRU value indicates a faster CO_2 uptake with respect to COS. This is the case for Hyytiälä where as in Siikaneva the opposite occurs (faster COS uptake than CO_2). For both ecosystems the ratio $\frac{[CO_2]}{[COS]}$ (eq. 3) is larger than 1, even if the Hyytiälä values are slightly higher than Siikaneva values. This indicates that the ratio $COS : CO_2$ fluxes is lower for Siikaneva than for Hyytiälä caused by the difference in vegetation. Lab experiments under optimal conditions done on liverwort and moss species different than the vegetation in Siikaneva, also found LRU values lower than 1 (Gimeno et al. 2017).

Since the ecosystem in Siikaneva is not only covered by mosses but also plants, it is a sink of CO_2 for high PAR levels and a CO_2 source for low PAR levels, the diurnal cycle of the calculated LRU (eq. 3) also changes from negative (-3.56 $\pm$ 1.313) during low PAR levels and positive (3.00 $\pm$ 0.472) during high PAR levels. This light dependence is also found in Hyytiälä (Kooijmans et al. 2019).

Finally fig. 24 shows spikes for the Siikaneva data between 1:30 and 3 am which can be caused by nighttime EC flux measurements which are not so accurate (Aubinet 2008). The negative spike around 14 h visible in both data sets can be explained with the presence of summer afternoon clouds which usually happen in this time of the year. Since both sites are close to each other we can assume similar meteorological circumstances. Fig. 29 shows indeed a little dip in PAR levels around the same time as the spikes in the GPP data occur. Moreover, fig. 30 from Mammarella et al. 2007 shows that during summer, around the same time also the mean vertical wind experiences a drop in velocity. This influences EC measurements and can be an explanation for the spikes in GPP data seen in fig. 24.

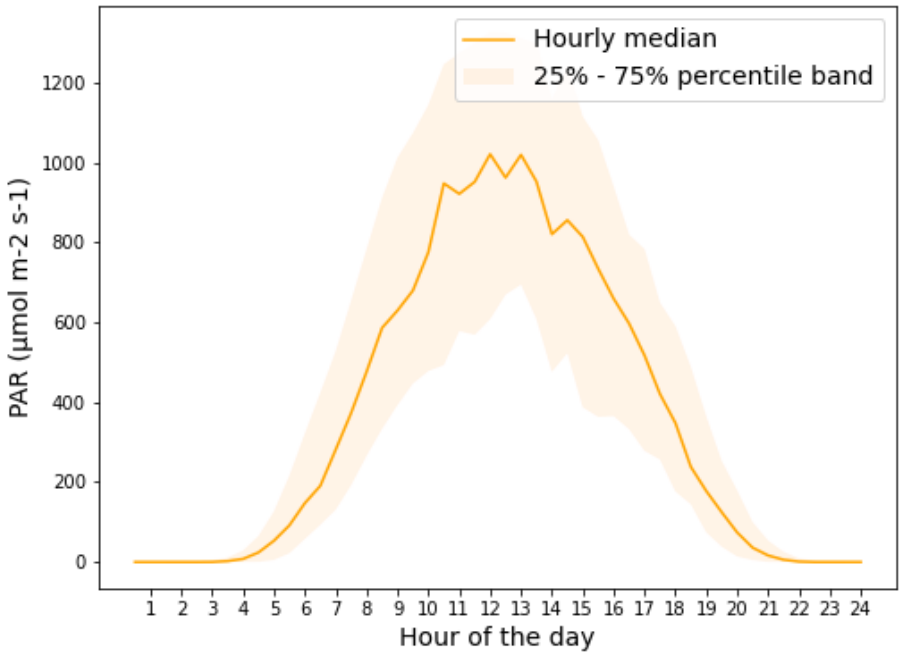

Fig. 29. Diurnal cycle median PAR levels with 25 and 75 percentiles.

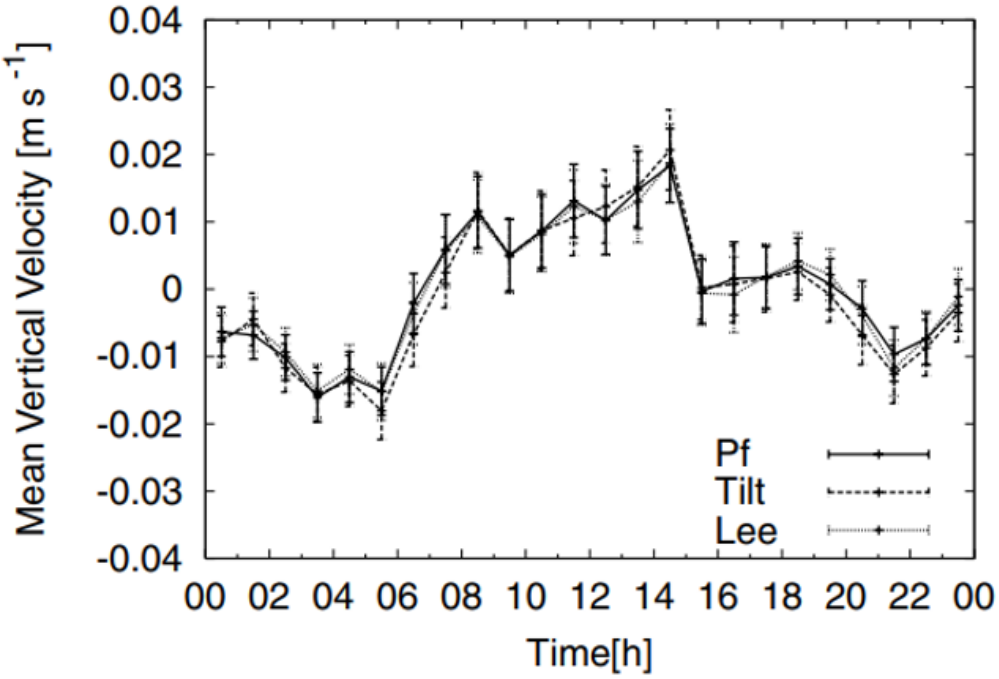

Fig. 30. Diurnal cycle of the mean vertical wind measured at Hyytiälä in the summer of 2004 by Mammarella et al. 2007

One possible reason influencing the difference between the GPP calculated by SmartSMEAR using CO_2 fluxes and the GPP fitted with the measured COS fluxes (fig. 24) can be the wind direction. During the analyzed period, the wind came from the northern region of the EC tower where the vegetation is rich in Sphagnum papillosum. This moss has lower photosynthetic capacity with respect to the Sphagnum majus dominating the southern side of the EC tower. Indeed CO_2 fluxes showed lower uptake during days with wind originating from the north with respect to days with opposite wind direction. However, COS fluxes were not affected by wind direction as the uptake is different from photosynthesis. This difference behaviour of the gases on the wind direction could give little variations in GPP estimations.

For Hyytiälä we see a time lag of around 1 hour between the fitted GPP values and the data (fig. 24 between 4 and 9 am). The GPP data is derived from net ecosystem CO_2 exchange (Aalto et al. 2019) while the fitted GPP from the measured COS and CO_2 fluxes. Chamber measurements done in Hyytiälä by Kooijmans et al. 2019 showed CO_2 fluxes have around 1 hour time lag with respect to COS fluxes due to the different light response. This can explain the similar time lag visible in our fit.

6.6 How do isotopic signatures of COS measured at Hyytiälä boreal forest and Siikaneva wetland compare/differ?

The similarity between the isotopic compositions found in Winter at Siikaneva and the ones found at 125 m in Hyytiälä is expected since they resemble the background values and the sites are located close to each other. Moreover, backwards wind trajectory (25) shows that the air came from similar direction for the winter samples and same direction for the spring samples. Nevertheless, as explain previously, most of the results do not follow the expectations based on wind direction so we wonder if the air provenance did affect our samples or not.

Since the temperatures were cold when the spring samples were taken, we suspect that both ecosystems were no clear COS sinks yet or that the wetland was even behaving as a source. Therefore the isotopic signatures at both sites are difficult to interpret. More information about similarities/differences between the sites could be gained if the sampling would be repeated in growing season and with more duplicates.

The Siikaneva data did not fit well in the three-isotope plot made with Hyytiälä data (fig. 14) which shows that at the wetland different fractionation took place as in Hyytiälä. Since the ecosystems differ and their behaviour against COS is hypothesized to differ, this is expected. Nevertheless, we need to keep in mind that we do cannot rely fully on our δ^{33}S values which also influences the interpretation of our three-isotope plot.

The relative high mixing ratio during winter in Siikaneva can be explained with the presence of the 1 m thick snow layer which 'sealed' of wetland activity while in Hyytiälä some COS uptake still could have taken place as the needles and stems of the trees were not covered by snow.
In spring the slightly higher mixing ratio found in Siikaneva with respect to Hyytiälä can be caused by more COS uptake in latter or more emission in the first ecosystem. Note however, that the difference is small and not significant.

7 Conclusions

In general we gained more knowledge on the interactions of COS with the biosphere by performing this research.

The EC flux data analysis we computed for the first time on a NH wetland fen, showed the fen to be a stable COS sink during the studied period. This new information helps to reduce the knowledge gap in the global COS budget.

The closely located Hyytiälä boreal forest showed, similarly to previous years, to be a sink of COS with a more pronounced daily cycle than Siikaneva as expected by the difference in vegetation. We were also able to fit the GPP on both sides.

In this project we also successfully sampled and measured for the first time the COS isotopic signature of sulfur and carbon at different heights in the boreal forest and on the wetland. The results fall within the expected ranges of literature and our plot of mixing ratio against the δ^{34}S signature suggests MDF. Lastly, these isotopic signature results show the convenience of the GC-IRMS developed at IMAU and can serve as invitation for further research.

A brief summary of the answers to all research questions is listed below. Finally, suggestions for further studies are written in the Outlook.

7.1 Is Hyytiälä boreal forest a COS source or sink and how does this differ among seasons?

The analyzed forest is found to behave as a COS sink as expected. The median COS flux on seasonal time scale is -8.26 pmol $m^{-2}s^{-1}$ with a 25%-75% range between -15.7 and -2.84 pmol $m^{-2}s^{-1}$ and -12.4 pmol $m^{-2}s^{-1}$ with a 25%-75% range between -19.9 and -5.91 pmol $m^{-2}s^{-1}$ for May till October 2020. The daily cycle is primarily driven by PAR. The sink strength increases during spring/summer and decreases towards winter due biological seasonal cycle. However, wintertime measurements are not reliable due to measurement breaks caused by EC wintertime challenges.

7.2 What is the isotopic composition of COS at different heights in Hyytiälä boreal forest during winter/spring?

The mean COS isotopic composition in winter/spring respectively is for δ^{34}S 13.79 ± 1.05 ‰/ 10.91 ± 0.90 ‰ which is within the literature range. For δ^{33}S the mean in winter/spring is 3.79 ± 2.61 ‰/ 0.11 ± 2.49 ‰, however, we do not trust our δ^{33}S values entirely.

The lower mean spring signatures of the sulfur isotope with respect to the winter mean can be a consequence of the downward drift of the GC-IRMS or higher BL in spring than in winter. This can also explain the higher mean mixing ratio found in early spring (530 ± 15 ppt) with respect to winter (474.51 ± 15 ppt).

The three-isotope plot appeared to not be the adequate tool to identify MDF for a complex ecosystem as our slope (1.84 ± 0.34) is different than the MDF line derived from lab experiments.

The mean δ^{13}C value in winter/spring is 3.78 ± 2.14 ‰/ 14.00 ± 2.14 ‰. We are the first reporting carbon isotopes of COS. More measurements are needed to frame these results.

Likewise, we did find some more enriched isotopic values with high PAR than with low PAR and higher up in the canopy layer than near the ground but additional measurements are needed to make these results more robust.

7.3 Is Siikaneva wetland a COS source or a sink and how does this differ among seasons?

We found that Siikaneva wetland behaves as a stable net COS sink for the whole analyzed period. The median COS flux on seasonal time scale is -9.15 pmol $m^{-2}s^{-1}$, with a 25%-75% percentile range between -16.2 and -4.42 pmol $m^{-2}s{-}1$. The sink strength tends to increase from May towards September with lower uptake in June and August caused by the extreme low WTD.

The diurnal cycle has a magnitude of around 5 pmol $m^{-2}s^{-1}$ which is mostly driven by PAR. Nevertheless, the found COS sink is very stable as a result of the vegetation (mosses and plants that have lost stomatal control) covering the fen.

7.4 What is the isotopic composition of COS at Siikaneva wetland during winter/spring?

The mean sulfur isotopes found in Siikaneva are for winter/spring respectively 13.85 ± 1.03 ‰/ 12.50 ± 0/83 ‰ for δ^{34}S and fit within literature range. For δ^{33}S the mean in winter/spring is 5.58 ± 2.56 ‰/ -7.60 ± 2.52 ‰ and for δ^{13}C 3.32 ± 2.14 ‰/ 23.27 ± 2.14 ‰. One explanation for the lower signatures found in spring than in winter is that the ecosystem was as COS sink in early spring while in winter, due to the snow/ice cover, we measured background values. Also the mixing ratio is higher in early spring (540.02 ± 15 ppt) than in winter (504.83 ± 15 ppt) which enforces this hypothesis. However, EC flux measurements of early spring and isotopic measurements in the growing season are needed to confirm this hypothesis.

7.5 How do EC COS flux measurements of Hyytälä boreal forest and Siikaneva wetland compare/differ?

We have shown that nighttime COS fluxes are similar in both ecosystems even if different years are compared. Daytime fluxes however, differ with a 1.68 ± 0.0860 times higher COS uptake by the boreal forest with respect to the fen wetland. The difference is caused by the different vegetation covering the sites with different LAI indexes. The daily cycle in Siikaneva is less pronounced since the site is mostly covered by mosses which do not have stomata and wetland plants that probably have lost their stomatal control.

7.6 How do isotopic signatures of COS measured at Hyytiälä boreal forest and Siikaneva wetland compare/differ?

The isotopic signature sampled in winter in both sites are similar. The similarity is even stronger between Siikaneva and 125 m at Hyytiälä as both resemble background air and the sites are closely located. Difference is suggested in the MDF process on both sites as the Siikaneva data did not fit in the three-isotope plot made for the Hyytiälä data. However, the data of both sites show negative trend between the mixing ratio and the δ^{34}S value as expected from MDF.

From both sites we get the impression that the ecosystems were not fully active when sampling as expected based on temperature. We recommend to sample again in growing season to be able to answer this research question.

7.7 Outlook

Since the found stable sink in Siikaneva wetland can have implications for the global COS budget, more research is advised on northern latitude wetlands. A longer time range of measurements as well as different wetland types could give the needed additional information on seasonality and differences among vegetation. This can help to understand better Northern latitude wetland ecosystem behaviour with respect to COS and help close the knowledge gap in the COS budget. For example, a comparison between COS fluxes at the fen and the bog,

which are situated next to each other and thus have the same environmental conditions but differ in ecosystem, is a potential place to start these measurements. Moreover, chamber measurements at Siikaneva both on mosses+soil and mosses+soil+plants could help disentangle the contribution of the plants with respect to net COS fluxes.

Finally, in this research we demonstrated the utility of the new GC-IRMS developed at IMAU, Utrecht. This opens a new range of study opportunities as isotopic signatures from diverse provenance can simply be measured now.

We suggest repeating the air sampling later in the growing season as at the time of our sampling campaign, temperatures were still low and the ecosystems seemed to be not fully active yet. Furthermore, our isotopic signatures are from different months than the flux data was measured. Therefore it is hard for us to derive general relationships between the EC flux data and the isotopic signatures. From the isotopic signature results we can deduce that the forest in both February as April is not a distinct sink of COS yet. This is indeed also found in the flux data but we cannot trust this flux data since the EC method is very sensitive to low temperatures. By measuring the isotopic signatures in growing season, a true comparison can be made among seasons and between both measurements methods. Moreover, to verify the hypothesis we made based on the isotopic signatures found in Siikaneva, that the wetland is a source of COS in early spring, EC measurements in this period would be very helpful. Another way to test this hypothesis is to do isotopic signatures measurements during the growing season. If the signatures would be more enriched in heavier isotope and the mixing ratio would be lower than the one we report here, it would be an indication of a bigger COS sink strength later in the growing season with respect to early spring.

All in all, this project opens the door for more interesting research. Like the famous quote based on Aristotle's Metaphysics says; "The more you know, the more you know you don't know."

8 Appendix

In the appendix a list of used theory, manuals and supplementary figures can be found. Moreover, we briefly analyze the EC *COS* fluxes measured at Kitinen River, Finland.

8.1 Raynolds' decomposition and averaging rules

Raynolds decomposition states we can devide any time-depentent quantity in the atmosphere into a time-mean (denoted with an overline) and fluctuating (denoted with an apostrophe) part. If we decompose the EC flux equation (eq. 21) we derive eq. 22.

$$F^{EC} = \overline{\rho_a w c} \tag{21}$$

With ρ_a the dry air molar density, w the vertical wind and c the gas mixing ratio ($c = \frac{\rho_c}{\rho_a}$).

$$F^{EC} = \overline{(\overline{\rho_a} + \rho_a')(\overline{w} + w')(\overline{c} + c')} \tag{22}$$

After opening the parentheses we come to equation 23:

$$F^{EC} = \overline{(\overline{\rho_a w c} + \overline{\rho_a w} c' + \overline{\rho_a} w' \overline{c} + \overline{\rho_a} w' c' + \rho_a' \overline{w c} + \rho_a' w' \overline{c} + \rho_a' \overline{w} c' + \rho_a' w' c')} \tag{23}$$

By applying Raynolds' averanging rules stating that the average deviation from the average is equal to zero, equation 23 is simplified to eq. 24:

$$F^{EC} = \overline{(\overline{\rho_a w c} + \overline{\rho_a} w' c' + \rho_a' w' \overline{c} + \rho_a' \overline{w} c' + \rho_a' w' c')} \tag{24}$$

Finally we assume no density variations and a negligible mean vertical flow since the surface is homogeneous and flat. This leads to eq. 6 describing the vertical flux (section 1.2.6). (Aubinet, Vesala, and Papale 2012, Stull 1988, Baldocchi 2003).

8.2 Error calculation examples

$$\partial f = \sqrt{(\frac{\partial f}{\partial x}\sigma x)^2 + (\frac{\partial f}{\partial y}\sigma y)^2} \tag{25}$$

For the error propagation calculations we use equation 25. Here we show an example for the error propogation calculation of the ratio between the maximum *COS* flux found in Siikaneva and Hyytiälä (equations 26, 27).

$$ratio = \frac{max_{Sii}}{max_{Hyy}} \tag{26}$$

$$error_{ratio} = \sqrt{(\frac{1}{max_{Hyy}}\sigma_{Hyy})^2 + (\frac{-max_{Sii}}{max_{Hyy}^2}\sigma_{Sii})^2} \tag{27}$$

8.3 Figures

	FCOS	FCO2	GPP	WD	PAR	Soiltemp0	Soiltemp5	WTD	Airtemp	RH	VPD	total_LAI	aer_LAI
FCOS	1.00	0.08	-0.06	-0.09	0.06	0.05	0.02	-0.03	0.11	-0.08	0.09	-0.07	-0.07
FCO2	0.08	1.00	-0.83	-0.08	-0.65	-0.51	-0.52	0.04	-0.40	0.54	-0.57	-0.66	-0.61
GPP	-0.06	-0.83	1.00	-0.06	0.65	0.81	0.81	-0.34	0.73	-0.48	0.67	0.85	0.82
WD	-0.09	-0.08	-0.06	1.00	0.10	-0.15	-0.12	0.07	-0.18	-0.04	-0.07	-0.00	-0.00
PAR	0.06	-0.65	0.65	0.10	1.00	0.41	0.36	0.04	0.44	-0.87	0.85	0.37	0.33
Soiltemp0	0.05	-0.51	0.81	-0.15	0.41	1.00	0.99	-0.46	0.91	-0.26	0.57	0.73	0.71
Soiltemp5	0.02	-0.52	0.81	-0.12	0.36	0.99	1.00	-0.50	0.87	-0.22	0.51	0.76	0.75
WTD	-0.03	0.04	-0.34	0.07	0.04	-0.46	-0.50	1.00	-0.44	-0.11	-0.08	-0.63	-0.70
Airtemp	0.11	-0.40	0.73	-0.18	0.44	0.91	0.87	-0.44	1.00	-0.30	0.67	0.60	0.60
RH	-0.08	0.54	-0.48	-0.04	-0.87	-0.26	-0.22	-0.11	-0.30	1.00	-0.85	-0.22	-0.17
VPD	0.09	-0.57	0.67	-0.07	0.85	0.57	0.51	-0.08	0.67	-0.85	1.00	0.39	0.35
total_LAI	-0.07	-0.66	0.85	-0.00	0.37	0.73	0.76	-0.63	0.60	-0.22	0.39	1.00	1.00
aer_LAI	-0.07	-0.61	0.82	-0.00	0.33	0.71	0.75	-0.70	0.60	-0.17	0.35	1.00	1.00

Fig. 31. Seasonal cycle correlation matrix Siikaneva wetland.

	FCOS	FCO2	GPP	WD	PAR	Soiltemp0	Soiltemp5	WTD	Airtemp	RH	VPD
FCOS	1.00	0.67	-0.71	-0.32	-0.66	0.29	0.62	-0.40	-0.50	0.43	-0.40
FCO2	0.67	1.00	-0.99	-0.62	-0.98	0.09	0.68	-0.23	-0.84	0.80	-0.79
GPP	-0.71	-0.99	1.00	0.64	0.97	-0.12	-0.70	0.25	0.83	-0.78	0.78
WD	-0.32	-0.62	0.64	1.00	0.58	0.53	-0.03	-0.41	0.85	-0.86	0.87
PAR	-0.66	-0.98	0.97	0.58	1.00	-0.14	-0.73	0.26	0.79	-0.75	0.75
Soiltemp0	0.29	0.09	-0.12	0.53	-0.14	1.00	0.78	-0.96	0.44	-0.52	0.53
Soiltemp5	0.62	0.68	-0.70	-0.03	-0.73	0.78	1.00	-0.82	-0.21	0.13	-0.12
WTD	-0.40	-0.23	0.25	-0.41	0.26	-0.96	-0.82	1.00	-0.30	0.37	-0.39
Airtemp	-0.50	-0.84	0.83	0.85	0.79	0.44	-0.21	-0.30	1.00	-0.99	0.98
RH	0.43	0.80	-0.78	-0.86	-0.75	-0.52	0.13	0.37	-0.99	1.00	-1.00
VPD	-0.40	-0.79	0.78	0.87	0.75	0.53	-0.12	-0.39	0.98	-1.00	1.00

Fig. 32. Diurnal cycle correlation matrix Siikaneva wetland.

Note the cross correlation between VPD, RH and air temperature. As well as soil temperature at 0 and 5 cm depth with WTD and GPP with CO_2 fluxes.

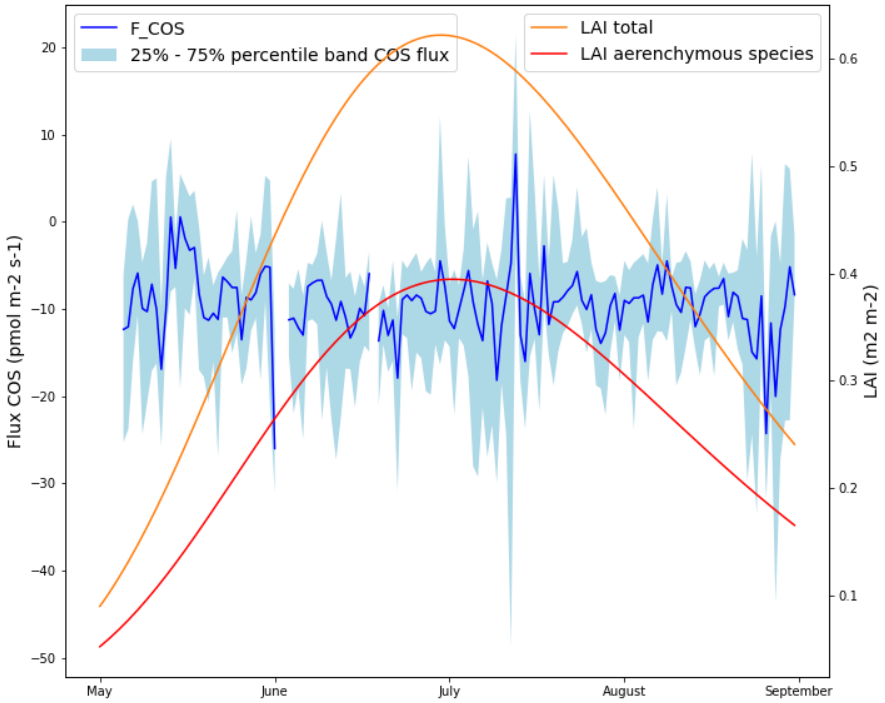

Fig. 33. Median seasonal cycle COS flux at Siikaneva wetland in blue with 25 and 75 percentiles, total LAI values in orange and aerenchymous species LAI in red.

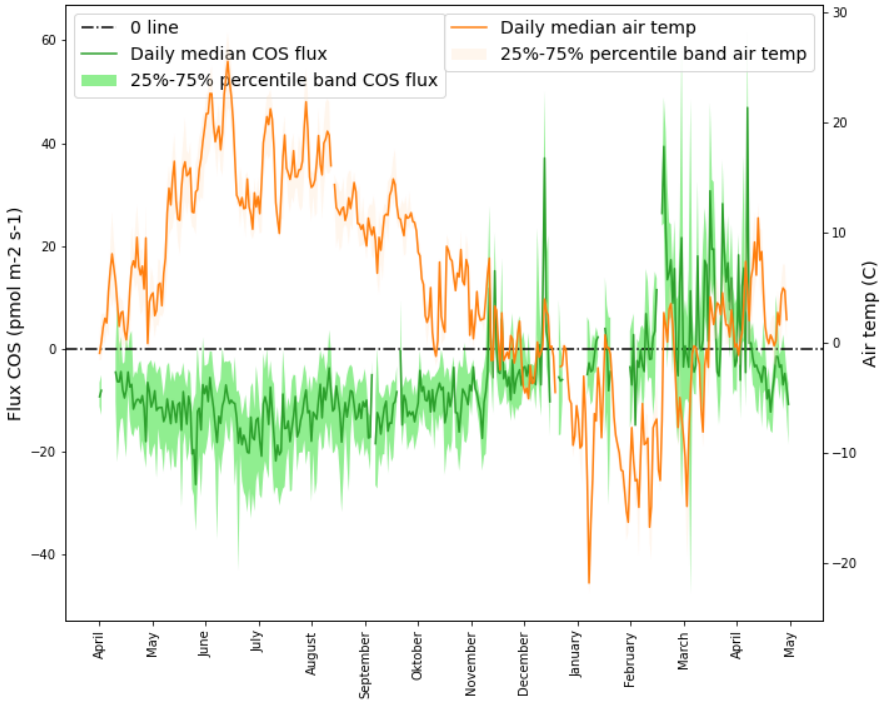

Fig. 34. Daily median *COS* fluxes and air temperature with 25 and 75 percentiles at Hyytälä. *COS* source reported as positive flux and *COS* sink reported as negative flux.

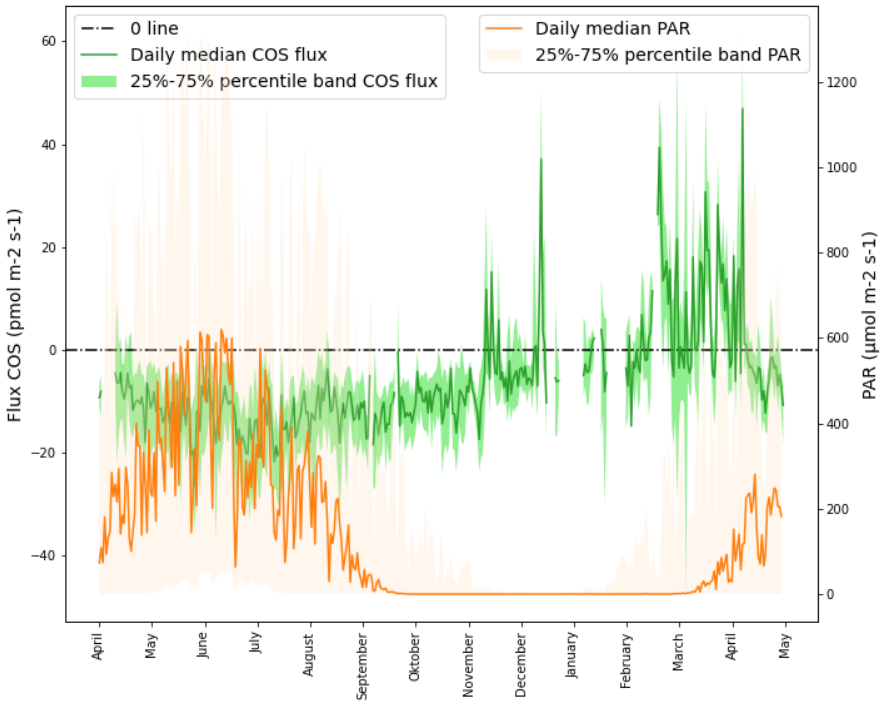

Fig. 35. Daily median *COS* fluxes and PAR levels with 25 and 75 percentiles at Hyytälä. *COS* source reported as positive flux and *COS* sink reported as negative flux.

Sample	δ^{34}S signature	δ^{33}S signature	δ^{13}C signature	mixing ratio (ppt)
Hyytiälä				
Winter 14 m height	14.58 ± 1.04 ‰	6.84 ± 2.58 ‰	1.76 ± 2.14 ‰	468.45 ± 15 ppt
	12.35 ± 1.04 ‰	-1.64 ± 2.6 ‰	1.37 ± 2.15 ‰	471.01 ± 15 ppt
Winter 23 m height	14.48 ± 1.04 ‰	6.65 ± 2.59 ‰	2.12 ± 2.15 ‰	476.51 ± 15 ppt
	12.85 ± 1.08 ‰	-1.69 ± 2.70 ‰	5.15 ± 2.15‰	441.81 ± 15 ppt
Winter 125 m height	$14.45 \pm 1,04$ ‰	7.58 ± 2.59 ‰	4.68 ± 2.15 ‰	482.91 ± 15 ppt
	14.04 ± 1.03 ‰	5.06 ± 2.56 ‰	7.57 ± 2.14 ‰	506.36 ± 15 ppt
Winter mean without outliers	13.79 ± 1.05 ‰	3.79 ± 2.61 ‰	3.78 ± 2.15 ‰	474.51 ± 15 ppt
Early spring 1 m height light	12.27 ± 0.98 ‰	-0.98 ± 2.51 ‰	21.92 ± 2.14 ‰	531.24 ± 15 ppt
Early spring 14 m height light	9.75 ± 0.97 ‰	-1.56 ± 2.48 ‰	25.66 ± 2.14 ‰	549.66 ± 15 ppt
Early spring 23 m height light	13.71 ± 0.98 ‰	5.09 ± 2.51 ‰	$-5.57 \pm .14$ ‰	515.83 ± 15 ppt
Early spring 125 m height light	9.79 ± 0.97 ‰	-2.61 ± 2.48 ‰	35.05 ± 2.14 ‰	533.95 ± 15 ppt
Early spring 1 m height dark	11.22 ± 0.99‰	-0.76 ± 2.53 ‰	4.05 ± 2.14 ‰	528.52 ± 15 ppt
Early spring 14 m height dark	9.88 ± 0.97 ‰	1.55 ± 2.47 ‰	18.85 ± 2.14 ‰	534.31 ± 15 ppt
Early spring 23 m height dark	8.62 ± 0.98‰	-3.55 ± 2.52‰	19.08 ± 2.14 ‰	526.90 ± 15 ppt
Early spring 125 m height dark	12.28 ± 0.35	3.66 ± 2.44	32.57 ± 2.14‰	522.18 ± 15 ppt
Early spring mean without outliers	$10,94 \pm 0.90$ ‰	0.11 ± 2.49 ‰	14.00 ± 2.14 ‰	530.32 ± 15 ppt
Siikaneva				
Winter 1 m height	13.85 ± 1.03 ‰	5.58 ± 2.56 ‰	3.32 ± 2.14 ‰	504.83 ± 15 ppt
Early spring 1 m height light	13.34 ± 1.00 ‰	-8.75 ± 2.53 ‰	23.27 ± 2.14 ‰	542.07 ± 15 ppt
	11.19 ± 1.00 ‰	-13.07 ± 2.53‰	31.20 ± 2.14‰	546.03 ± 15 ppt
Early spring 1 m height dark	11.91 ± 0.35 ‰	-17.47 ± 2.44‰	32.23 ± 2.14‰	570.23 ± 15 ppt
	13.54 ± 0.97‰	-0.98 ± 2.49 ‰	-19.00 ± 2.14 ‰	531.94 ± 15 ppt
Early spring mean without outliers	12.50 ± 0.83 ‰	-7.60 ± 2.52 ‰	23.27 ± 2.14 ‰	540.02 ± 15 ppt

Tab. 3. Isotopic signatures Hyytiälä boreal forest and Siikaneva wetland samples. Orange results are drifted values and red results are outliers.

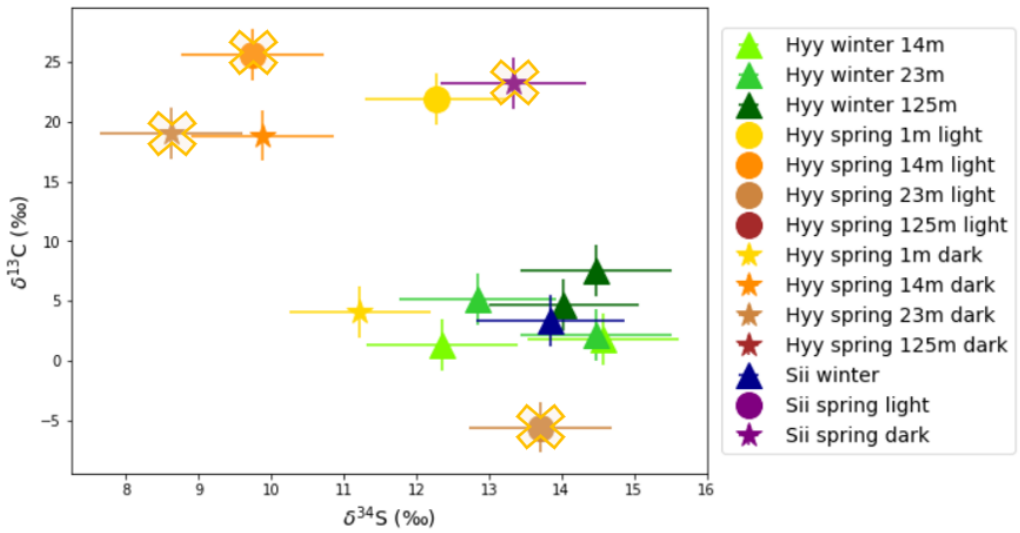

Fig. 36. δ^{34}**S plotted against** δ^{13}**C for all samples without outliers.** Orange crosses on the drifted values.

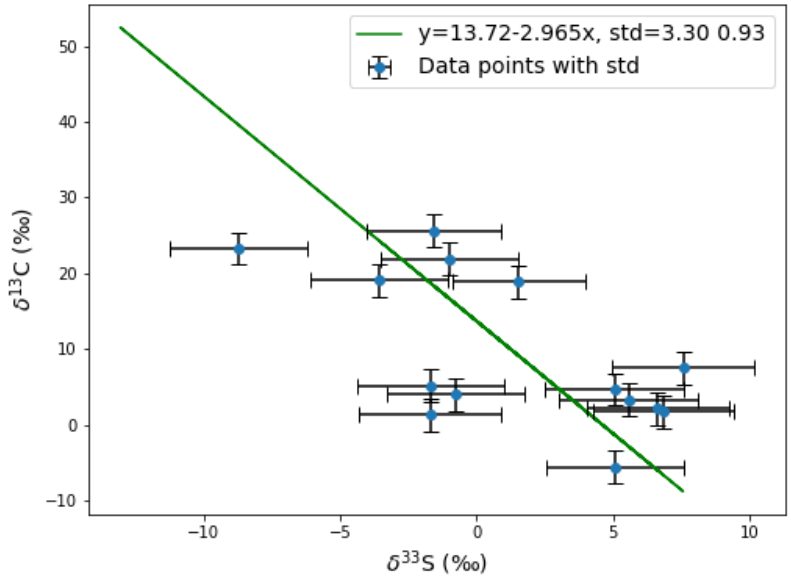

Fig. 37. δ^{33}S plotted against δ^{13}C for all samples without outliers and explicit orthogonal distance regression fit.

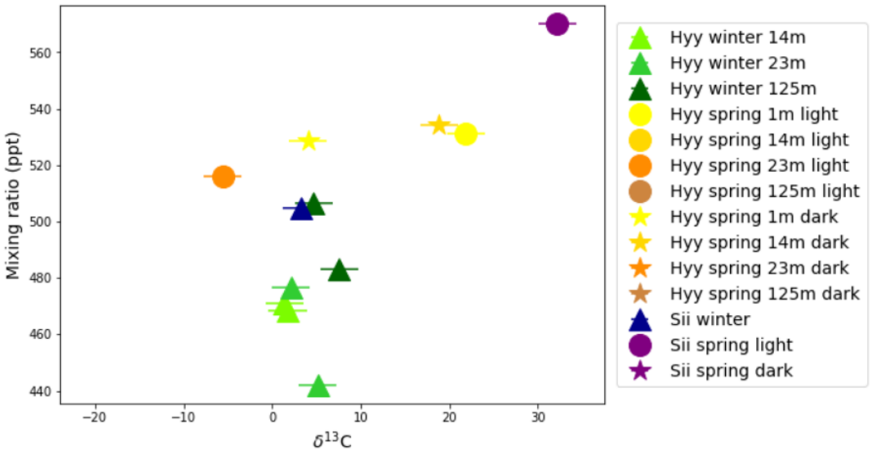

Fig. 38. δ^{13}C plotted against the mixing ratio for all samples without outliers and drifted samples.

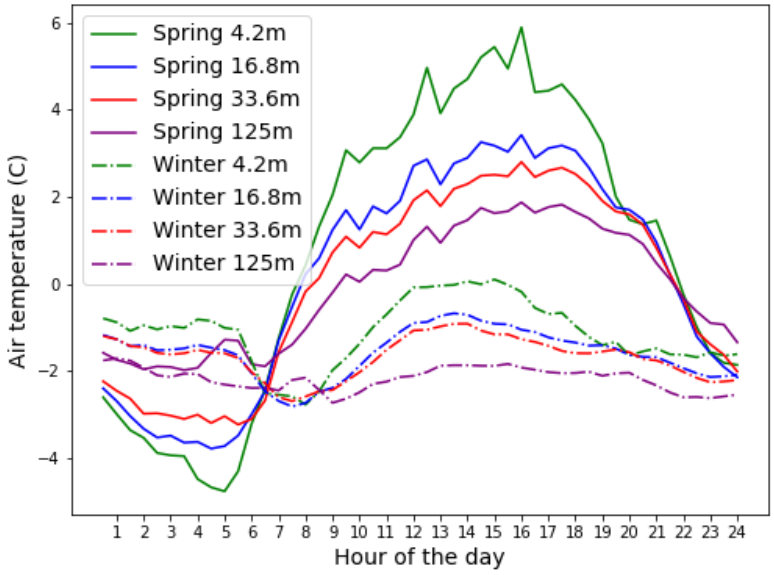

Fig. 39. Diurnal cycle of the air temperature on the sampling days (Aalto et al. 2019)

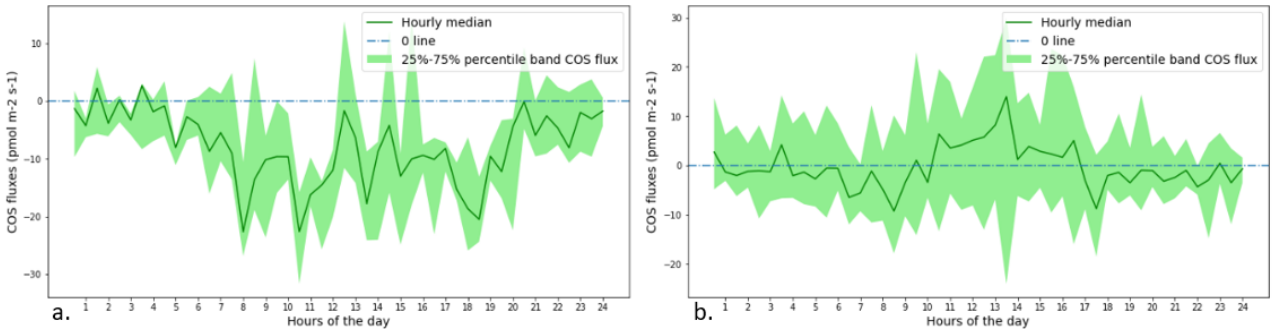

Fig. 40. Diurnal cycle of *COS* flux with 25 and 75 percentiles for April 2020 in a and April 2021 in b. *COS* source reported as positive flux and *COS* sink reported as negative flux.

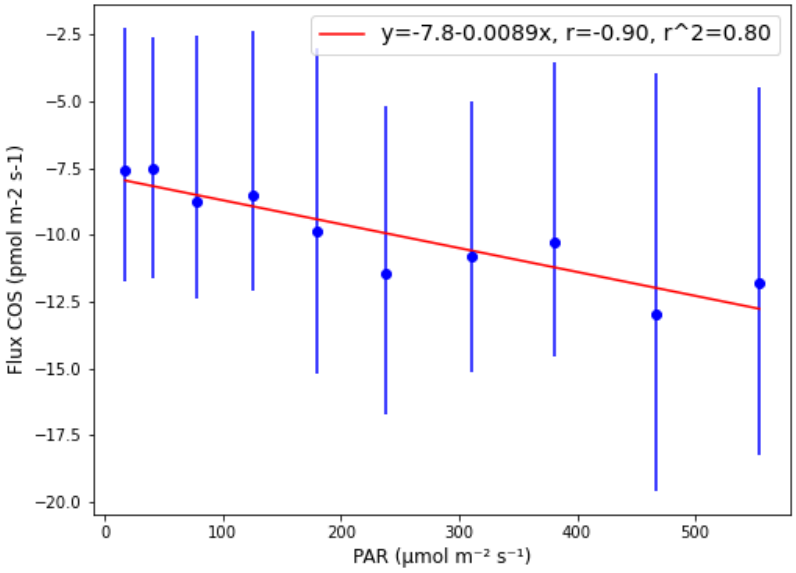

Fig. 41. *COS* **fluxes against low PAR levels.**

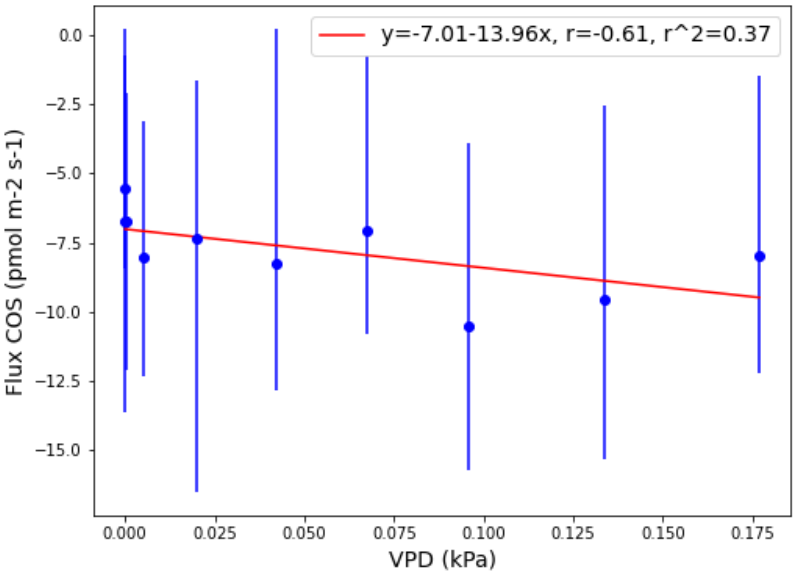

Fig. 42. *COS* **fluxes against low VPD levels.**

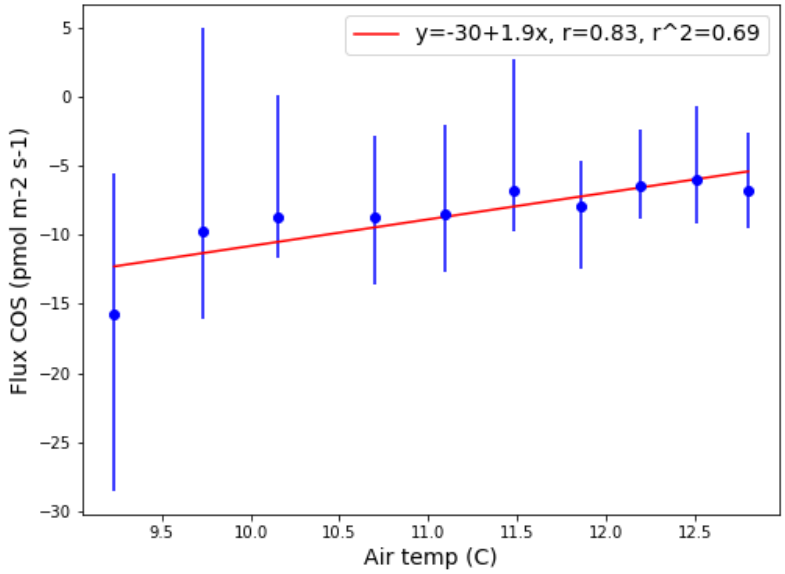

Fig. 43. *COS* **fluxes against air temperature range.**

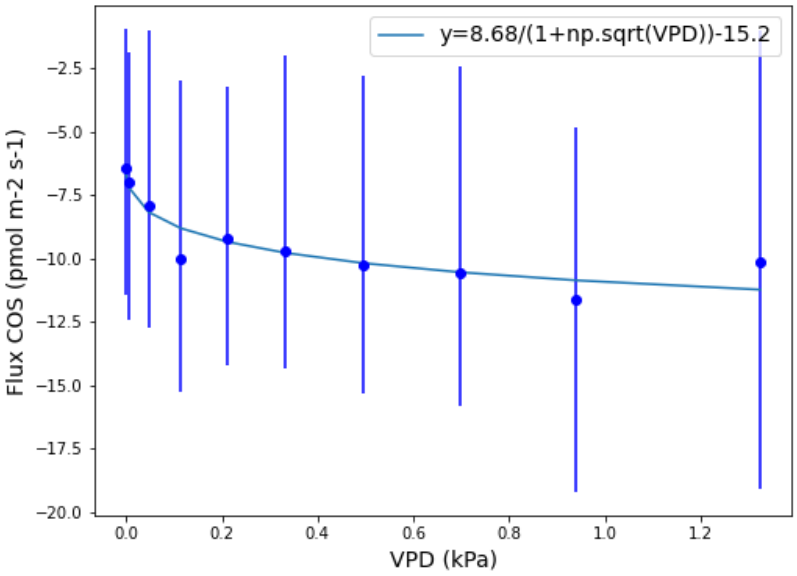

Fig. 44. *COS* **flux and fit using equation 19 against VPD values.** Data is collected in 10 equally sized binns. Errorbars represent 25 and 75 percentiles.

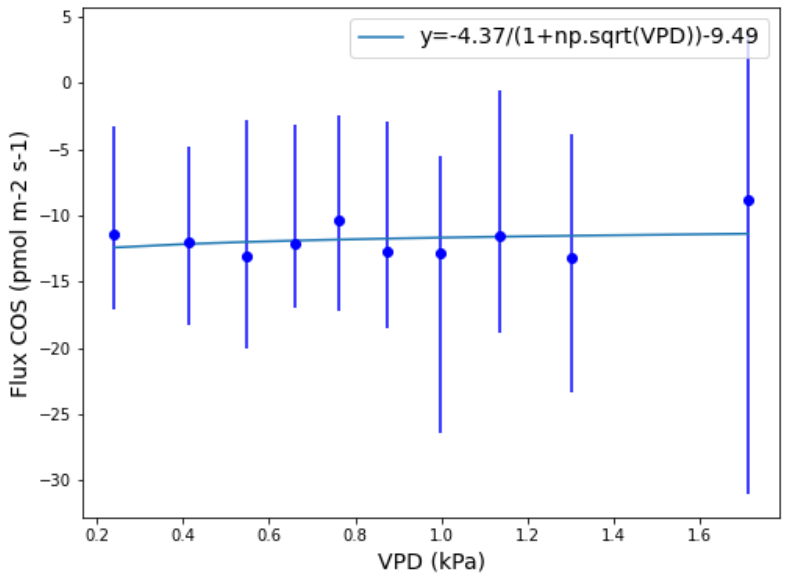

Fig. 45. *COS* **flux measured with PAR values higher than 600** μ**mol** $m^{-2}s^{-1}$ **and fit using equation 19 against VPD values.** Data is collected in 10 equally sized binns. Errorbars represent 25 and 75 percentiles.

	FCOS	FCO2	PAR	RH	prec	Tair	Tsoil_5	wsoil_5
FCOS	1.00	0.25	0.09	-0.32	-0.12	0.01	-0.28	-0.12
FCO2	0.25	1.00	-0.73	0.53	0.38	-0.40	-0.25	0.01
PAR	0.09	-0.73	1.00	-0.83	-0.40	0.43	-0.00	0.03
RH	-0.32	0.53	-0.83	1.00	0.46	-0.31	0.24	-0.05
prec	-0.12	0.38	-0.40	0.46	1.00	-0.10	0.10	-0.12
Tair	0.01	-0.40	0.43	-0.31	-0.10	1.00	0.78	-0.49
Tsoil_5	-0.28	-0.25	-0.00	0.24	0.10	0.78	1.00	-0.57
wsoil_5	-0.12	0.01	0.03	-0.05	-0.12	-0.49	-0.57	1.00

Fig. 46. Daily mean correlation matrix Hyytiälä forest for May-Sept 2020.

	FCOS	FCO2	PAR	RH	prec	Tair	Tsoil_5	wsoil_5
FCOS	1.00	0.93	-0.93	0.47	-0.16	-0.45	0.69	-0.08
FCO2	0.93	1.00	-1.00	0.70	-0.22	-0.67	0.53	0.10
PAR	-0.93	-1.00	1.00	-0.67	0.22	0.63	-0.57	-0.04
RH	0.47	0.70	-0.67	1.00	-0.47	-1.00	-0.23	0.70
prec	-0.16	-0.22	0.22	-0.47	1.00	0.48	0.25	-0.42
Tair	-0.45	-0.67	0.63	-1.00	0.48	1.00	0.27	-0.73
Tsoil_5	0.69	0.53	-0.57	-0.23	0.25	0.27	1.00	-0.70
wsoil_5	-0.08	0.10	-0.04	0.70	-0.42	-0.73	-0.70	1.00

Fig. 47. Diurnal cycle correlation matrix Hyytiälä forest for May-Sept 2020.

8.4 Manuals

8.4.1 Air sampler manual

8.4.2 Cannister evacuation manual

8.4.3 Dryer preparation manual

8.5 Kitinen River

In this section, the EC COS flux data measured over Kitinen river is discussed. We present the results without in depth analysis and hope someone wants to proceed with this study.

8.5.1 EC measurements site

The COS fluxes were measured near the Sodankylä observatory ($67°22'N$, $26°37'E$) by Dr. Kukka-Maaria Kohonen. The setup was placed 15 m offshore, 2 m above water level.

An Aerodyne QCLS was used for the mixing ratio measurements and a Metek USA-3 at a frequency of 10 Hz for the wind components.

The EC flux data was processed by Dr. Kukka-Maaria Kohonen (Helsinki University).

8.5.2 Research question and hypothesis

In this report we try to answer the following research question:

"Is Kitinen river a COS source or sink in the analyzed period and does the site show a diurnal COS flux cycle?"

Forming a hypothesis for this question is difficult as freshwater COS flux measurements are rare.

COS can be produced in freshwater photochemically from chromophoric dissolved organic matter ($CDOM$) (Ferek and Andreae 1984, Whelan et al. 2018) and in smaller extend light independently trough sulfur radical formation and indirectly by CS_2 (Flöck, Andreae, and Dräger 1997, Zhang, Walsh, and Cutter 1998, Whelan et al. 2018). Sinks are abiotic hydrolysis, which depends on the pH, salinity and temperature of the water, and algae uptake (Whelan et al. 2018).

8.5.3 Method

For the Kitinen river data file we needed to take into account the wind direction since the measurement tower is located at the shore of the river. Winds blowing from the land site influences the fluxes disturbing the river signal of our interest. All fluxes measured with values of wind direction below 150 and above 320 were filtered out.

8.5.4 Results

The median COS flux found over all daily medians is -0.305 pmol $m^{-2}s^{-1}$ with a $25\% - 75\%$ range between -3.94 and 4.79 pmol $m^{-2}s^{-1}$.

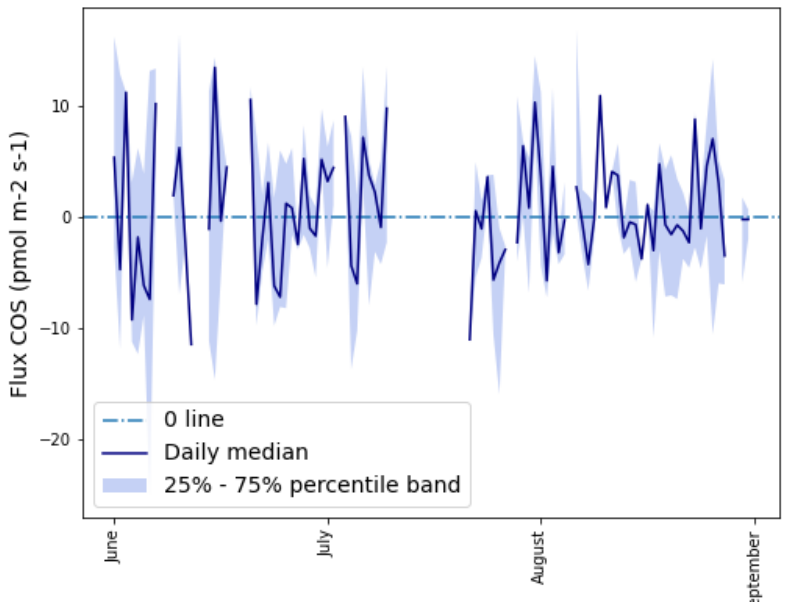

Fig. 48. Daily median *COS* fluxes with 25 and 75 percentiles. *COS* source reported as positive flux and *COS* sink reported as negative flux.

When calculating the median *COS* flux over the diurnal cycle, the results is slightly positive; 0.136 pmol $m^{-2}s^{-1}$ with a $25\% - 75\%$ range between -5.35 and 5.08 pmol $m^{-2}s^{-1}$. Both medians show a percentile band suggesting no significant *COS* sink nor source. Overall in the river the *COS* fluxes tend to cancel out.

The diurnal cycle (fig. 49) however, shows the river to be a *COS* source during day and sink during night.

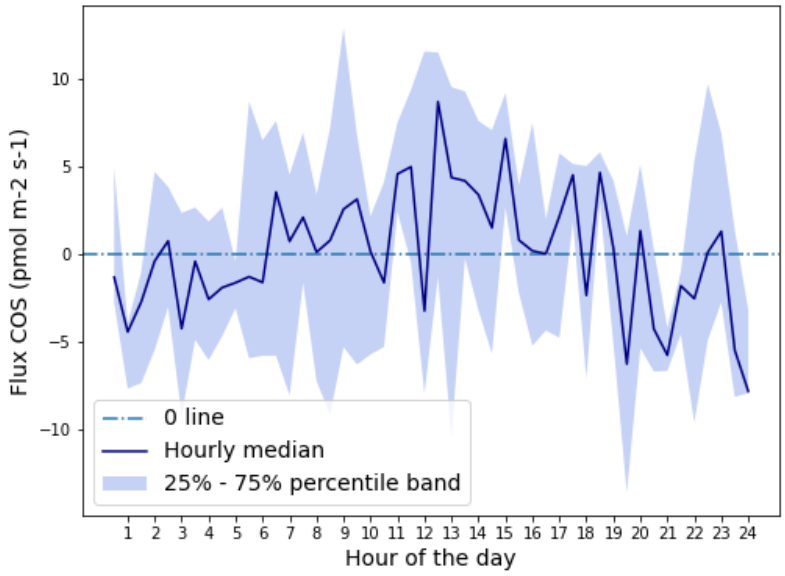

Fig. 49. Diurnal cycle *COS* flux with 25 and 75 percentiles. *COS* source reported as positive flux and *COS* sink reported as negative flux.

Figure 50 shows the correlation matrix on the diurnal cycle of the data. No specific high correlation is found.

	FCOS	FCO2	PAR	RH	Tair	Tw	WD
FCOS	1.00	-0.44	0.53	-0.58	0.55	0.25	0.34
FCO2	-0.44	1.00	-0.64	0.79	-0.77	-0.33	-0.81
PAR	0.53	-0.64	1.00	-0.76	0.69	0.06	0.48
RH	-0.58	0.79	-0.76	1.00	-0.99	-0.62	-0.70
Tair	0.55	-0.77	0.69	-0.99	1.00	0.70	0.69
Tw	0.25	-0.33	0.06	-0.62	0.70	1.00	0.29
WD	0.34	-0.81	0.48	-0.70	0.69	0.29	1.00

Fig. 50. Diurnal cycle correlation matrix Kitinen river June-Sept 2018

Notable is the cross - correlation with RH and air temperature.

Figure 51 shows the data binned against PAR, RH, air temperature and water temperature as done for the Siikaneva data.

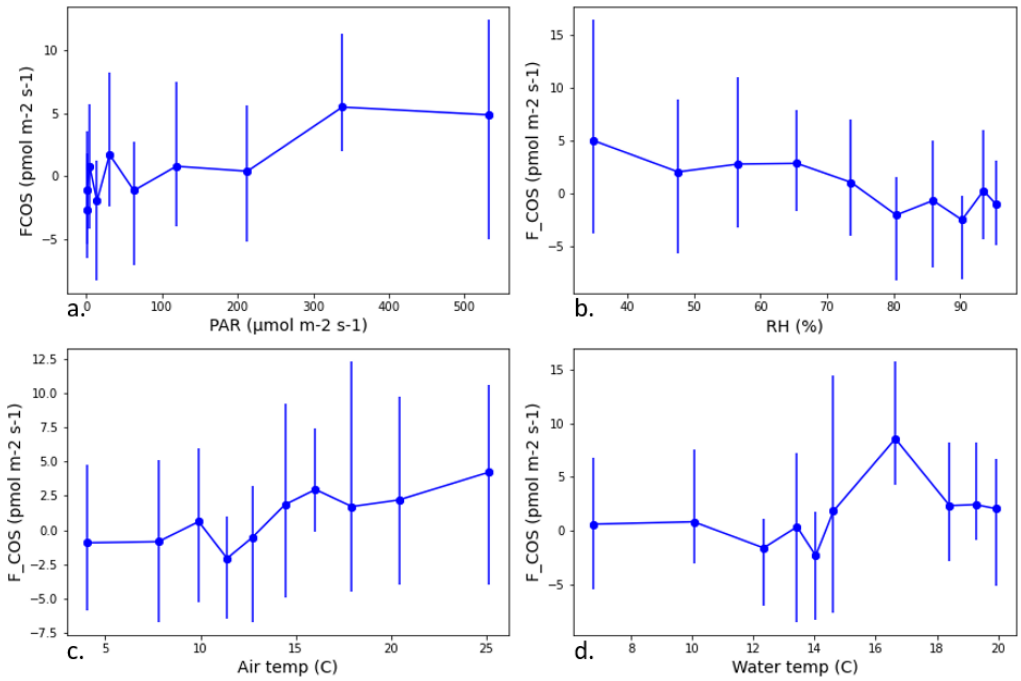

Fig. 51. *COS* **flux relationship with meteorological variables.** Data is collected in 10 equally sized binns. Errorbars represent 25 and 75 percentiles.

We also checked if there is a correlation between the fluctuating part of the vertical wind direction and the *COS* fluxes, but this was absent.

8.5.5 Discussion

On seasonal time scale we see a gap in measurements in July (fig. 48) as there were problems with the instrumentation. Other gaps in data can be caused by the same or can be appeared after the correction for wind direction.

Overall no net flux was found but when looking at the diurnal cycle we see that the river studied, is a source during day which can be explained trough photochemical COS production. While during night hydrolysis dominated making the river a sink.

Indeed, figure 51a,c., shows increasing COS fluxes with increasing PAR fluxes and with increasing air temperature. Even if the correlations are low (around 0.5 for both), when plotting the diurnal cycle of the fluxes and meteorological parameters, the correlation seems higher, especially for air temperature (fig 52 and 53).

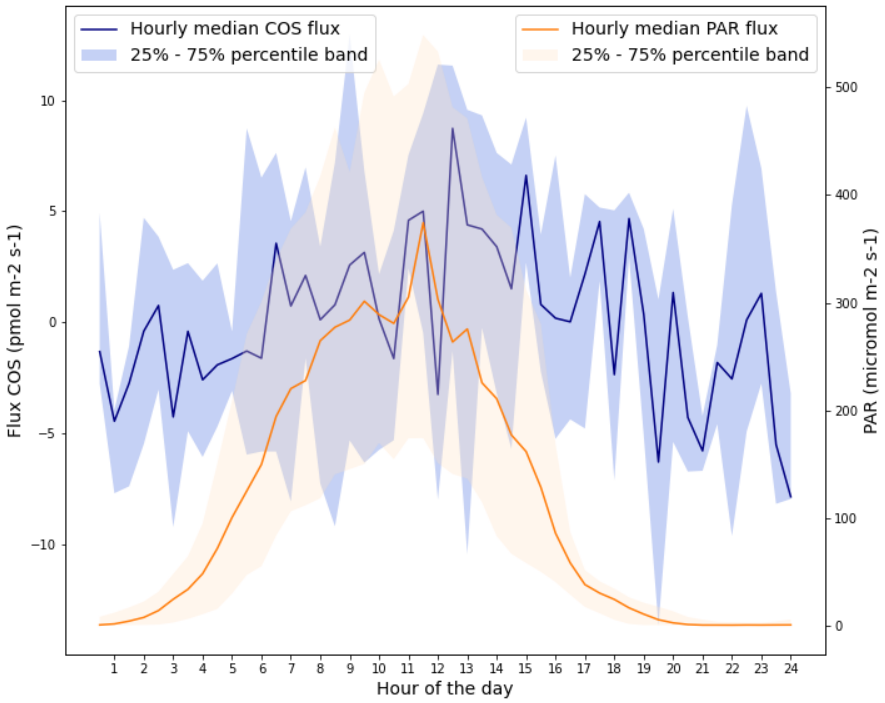

Fig. 52. Diurnal cycle COS and PAR fluxes.

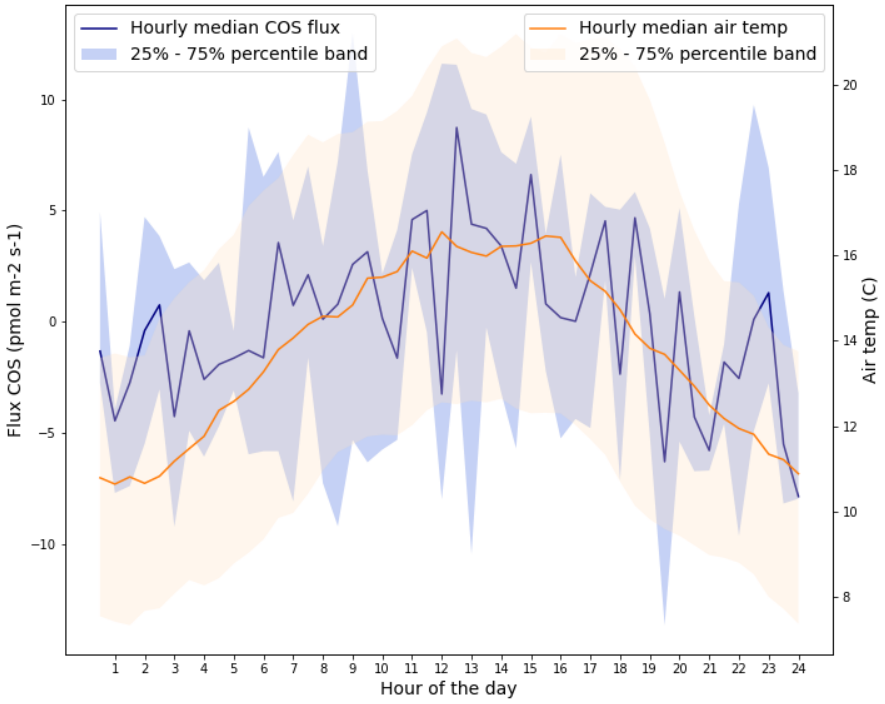

Fig. 53. Diurnal cycle COS fluxes and air temperature.

Moreover, a spike in COS source is found at water temperatures of 17 °C suggesting an optimal COS production temperature (fig. 51d.). However, within uncertainty ranges this optimum is only small.

Further research is needed to verify if more pronounced correlation between PAR, air temperature and water temperature exists.

8.5.6 Conclusion

No significant net sink/source is found for the studied period (June-Sept 2018) over Kitinen river. However, a small diurnal cycle with COS emission during high PAR levels, has been found.

More research on this data is needed to identify potential drivers for the daily COS flux cycle found at Kitinen river. Moreover, if EC measurements over a longer period can be done, a better view of the seasonal cycle will be gained.

References

Masson-Delmotte, V. et al. (2021). "Climate Change 2021, The Physical Science Basis, Working Group I Contribution to the Sixth Assessment Report of the Intergovernmental Panel on Climate Change". In.

Aubinet, Marc (2008). "Eddy covariance CO2 flux measurements in nocturnal conditions: an analysis of the problem". In: *Ecological applications* 18.6, pp. 1368–1378.

Kohonen, Kukka-Maaria et al. (2022). "Carbonyl sulfide fluxes and relation to photosynthesis in the boreal region". In.

Keenan, Trevor F et al. (2019). "Widespread inhibition of daytime ecosystem respiration". In: *Nature ecology & evolution* 3.3, pp. 407–415.

Kooijmans, L. M. J. et al. (2017). "Canopy uptake dominates nighttime carbonyl sulfide fluxes in a boreal forest". In: *Atmospheric Chemistry and Physics* 17.18, pp. 11453–11465. DOI: 10.5194/acp-17-11453-2017. URL: https://acp.copernicus.org/articles/17/11453/2017/.

Montzka, S. A. et al. (2007). "On the global distribution, seasonality, and budget of atmospheric carbonyl sulfide (COS) and some similarities to CO2". In: *Journal of Geophysical Research: Atmospheres* 112.D9. DOI: https://doi.org/10.1029/2006JD007665. URL: https://agupubs.onlinelibrary.wiley.com/doi/abs/10.1029/2006JD007665.

Whelan, M. E. et al. (2018). "Reviews and syntheses: Carbonyl sulfide as a multi-scale tracer for carbon and water cycles". In: *Biogeosciences* 15.12, pp. 3625–3657. DOI: 10.5194/bg-15-3625-2018. URL: https://bg.copernicus.org/articles/15/3625/2018/.

Ma, J. et al. (2021). "Inverse modelling of carbonyl sulfide: implementation, evaluation and implications for the global budget". In: *Atmospheric Chemistry and Physics* 21.5, pp. 3507–3529. DOI: 10.5194/acp-21-3507-2021. URL: https://acp.copernicus.org/articles/21/3507/2021/.

Brühl, C et al. (2012). "The role of carbonyl sulphide as a source of stratospheric sulphate aerosol and its impact on climate". In: *Atmospheric Chemistry and Physics* 12.3, pp. 1239–1253.

Lennartz, Sinikka T et al. (2017). "Direct oceanic emissions unlikely to account for the missing source of atmospheric carbonyl sulfide". In: *Atmospheric chemistry and physics* 17.1, pp. 385–402.

Biotechnology Information, National Center for (2022). *PubChem Compound Summary for CID 10039, Carbonyl sulfide.* URL: https://pubchem.ncbi.nlm.nih.gov/compound/Carbonyl-sulfide (visited on 01/05/2022).

Chin, Mian and DD Davis (1995). "A reanalysis of carbonyl sulfide as a source of stratospheric background sulfur aerosol". In: *Journal of Geophysical Research: Atmospheres* 100.D5, pp. 8993–9005.

Kooijmans, Linda Maria Johanna (2018). "Carbonyl sulfide, a way to quantify photosynthesis". English. PhD thesis. University of Groningen. Chap. 1 Introduction. ISBN: 978-94-034-1079-1.

Baartman, Sophie L et al. (2021). "A GC-IRMS method for measuring sulfur isotope ratios of carbonyl sulfide from small air samples". In: *Open Research Europe* 1.105, p. 105.

Du, Qianqian et al. (2017). "Photochemical production of carbonyl sulfide, carbon disulfide and dimethyl sulfide in a lake water". In: *Journal of Environmental Sciences* 51, pp. 146–156. ISSN: 1001-0742. DOI: https://doi.org/10.1016/j.jes.2016.08.006. URL: https://www.sciencedirect.com/science/article/pii/S1001074216303746.

Schmidt, JA et al. (2012). "Predictions of the sulfur and carbon kinetic isotope effects in the OH+ OCS reaction". In: *Chemical Physics Letters* 531, pp. 64–69.

Wikimedia Commons, public domain (2007). *File:Carbonyl-sulfide.png.* URL: https://commons.wikimedia.org/w/index.php?curid=621705 (visited on 01/05/2022).

Kettle, AJ et al. (2002). "Global budget of atmospheric carbonyl sulfide: Temporal and spatial variations of the dominant sources and sinks". In: *Journal of Geophysical Research: Atmospheres* 107.D22, ACH–25.

Stinecipher, James R et al. (2019). "Biomass burning unlikely to account for missing source of carbonyl sulfide". In: *Geophysical Research Letters* 46.24, pp. 14912–14920.

Zumkehr, Andrew et al. (2018). "Global gridded anthropogenic emissions inventory of carbonyl sulfide". In: *Atmospheric Environment* 183, pp. 11–19.

Berry, Joe et al. (2013). "A coupled model of the global cycles of carbonyl sulfide and CO2: A possible new window on the carbon cycle". In: *Journal of Geophysical Research: Biogeosciences* 118.2, pp. 842–852.

Kesselmeier, J, N Teusch, and U Kuhn (1999). "Controlling variables for the uptake of atmospheric carbonyl sulfide by soil". In: *Journal of Geophysical Research: Atmospheres* 104.D9, pp. 11577–11584.

Shohei Hattori, Tokyo Institute of Technology (2020). *Scientists identify missing source of atmospheric carbonyl sulfide.* URL: https://phys.org/news/2020-08-scientists-source-atmospheric-carbonyl-sulfide.html.

Kooijmans, Linda MJ et al. (2016). "Continuous and high-precision atmospheric concentration measurements of COS, CO 2, CO and H 2 O using a quantum cascade laser spectrometer (QCLS)". In: *Atmospheric Measurement Techniques* 9.11, pp. 5293–5314.
Vesala, Timo et al. (2022). "Long-term fluxes of carbonyl sulfide and their seasonality and interannual variability in a boreal forest". In: *Atmospheric Chemistry and Physics* 22.4, pp. 2569–2584.
Sun, Wu et al. (2018). "Soil fluxes of carbonyl sulfide (COS), carbon monoxide, and carbon dioxide in a boreal forest in southern Finland". In: *Atmospheric Chemistry and Physics* 18.2, pp. 1363–1378.
Kooijmans, Linda MJ et al. (2021). "Evaluation of carbonyl sulfide biosphere exchange in the Simple Biosphere Model (SiB4)". In: *Biogeosciences* 18.24, pp. 6547–6565.
Asaf, David et al. (2013). "Ecosystem photosynthesis inferred from measurements of carbonyl sulphide flux". In: *Nature Geoscience* 6.3, pp. 186–190.
Protoschill-Krebs, G and J Kesselmeier (1992). "Enzymatic pathways for the consumption of carbonyl sulphide (COS) by higher plants". In: *Botanica Acta* 105.3, pp. 206–212.
Blonquist Jr, J Mark et al. (2011). "The potential of carbonyl sulfide as a proxy for gross primary production at flux tower sites". In: *Journal of Geophysical Research: Biogeosciences* 116.G4.
Sandoval-Soto, L et al. (2005). "Global uptake of carbonyl sulfide (COS) by terrestrial vegetation: Estimates corrected by deposition velocities normalized to the uptake of carbon dioxide (CO 2)". In: *Biogeosciences* 2.2, pp. 125–132.
Campbell, J Elliott et al. (2008). "Photosynthetic control of atmospheric carbonyl sulfide during the growing season". In: *Science* 322.5904, pp. 1085–1088.
Kooijmans, Linda M. J. et al. (2019). "Influences of light and humidity on carbonyl sulfide-based estimates of photosynthesis". In: *Proceedings of the National Academy of Sciences* 116.7, pp. 2470–2475. ISSN: 0027-8424. DOI: 10.1073/pnas.1807600116. eprint: https://www.pnas.org/content/116/7/2470.full.pdf. URL: https://www.pnas.org/content/116/7/2470.
Kesselmeier, J and L Merk (1993). "Exchange of carbonyl sulfide (COS) between agricultural plants and the atmosphere: Studies on the deposition of COS to peas, corn and rapeseed". In: *Biogeochemistry* 23.1, pp. 47–59.
Protoschill-Krebs, G, C Wilhelm, and J Kesselmeier (1996). "Consumption of carbonyl sulphide (COS) by higher plant carbonic anhydrase (CA)". In: *Atmospheric Environment* 30.18, pp. 3151–3156.
Meija, Juris et al. (2016). "Atomic weights of the elements 2013 (IUPAC Technical Report)". In: *Pure and Applied Chemistry* 88.3, pp. 265–291. DOI: doi:10.1515/pac-2015-0305. URL: https://doi.org/10.1515/pac-2015-0305.
Stute, Martin (n.d.). *Carbon Isotopes (12C, 13C, 14C)*. URL: https://www.ldeo.columbia.edu/~martins/isohydro/carbon1.html.
Röckmann, Thomas (2017). *Atmospheric Composition and Chemical Processes*. Utrecht University, Institute for marine and atmospheric research, pp. 129–140.
Nagori, Juhi et al. (2022). "Modelling the atmospheric 34 S-sulfur budget in a column model under volcanically quiescent conditions". In: *Atmospheric Chemistry and Physics Discussions*, pp. 1–30.
Angert, Alon et al. (2019). "Sulfur isotopes ratio of atmospheric carbonyl sulfide constrains its sources". In: *Scientific reports* 9.1, pp. 1–8. DOI: https://doi-org.proxy.library.uu.nl/10.1038/s41598-018-37131-3.
Hattori, Shohei, Kazuki Kamezaki, and Naohiro Yoshida (2020). "Constraining the atmospheric OCS budget from sulfur isotopes". In: 117.34, pp. 20447–20452. DOI: 10.1073/pnas.2007260117.
Davidson, Chen, Alon Amrani, and Alon Angert (2021). "Tropospheric carbonyl sulfide mass balance based on direct measurements of sulfur isotopes". In: *Proceedings of the National Academy of Sciences* 118.6.
Aubinet, Marc, Timo Vesala, and Dario Papale (2012). *Eddy covariance: a practical guide to measurement and data analysis*. Springer Science & Business Media.
Baldocchi, Dennis D (2003). "Assessing the eddy covariance technique for evaluating carbon dioxide exchange rates of ecosystems: past, present and future". In: *Global change biology* 9.4, pp. 479–492.
Montagnani, Leonardo et al. (2018). "Estimating the storage term in eddy covariance measurements: the ICOS methodology". In: *International Agrophysics* 32.4, pp. 551–567.
Kohonen, K.-M. et al. (2020). "Towards standardized processing of eddy covariance flux measurements of carbonyl sulfide". In: *Atmospheric Measurement Techniques* 13.7, pp. 3957–3975. DOI: 10.5194/amt-13-3957-2020. URL: https://amt.copernicus.org/articles/13/3957/2020/.

Hattori, Shohei et al. (2015). "Determination of the sulfur isotope ratio in carbonyl sulfide using gas chromatography/isotope ratio mass spectrometry on fragment ions 32S+, 33S+, and 34S+". In: *Analytical chemistry* 87.1, pp. 477–484.

Farquhar, James and Boswell A Wing (2003). "Multiple sulfur isotopes and the evolution of the atmosphere". In: *Earth and Planetary Science Letters* 213.1-2, pp. 1–13.

Ono, Shuhei et al. (2006). "High precision analysis of all four stable isotopes of sulfur (32S, 33S, 34S and 36S) at nanomole levels using a laser fluorination isotope-ratio-monitoring gas chromatography–mass spectrometry". In: *Chemical Geology* 225.1-2, pp. 30–39.

Ghiasi, Mina, Samira Gholami, and Samira Nasiri (2021). "QM study of carbon dioxide (CO2) and carbonyl sulfide (COS) degradation by cluster model of Carbonic anhydrase enzyme". In: *Computational and Theoretical Chemistry* 1199, p. 113188.

Angeli, Andrea, Fabrizio Carta, and Claudiu T Supuran (2020). "Carbonic anhydrases: Versatile and useful biocatalysts in chemistry and biochemistry". In: *Catalysts* 10.9, p. 1008.

Kamezaki, Kazuki et al. (2016). "Sulfur isotopic fractionation of carbonyl sulfide during degradation by soil bacteria". In: *Environmental Science & Technology* 50.7, pp. 3537–3544.

Fried, Alan, Lee F Klinger, and David J Erickson III (1993). "Atmospheric carbonyl sulfide exchange in bog microcosms". In: *Geophysical research letters* 20.2, pp. 129–132.

DeLaune, RD, I Devai, and CW Lindau (2002). "Flux of reduced sulfur gases along a salinity gradient in Louisiana coastal marshes". In: *Estuarine, Coastal and Shelf Science* 54.6, pp. 1003–1011.

De Mello, William Z and Mark E Hines (1994). "Application of static and dynamic enclosures for determining dimethyl sulfide and carbonyl sulfide exchange in Sphagnum peatlands: Implications for the magnitude and direction of flux". In: *Journal of Geophysical Research: Atmospheres* 99.D7, pp. 14601–14607.

Artz, Rebekka RE (2009). "Microbial community structure and carbon substrate use in northern peatlands". In: *Washington DC American Geophysical Union Geophysical Monograph Series* 184, pp. 111–129.

Zeiger, Eduardo, Graham D Farquhar, and IR Cowan (1987). *Stomatal function*. Stanford University Press.

Seco, Roger et al. (2020). "Volatile organic compound fluxes in a subarctic peatland and lake". In: *Atmospheric Chemistry and Physics* 20.21, pp. 13399–13416.

Woods-Hole-Oceanographic-Institution (n.d.). *Lecture 15, Physical Principles of Isotopic Fractionation*. URL: https://www.whoi.edu/fileserver.do?id=136144&pt=2&p=146969.

Aalto, J et al. (2019). "SMEAR II Hyytiälä forest meteorology, greenhouse gases, air quality and soil (Version 1), University of Helsinki". In: *Institute for Atmospheric and Earth System Research [data set], available at: http://urn. fi/urn: nbn: fi: att: a8e81c0e-2838-4df4-9589-74a4240138f8, last access* 5.

Rinne, Janne et al. (2018). "Temporal variation of ecosystem scale methane emission from a boreal fen in relation to temperature, water table position, and carbon dioxide fluxes". In: *Global Biogeochemical Cycles* 32.7, pp. 1087–1106.

Stein, AF et al. (2015). "NOAA's HYSPLIT atmospheric transport and dispersion modeling system". In: *Bulletin of the American Meteorological Society* 96.12, pp. 2059–2077.

Rolph, Glenn, Ariel Stein, and Barbara Stunder (2017). "Real-time environmental applications and display system: READY". In: *Environmental Modelling & Software* 95, pp. 210–228.

handbook, Engeneering statistics (n.d.). *1.3.5.11.Measures of Skewness and Kurtosis*. URL: https://www.itl.nist.gov/div898/handbook/eda/section3/eda35b.htm (visited on 01/14/2022).

Leys, Christophe et al. (2013). "Detecting outliers: Do not use standard deviation around the mean, use absolute deviation around the median". In: *Journal of experimental social psychology* 49.4, pp. 764–766.

Whelan, Mary E and Robert C Rhew (2016). "Reduced sulfur trace gas exchange between a seasonally dry grassland and the atmosphere". In: *Biogeochemistry* 128.3, pp. 267–280.

Xu, Jiren et al. (2018). "PEATMAP: Refining estimates of global peatland distribution based on a meta-analysis". In: *Catena* 160, pp. 134–140.

Olefeldt, David et al. (2021). "The Boreal–Arctic Wetland and Lake Dataset (BAWLD)". In: *Earth system science data* 13.11, pp. 5127–5149.

Krinner, Gerhard et al. (2005). "A dynamic global vegetation model for studies of the coupled atmosphere-biosphere system". In: *Global Biogeochemical Cycles* 19.1.

Tootchi, Ardalan, Anne Jost, and Agnès Ducharne (2019). "Multi-source global wetland maps combining surface water imagery and groundwater constraints". In: *Earth System Science Data* 11.1, pp. 189–220.

Gimeno, Teresa E et al. (2017). "Bryophyte gas-exchange dynamics along varying hydration status reveal a significant carbonyl sulphide (COS) sink in the dark and COS source in the light". In: *New Phytologist* 215.3, pp. 965–976.

Mammarella, Ivan et al. (2007). "Determining the contribution of vertical advection to the net ecosystem exchange at Hyytiälä forest, Finland". In: *Tellus B: Chemical and Physical Meteorology* 59.5, pp. 900–909.

Stull, Roland B (1988). *An introduction to boundary layer meteorology*. Vol. 13. Springer Science & Business Media.

Ferek, RJ and MO Andreae (1984). "Photochemical production of carbonyl sulphide in marine surface waters". In: *Nature* 307.5947, pp. 148–150.

Flöck, Otmar R, Meinrat O Andreae, and M Dräger (1997). "Environmentally relevant precursors of carbonyl sulfide in aquatic systems". In: *Marine Chemistry* 59.1-2, pp. 71–85.

Zhang, Li, Russell S Walsh, and Gregory A Cutter (1998). "Estuarine cycling of carbonyl sulfide: production and sea–air flux". In: *Marine chemistry* 61.3-4, pp. 127–142.